# THE BLOCKING OF MID-LATITUDE WESTERLY WINDS BY STATIONARY ANTICYCLONES

by

Jillian Frances AUSTIN

Atmospheric Physics Group
Department of Physics
Imperial College, London

A thesis submitted for the degree of
Doctor of Philosophy
to the University of London

ABSTRACT

THE BLOCKING OF MID-LATITUDE WESTERLY WINDS BY STATIONARY ANTICYCLONES

by J.F. Austin

This study is concerned with a phenomenon commonly known as blocking. A survey is made of the observations in order to determine the essential features of blocking which a numerical model should be able to reproduce. As for mechanisms responsible for blocking, there is no agreement in the literature on these, so a number of possible mechanisms are reviewed. These include barotropic instability, baroclinic instability, hydraulic jumps and orographically forced long waves. It is found that long waves on normal charts, which represent the stationary response of the atmosphere to orographic forcing, interfere to give ridges at 500 mb. in the regions where blocking anticyclones most frequently occur. Long waves are further examined in case studies of the tropospheric flow in the Northern Hemisphere in January 1968, December 1963 and January 1966. These case studies concentrate on the Fourier spectra associated with blocking in different regions; the results indicate that short lived blocking situations are due to the interference of long waves at 500 mb. and thus are spatially isolated. However, persistent blocking situations are associated with the amplification of a single wavenumber. It is inferred that an additional mechanism is at work in persistent blocking situations and it seems likely that this is an interaction between the long waves and smaller scale baroclinic waves. The baroclinic waves grow in the temperature gradients produced by the long waves and damp the long waves by transferring heat down-gradient. However, there is also a non-Fickian transfer of momentum by the baroclinic waves and it is found that a simple model of this process reproduces well the observed features of blocking. A resonance is possible at the stationary barotropic Rossby wavelength, which is the wavelength most commonly observed in persistent blocking situations.

Contents


| | | Page |
|---|---|---|
| Introduction | | |
| Chapter One - The Observations | | 1 |
| 1.1 | Definition of Blocking Anticyclones | 2 |
| 1.2 | Statistical Surveys | 4 |
| | 1.2.1 Geographical Distribution | 8 |
| | 1.2.2 Monthly Occurence | 10 |
| | 1.2.3 Monthly Position | 10 |
| | 1.2.4 Duration of Blocking | 10 |
| | 1.2.5 Annual Variations | 13 |
| 1.3 | Rotation of the Sun | 13 |
| 1.4 | Summary | 21 |
| Chapter Two - The Mechanisms | | 23 |
| 2.1 | Introduction | 24 |
| 2.2 | Hydraulic Jump | 26 |
| 2.3 | Barotropic Instability | 30 |
| 2.4 | Sensible Heat Exchange from the Oceans | 31 |
| 2.5 | Rossby Waves | 32 |
| 2.6 | Summary | 52 |
| Chapter Three - Pacific Blocking | | 53 |
| 3.1 | Introduction | 54 |
| 3.2 | Wintertime Pacific Blocking- January 1968 | 54 |
| 3.3 | Behaviour of Wavenumber One | 70 |
| 3.4 | Zonal Winds | 78 |
| 3.5 | Stratospheric Warmings | 82 |
| 3.6 | Summary | 86 |
| Chapter Four - Atlantic and Double Blocking | | 87 |
| 4.1 | Introduction | 88 |
| 4.2 | Pacific and Double Blocking - January 1966 | 88 |
| 4.3 | Atlantic, Pacific and Double Blocking - December 1963 | 99 |
| 4.4 | General Conclusions from Case Studies | 115 |

Chapter Five - The Interaction between the Long Waves and Baroclinic Waves

Part One - Transfer of Heat 121

5.1 Introduction 122

5.2 Effect of Eddy Diffusivity of Heat on Stationary Rossby Waves 122

5.3 A Two-Layer Baroclinic Model 126

5.4 Conclusion 132

Chapter Six - The Interaction between the Long Waves and Baroclinic Waves

Part Two - Transfer of Momentum 133

6.1 Introduction 134

6.2 Momentum Forcing constant with Height 137

6.3 Effect of Friction 142

6.4 Momentum Forcing varying with Height 145

6.5 Inclusion of Spherical Geometry and Wind Shear 151

6.6 Energy Transmitting Upper Boundary Condition 156

6.7 Numerical Solutions 157

6.8 Conclusion 163

Appendix One - Catalogue of Blocking Dates 164

Appendix Two - Errors in Long Wave Calculations 168

Appendix Three - Harmonic Analysis of Normal Charts (Eliasen) 171

References 172

Acknowledgements 176

Introduction

For a long time meteorologists paid little attention to anticyclones because the latter were not usually accompanied by any dangerous weather. The term anticyclone was introduced by Galton in 1861 in his "Meteorographica". Galton correctly noted the basic feature of anticyclones, which are the predominance of light winds, the clockwise rotation of air flows and the downward motion of the air. By contrast, the term cyclone had first been used by H. Piddington in 1848 (Sailors' Horn Book and winds) to describe storms in which the wind had a circular or whirling course.

The theory of anticyclones has always been intimately connected with the theory of cyclones. In the nineteenth century the prevelant view of cyclones was that they were isolated convection cells due to heating at the ground. Ferrel, a supporter of this theory, realised the implication that every cyclone must be surrounded by a ring of elevated pressure. Outside this area the pressure much drop once again and the winds would be anticyclonic in nature. The fact that there are no annular anticyclones in nature did not unduly disturb Ferrel. He merely noted that such phenomena "- - - are not revealed directly by observation, but to deny their existence would be to deny the validity of certain fundamental, well established principles of mechanics." In Ferrel's opinion, anticyclones were produced as a result of the interference of rings of high pressure around two adjacent cyclones. However, he later thought that anticyclones might be due to cooling and a consequent accumulation of heavier air at one place. Theories of anticyclones at this time were further confused by a lack of understanding of adiabatic processes. For example, in 1874 the American meteorologist Loomis explained the cold weather in anticyclones as "a result of the downward motion of air from the upper atmosphere."

J. Hann, one of the greatest of nineteenth century meteorologists, came out against the convection theory of cyclones. As early as 1875 he believed that "most of the lowering of a barometer during a storm can be explained mechanically." Hann carried out a considerable programme of mountain observations and recorded the temperature variations with height in cyclones and anticyclones. From these observations he drew the important conclusion that "- - - the pressure conditions in an anticyclone are a consequence not of the temperature conditions but rather of the type of motion of the air masses in it. The temperature conditions depend on the type of motion and thus are a consequence, like the dryness of air and the absence of cloud."

In his study Hann was actually describing a warm anticyclone in a mature baroclinic wave. In subsequent years a controversy developed between Hann and some American meteorologists whether anticyclones were warm or cold. This issue was not finally settled until about 1908, when it was acknowledged that both types of anticyclone existed in the atmosphere.

The idea that anticyclones are somewhat secondary in synoptic meteorology was refuted once and for all with the advent of long-term weather forcasting. In 1880 Teisserenc de Bort was the first to introduce the idea of "centres of action" in the atmosphere; he was spurred on in his research by the anomalous winter of 1879. de Bort concluded that the European weather of an entire season is determined by the intensity variation and the migration of "centres of action" in the atmosphere. For Europe, the centres which turned out to be the most important were the Azores and Siberian highs and the Icelandic low. In an attempt to express this more graphically, he referred to anticyclones as "weather regulators." The first scientific long-term weather

forcasts began with attempts to predict good or bad summer monsoons for India. The first of these was produced by Blanford in 1886, based on the amount of snow which fell in the Himalayas and the Sulaiman Mountains from January to May.

Thus, with their importance firmly established, anticyclones have received much study in the twentieth century. Thanks to the work of Eady (1949), transient highs and lows are now known to be due to baroclinic instability of the zonal flow. Theories of stationary disturbances, the "centres of action" of Teisserenc de Bort, have been less successful. Perhaps the most spectacular of these stationary disturbances is the winter Siberian anticyclone. In 1873 the great Russian meteorologist A.I. Voeikov realised that the winter cooling of a large continent must create an anticyclonic rotation in the lower layers of the atmosphere and a pressure minimum in the upper. This idea still forms the basis for our present understanding of cold continental anticyclones, but only in recent years has it been realised that these anticyclones are not shallow phenomena but extend their influence as high as the mesosphere.

The erratic appearance of stationary warm anticyclones in middle latitudes has almost completely defied explanation. These quite commonly occur on the western coasts of the two main continents in the Northern Hemisphere; they bring about heat waves and droughts in the summer and particularly severe weather in the winter. Thus the short-term effect of these anticyclones on the climate is spectacular; the long-term effects have only been speculated about. Lamb (1973) has implied that they are associated with the onset of ice-ages, while Rex (1952) has expressed the opposite point of view. Rex argued that, as the stationary anticyclone deviates warm middle latitude air over Scandinavia, this would

retard the progress of glaciers there.

It is quite clear that these stationary anticyclones present a formidable problem in modern meteorology. This study is concerned with most aspects of the problem as observed in the Northern Hemisphere. Van Loon (1956) has suggested similar disturbances occur in the Southern Hemisphere but lack of 500 mb. data there makes it almost impossible to verify this.

# Chapter ONE

## The Observations

''As the days lengthen

The cold strengthens''

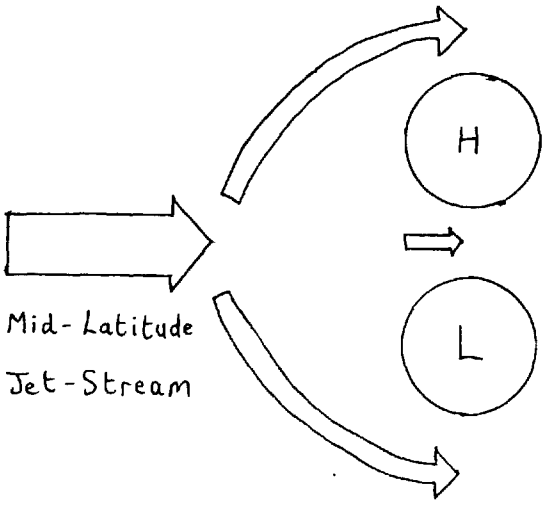
English Weather Lore

## Chapter One The Observations

### 1.1 Definition of Blocking Anticyclones

One of the most difficult and important problems in medium-range weather forcasting is the prediction of stationary high pressure cells in regions where westerly winds normally prevail. The generally accepted term for these anticyclones is blocking anticyclones. This is because they are thought of as ''blocks'' around which travelling troughs and ridges must detour. The implication of this terminology is that the high pressure area is somehow ''different'' from the baroclinic disturbances associated with the more zonal flow.

Sometimes the anticyclone block can take the form of a high pressure ridge, which extends up from the tropics and deviates the zonal flow to the north. However, either these cases do not persist very long, or the ridge develops into a high pressure cell at about $60^{\circ}N$ with a low pressure cell to the south at about $40^{\circ}N$. This is the usual configuration in blocking siutations which persist for more than a week. This pressure pattern splits the main jet-stream to the north of the high and the south of the low. There is a ''col'' region between the high pressure and low pressure where the winds are very weak and can be either westerly or easterly. The splitting of the jet stream is particularly obvious at 500 mb.




Split Jet-Stream

H = high pressure cell
L = low pressure cell

However, it is clear from the literature that there is no objective definition of blocking; it can nd does mean different things to different authors. Authors who have studied the problem from a synoptic point of view have usually presented descriptions similar to the one outlined above. However, the term blocking is used rather loosely in numerical modelling, for example to describe any long wave of large amplitude. The conflict in the terminology is genuine. Is a blocking anticyclone a localised disturbance or part of a global scale wave? The answer is not obvious but a study of synoptic charts does suggest that short lived blocking anticyclones (persistence of about a week) are localised phenomena. However in severe cases of blocking, such as January 1963, the whole tropospheric and stratospheric circulation was affected. This suggests that different mechanisms may be involved in short-lived and long-lived blocking situations.

The purpose of this chapter is to survey the observations on blocking anticyclones and hence identify the essential features of blocking which a numerical model should be able to reproduce.

The most important thing to notice about a blocking anticyclone is that it is warm in the troposphere and cold in the stratosphere. Hence the anticyclone intensifies with height in the troposphere and is then damped with height in the stratosphere. This is in marked contrast to the stationary anticyclone over Siberia in the winter, which is cold in the lower troposphere. In the case of the Siberian anticyclone, low level radiational cooling causes the low-lying air to sink and compress the vortex tubes associated with the earth's vorticity. This produces a low-level, cold anticyclone. However, the low-level sinking causes the vortex tubes higher in the atmosphere

to be stretched and so produce cyclonic vorticity. Thus the surface anticyclone is accompanied by a cyclone aloft in the troposphere; that is to say the disturbance ''changes sign'' with height in the troposphere.

January 1963 was a month in which the circulation was dominated by blocking anticylones in the Atlantic and Pacific. Fig. 1(1) shows the sea level chart for Europe and the Atlantic on January 11th. 1963 (taken from Daily Synoptic Weather Maps published by N.O.A.A.). Two anticyclones can be seen, one over the Atlantic ($-3^{\circ}C$) and the other over Siberia ($-12^{\circ}C$). The 500 mb. chart for the same day is shown in Fig 1(2). This clearly shows that there is a warm high pressure cell over the Atlantic and an area of weak low pressure over Siberia, illustrating the difference between the two phenomena.

To further emphasise the vertical structure of a blocking anticyclone, a diagram is reproduced in Fig 1(3) from Elliot and Smith (1949). This shows a time-height cross-section of the temperature at Longview, Alaska during the formative stages of a blocking anticyclone in the region. During the period 31st March to 3rd April 1948 an anticyclone developed over the central Aleutians and remained more or less stationary in this region during April. It can be seen that warming through the depth of the troposphere and cooling in the stratosphere were features of the development of the blocking anticyclone.

## 1.2 Statistical Surveys

A number of independent statistical surveys have been carried out on the occurence, position and duration of blocking anticyclones and it is interesting to compare these results. The definitions of blocking vary, but a deep stationary anticyclone in mid or high latitudes with

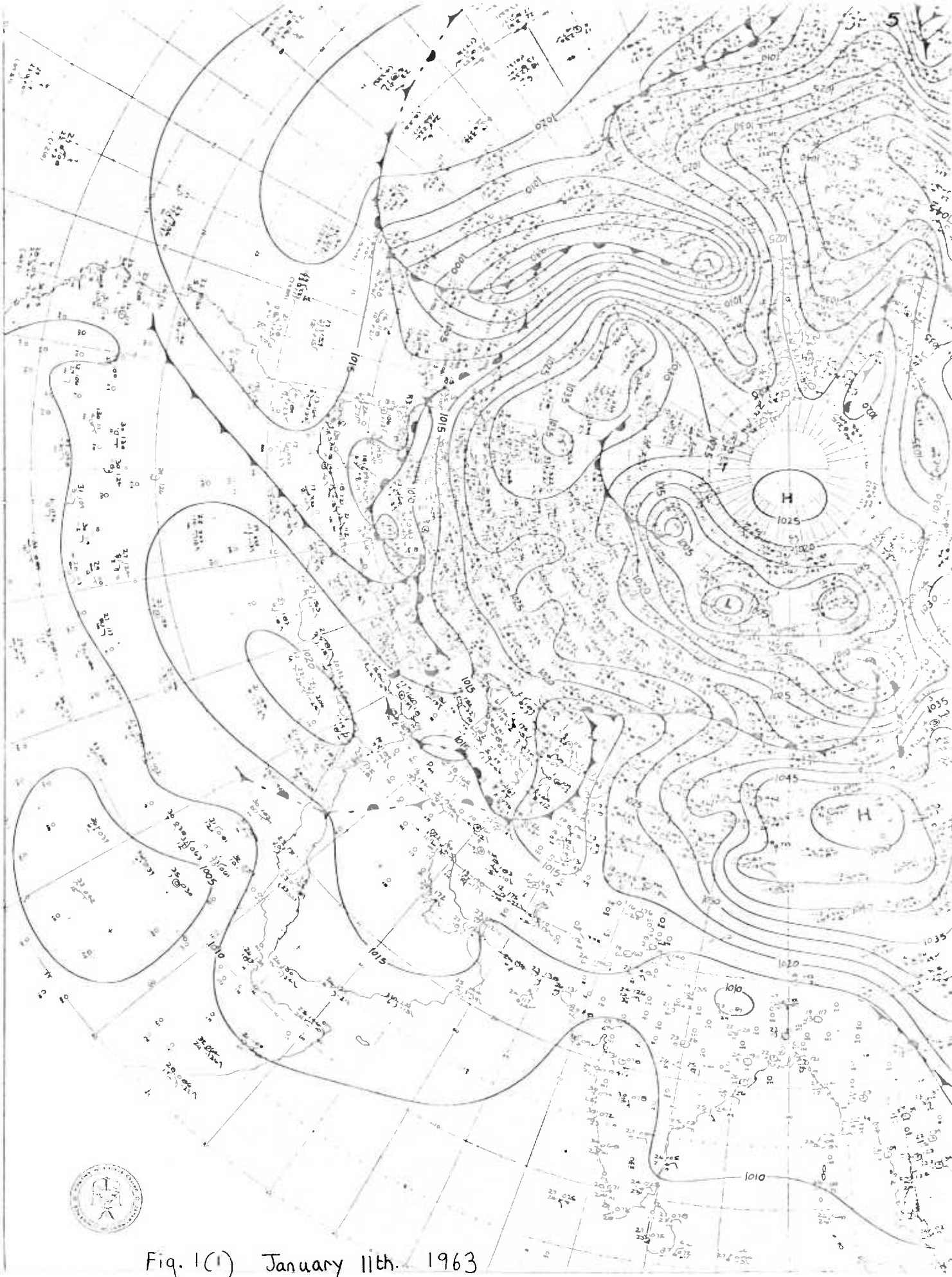



Fig. 1(1) January 11th. 1963
(sea level)

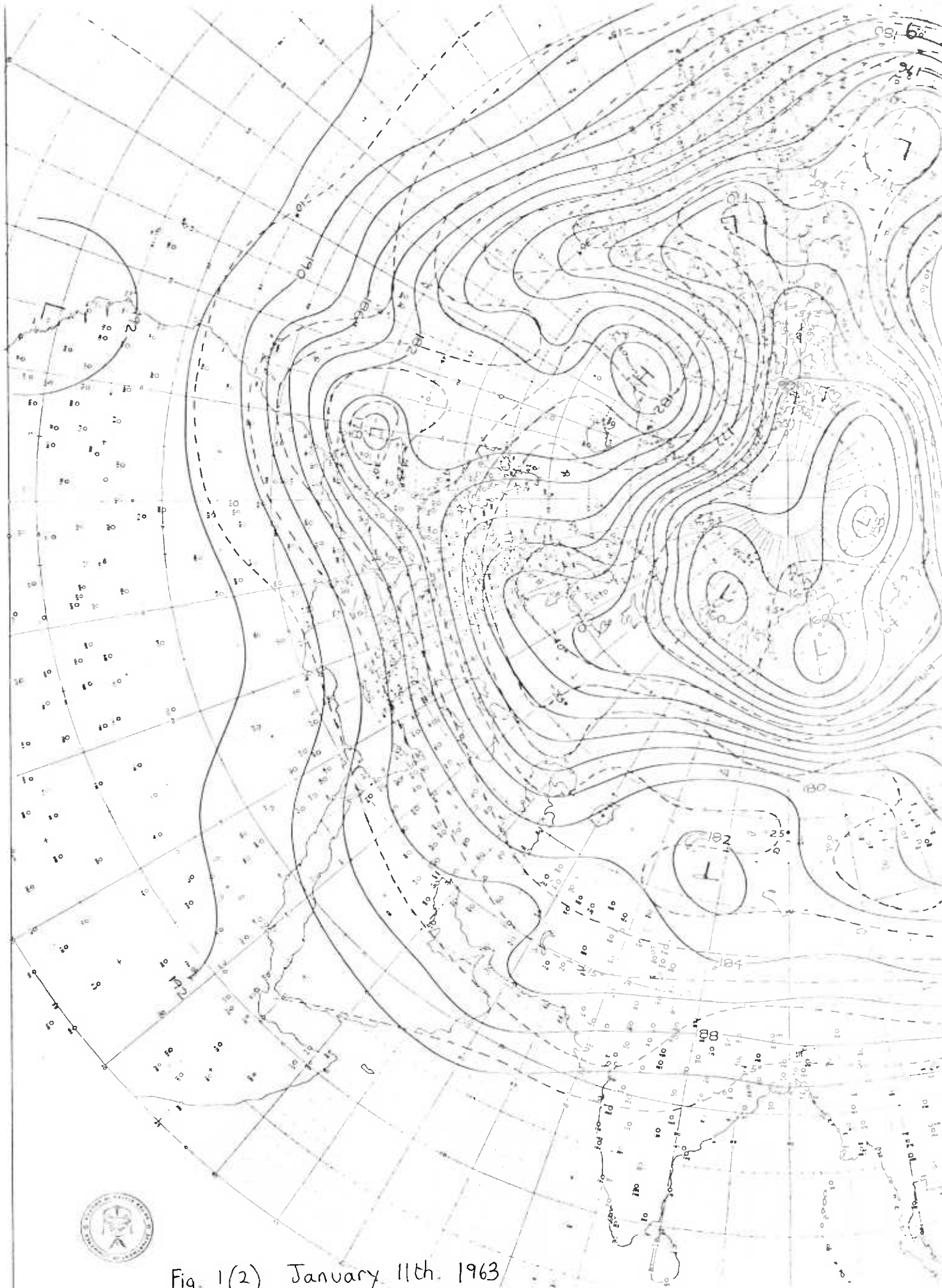
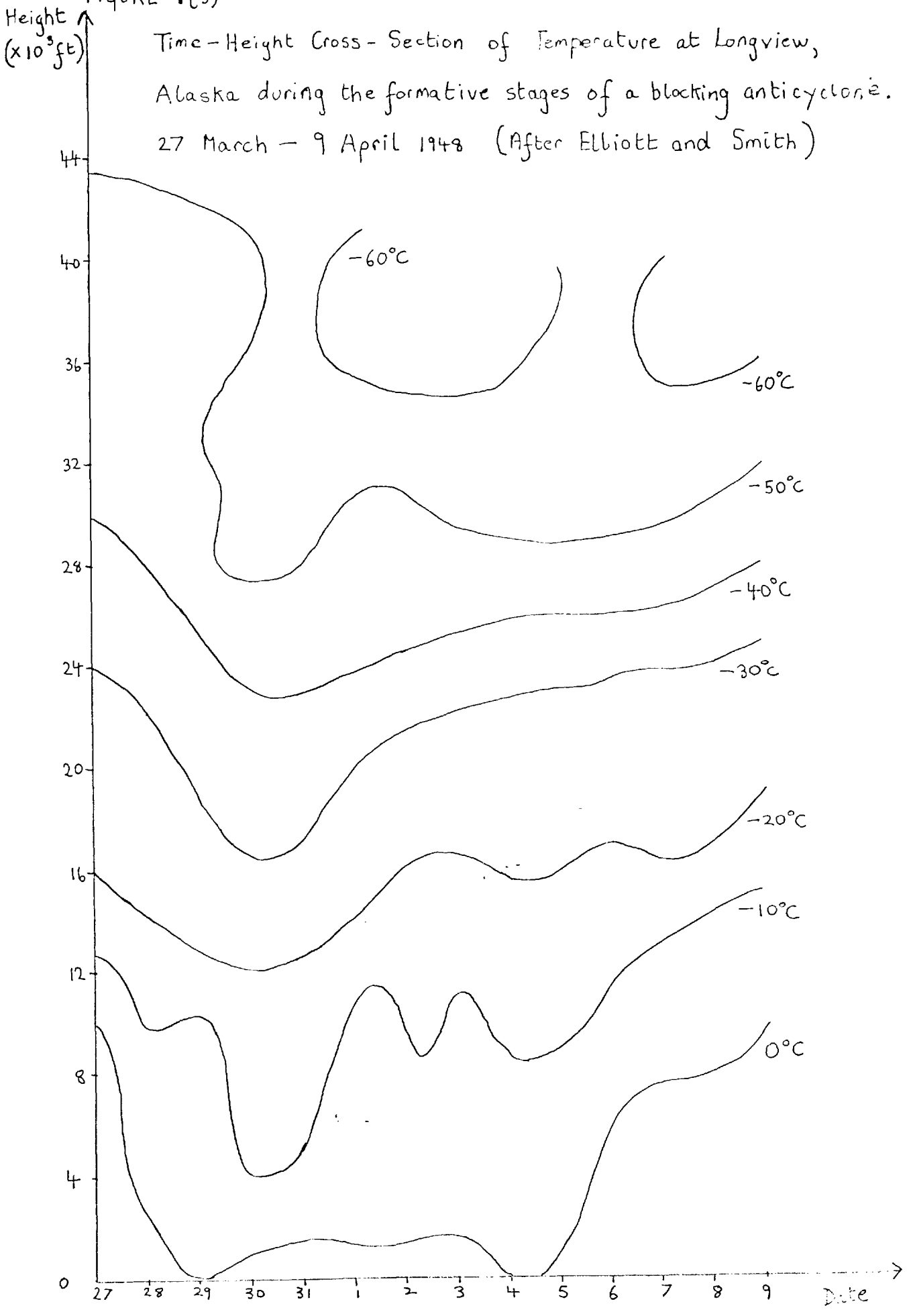


Fig. 1(2) January 11th. 1963

(500mb.)

FIGURE 1(3)

Time-Height Cross-Section of Temperature at Longview, Alaska during the formative stages of a blocking anticyclone. 27 March – 9 April 1948 (After Elliott and Smith)



an associated split jet-stream seem to be the main requirements. Statistics were used from the following authors:

Rex (1950), who used 500 mb. charts for the period 1932 to 1950 and required a minimum persistence of the stationary anticyclone of 10 days.

Montalto, Conte and Urbani (1971), who used 500 mb. charts for the period 1951 to 1970 and required a minimum persistence of five days.

Sanders (1953), who used surface charts for the period 1899 to 1938 and required no minimum persistence. [This makes his results rather unreliable as it is difficult to know how he differentiated between the ridges of travelling baroclinic waves and blocking anticyclones.]

Austin, who used surface charts for the period 1966 to 1976 and required a minimum persistence of six days. These results are given in Appendix One.

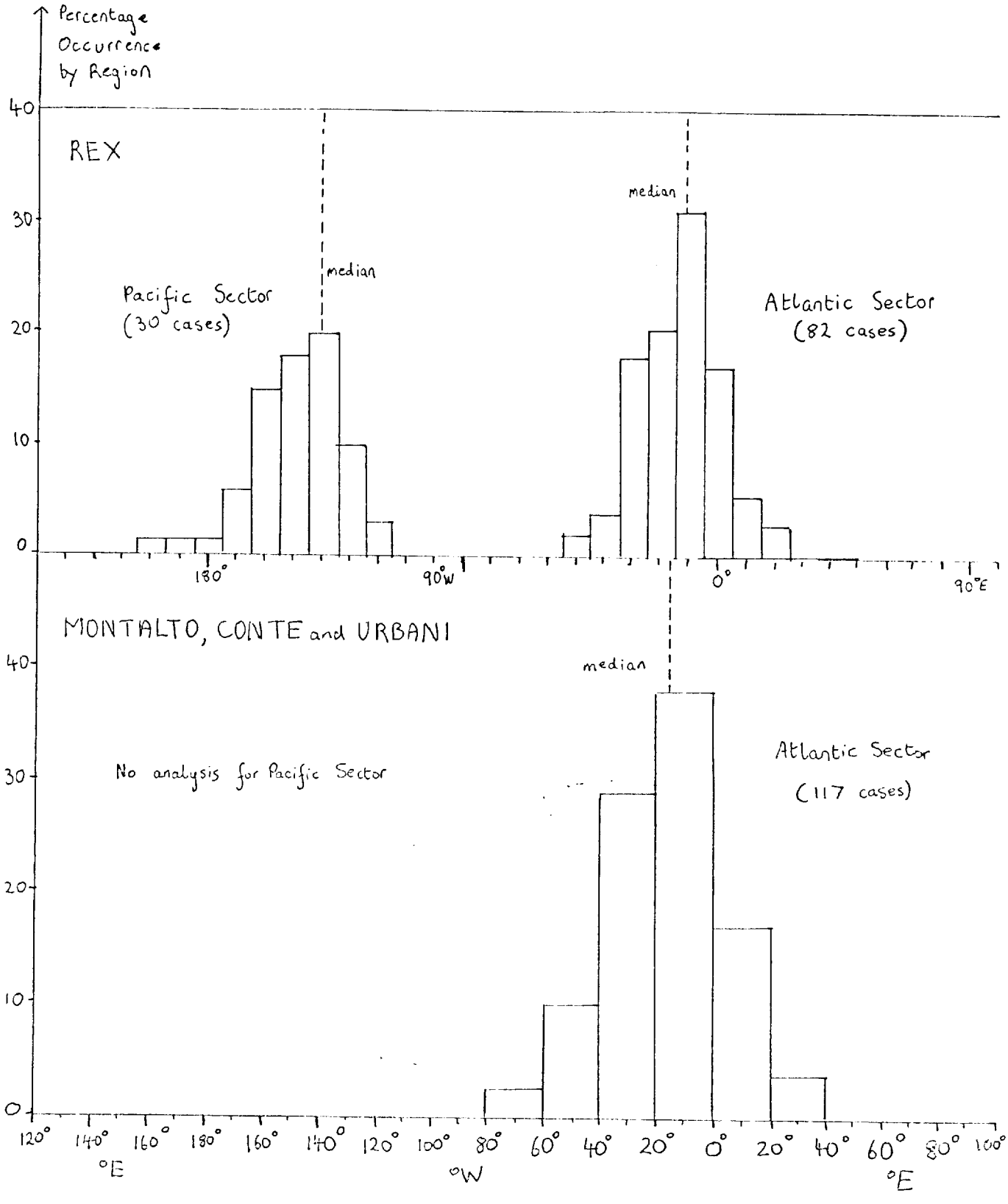
1.2.1 Geographical Distribution of Blocking Anticyclones

It is widely accepted in the literature that the two main regions for blocking anticyclones in the Northern Hemisphere are centred on the N.E. Atlantic and the N.E. Pacific. In future these regions will be referred to as the Atlantic and Pacific sectors respectively. Rex used hemispheric charts in his study but the other authors concentrated on Western Europe and the Atlantic.

Both Rex and Montalto, Conte and Urbani published histograms for the longitude of the initial splitting of the jet stream at the onset of blocking. Their results in Fig 1(4) show very good agreement

FIGURE 1(4)

Geographical Distribution of Blocking: Longitude of initial splitting of the jet-stream at 500 mb.



in the Atlantic sector, while Rex also provided figures for the Pacific sector. Rex's results show that two thirds of the cases he studied occured in the Atlantic sector. This bias towards the Atlantic sector has been confirmed by other authors. For example, Elliot and Smith (1949) did not publish such statistics but stated that there was a marked tendency for blocking activity to occur in the N.E. portions of the Atlantic and the Pacific, with the highest frequency of occurence in the band $0^{o}$W. to $25^{o}$W.

1.2.2 Monthly Occurence of Blocking Anticyclones in the Atlantic Sector

Fig 1(5) shows the average monthly occurence of blocking in the Atlantic sector throughout the year. There does seem to be a tendency for a late spring maximum in the different curves, but it is not very striking. Blocking obviously occurs throughout the year.

1.2.3 Monthly Position of Blocking Anticyclones in the Atlantic Sector

Fig 1(6) shows the monthly distribution of the longitude of the splitting of the jet at the onset of blocking in the Atalantic sector. The agreement between Rex and Montalto, Conte and Urbani is striking, particularly as their statistics apply to different sets of years. These results suggest that the position of the blocking anticyclone is most likely to be on the coast or in mid-Atlantic at the equinoxes and, to a lesser extent, in mid-winter. However, in the summer the anticyclone is most likely to be over France or Denmark. Some of the dispersion of longitude in Fig 1(4) is presumably due to this effect.

1.2.4 Duration of Blocking in the Atlantic Sector

Rex's survey of duration of blocking in the Atlantic sector showed a well defined peak at fourteen days, which he considered to be important. However, this peak has not been confirmed by other authors.

FIGURE 1(5)

Monthly Occurrence of Blocking

Percentage of days in the month on which blocking occurred.

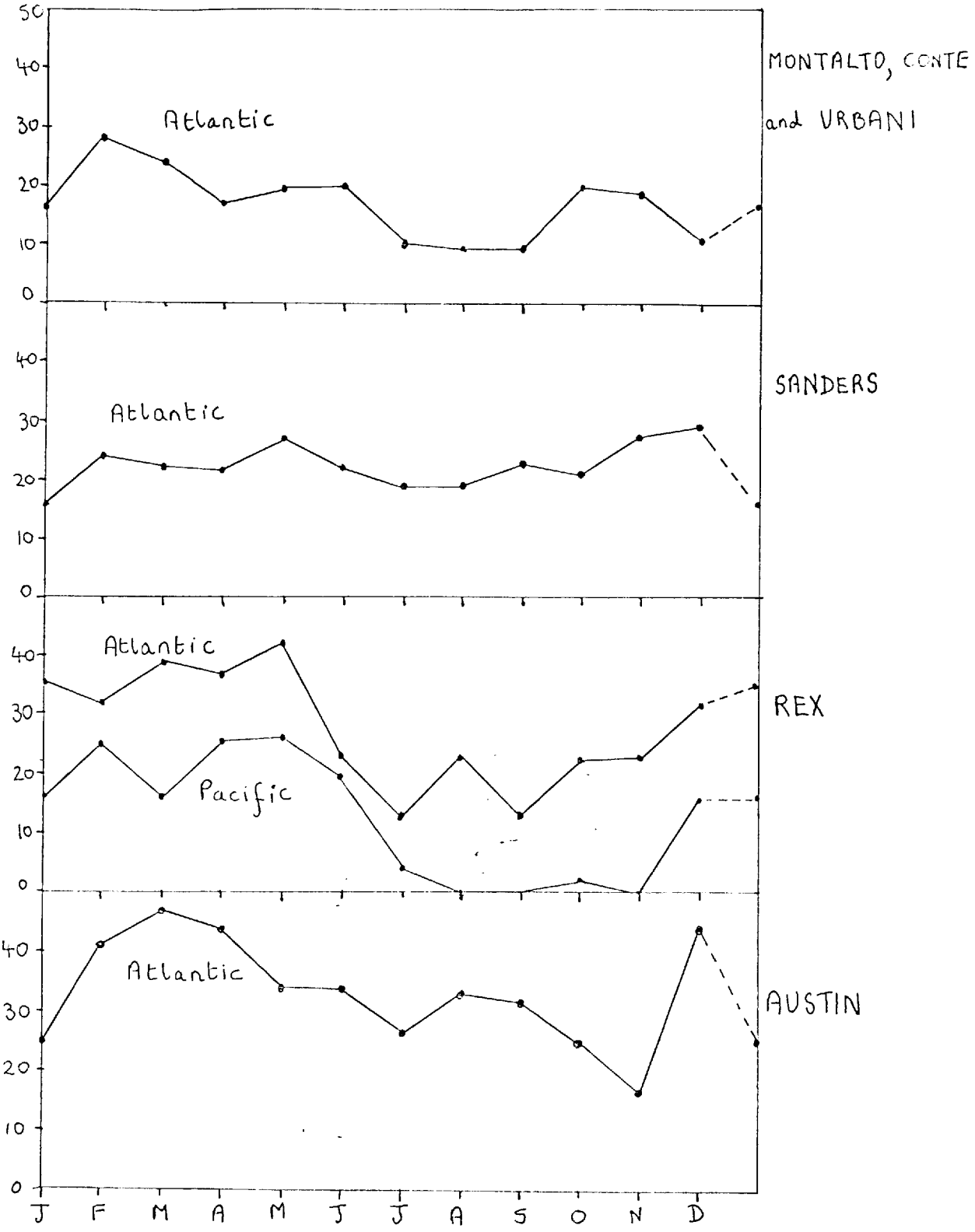
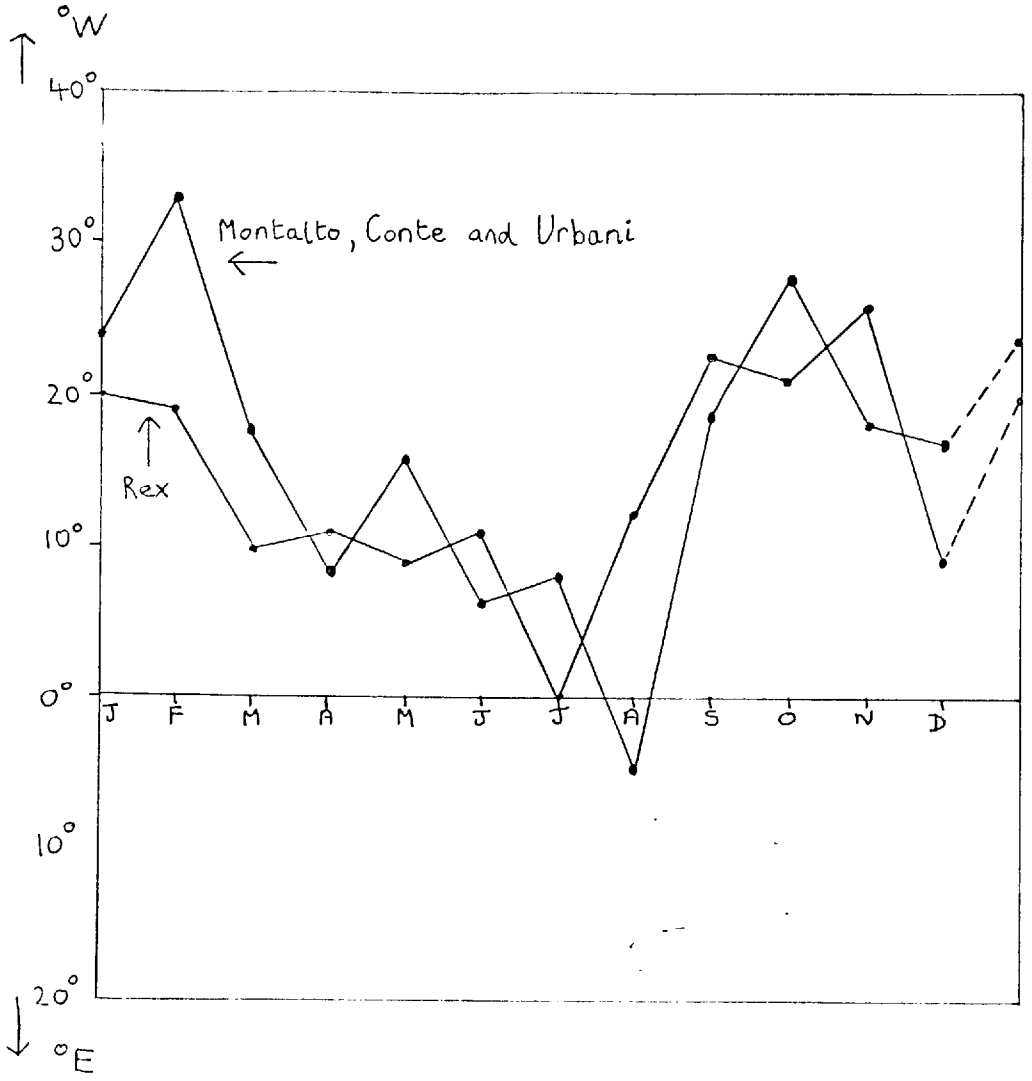


FIGURE 1(6)

Monthly Mean of Position of Blocking in the Atlantic Sector

(Longitude of the initial splitting of the jet at 500mb.)



For example, Austin's data on duration of blocking in the Atlantic shows rather weak maxima at eight days and twelve days. Both surveys show that blocking situations which persist for more than about thirty days are uncommon events. This data is shown in Fig 1(7).

1.2.5 Annual Variations in Blocking

All authors are agreed that the amount of blocking varies considerably from year to year. It is not known why this should be so, or whether any long term trends or periodicities are involved. Lamb (1973) has constructed a graph of the frequency of S.W. 'ly surface winds in S.E. Britain since 1340 and this data shows a 200 year cycle within this period. The presence of surface S.W. 'ly winds is a good indication of depressions travelling in from the Atlantic and hence no blocking.

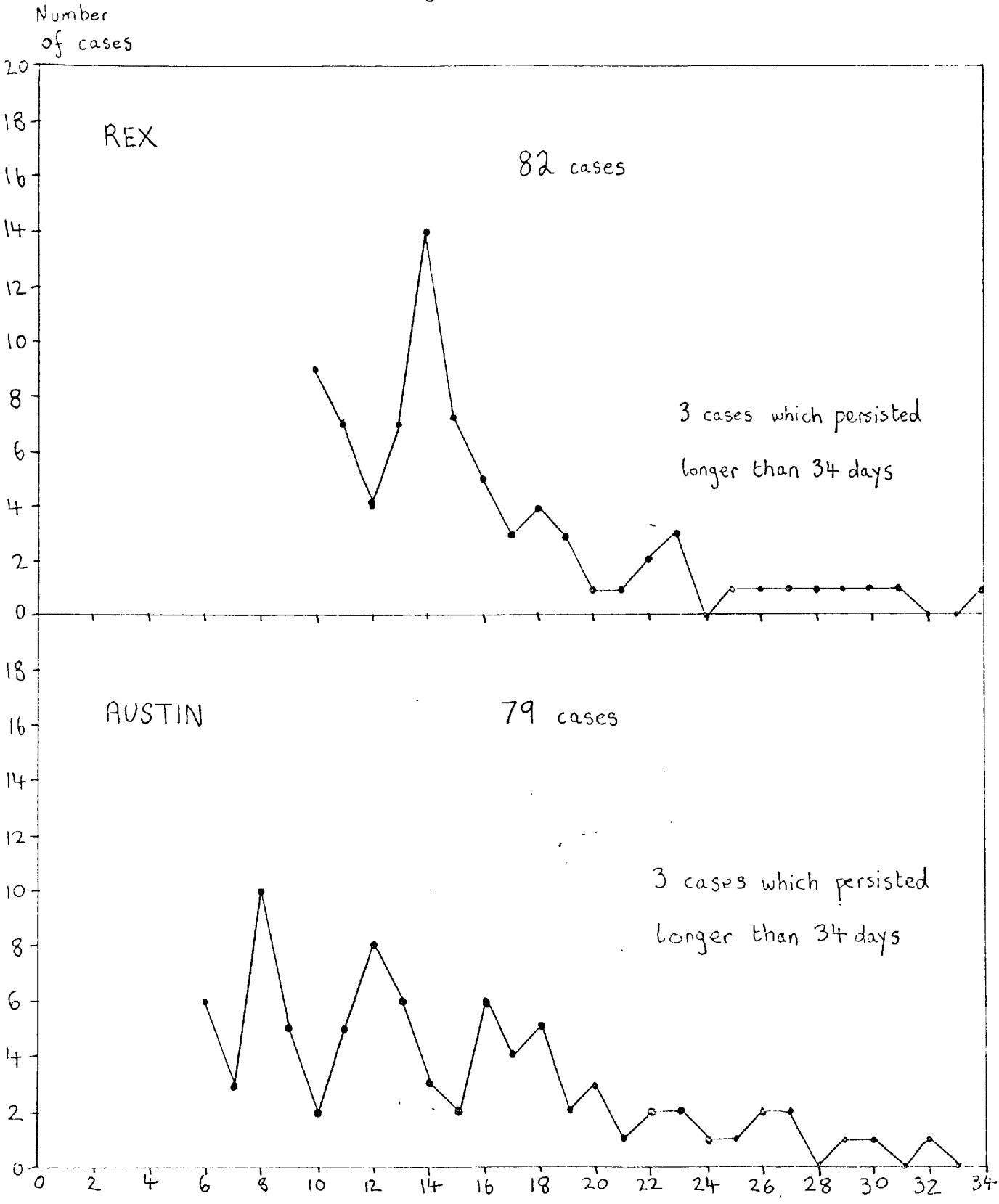
It has been suggested that blocking is associated with the eleven year sunspot cycle, for example by Wexler in 1956. He produced northern hemisphere maps showing prevailing January pressures all over the Arctic during sunspot maximum to be higher than during sunspot minimum in the sunspot cycles between 1900 and 1939. The peak value of this difference was 9.5 mb. near Alaska. More recent data on this topic has been presented by Lamb (1972), from unpublished work by B.N. Parker. This data covers the period 1750 to 1958 and shows that during this period there have been statistically significant surface pressure anomalies associated with certain phases of the sunspot cycle. These anomalies were larger in the winter than in the summer.

1.3 Rotation of the Sun

It has been suggested that the earth's weather may be directly

FIGURE 1(7)

Duration of Blocking in the Atlantic



affected by disturbed regions on the sun, although the mechanism for this has not been established. The approximate 27 day rotation period of the sun about its axis is likely to bring round the same disturbed regions to the central meridian facing the earth at about this interval (27 days) for features near the sun's equator, 28 days near solar latitude $30^{\circ}$, providing the solar disturbance lasts long enough. Therefore, a periodicity of this order may operate from time to time in any terrestrial responses to the solar disturbance. King (private communication) has investigated this possibility using a technique known as super-posed epoch analysis. Key dates, separated by a constant time interval which in this case is 27.5 days, are identified in a run of data. The data is then ''folded over'' on itself to discover if some sequence of events is repeated regularly at intervals of 27.5 days. This technique has several advantages over Fourier Analysis, providing one has some indication of how to choose the key dates. Firstly, it eliminates noise and can reveal the shape of the pulse and its phasing with respect to the key date. Secondly, breaks in the data run do not matter so long as the pattern of key dates is maintained. This enables, for example, successive winters to be analysed together.

Fig. 1(8) shows some of the results of King's analysis of the height of the 500 mb. surface at $70^{\circ}$N for ten winters (1963-1972). The key dates used by King are listed in ''Solar-Terrestrial Physics and Meteorology: Working Document II.'' (1977). The height of the 500 mb. surface relative to the climatic mean is shown as a function of longitude on day 8 and day 22 after the key date. The data shows that the height of the 500 mb. surface changed regularly over the period 27.5 days, with the largest change of 9 dm. at about $0^{\circ}$ long.

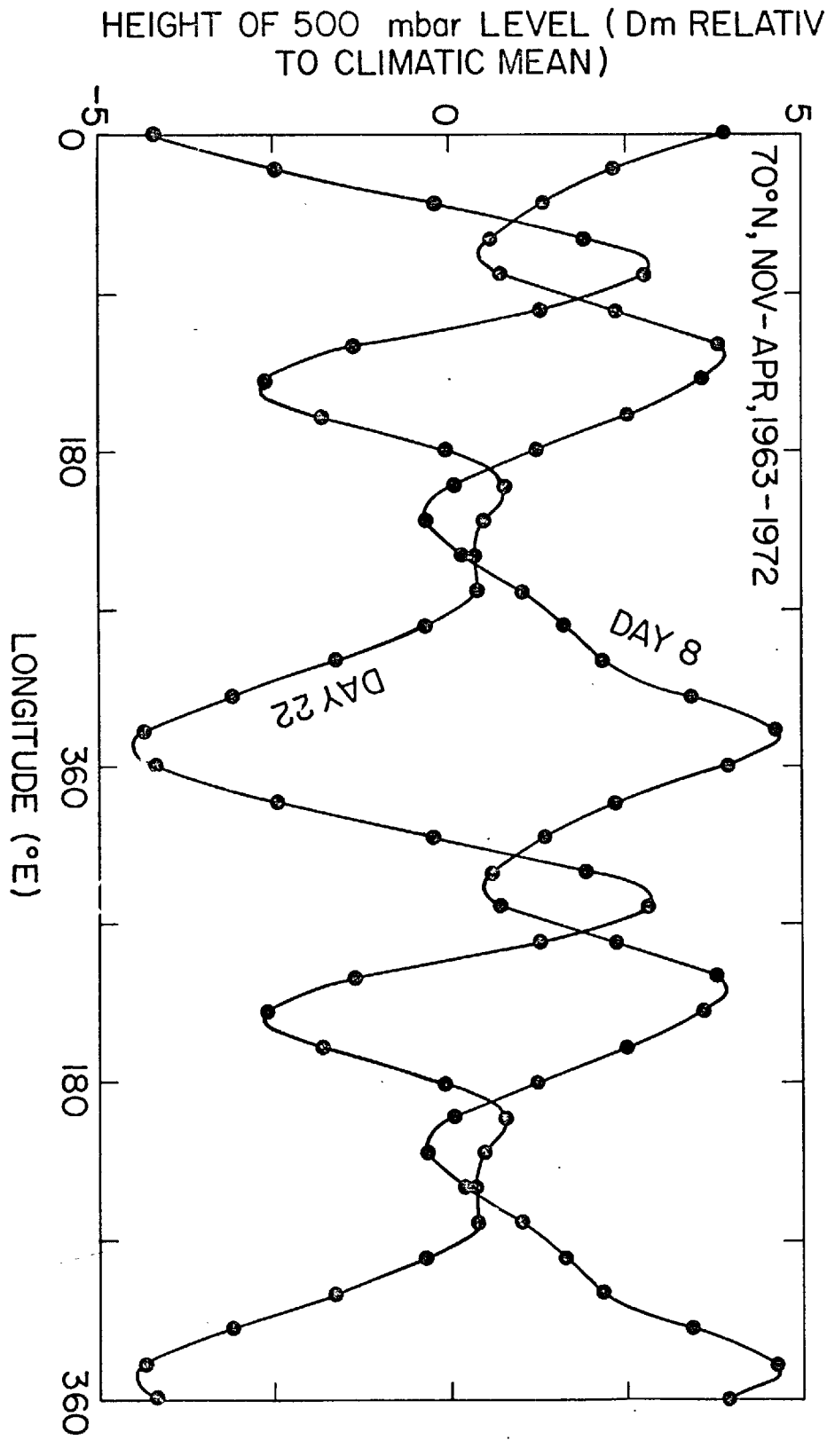

HEIGHT OF 500 mbar LEVEL ( Dm RELATIVE TO CLIMATIC MEAN)
-5
0
5
0
180
360
180
360
LONGITUDE (°E)
70°N, NOV-APR, 1963-1972
DAY 8
DAY 22

Figure 1(8)

The standard deviation of the 500 mb. height at these latitudes is about 20 dm. but, when averaged over about 60 days, this is reduced to $2\frac{1}{2}$ dm. Thus the fluctuations observed by King are of the order of 3 standard deviations at $0^{o}$ long. and cannot be considered the result of random events. These results suggested that blocking in the Atlantic sector should also be modulated by a 27.5 day period. Hence, King (private communication) carried out the same analysis on the blocking dates for the Atlantic sector given in Appendix One.

These results are shown in Fig. 1(9). There is clearly a systematic variation of blocking with a 27.5 day period; the maximum occurence of blocking is 8 days after the key date and the minimum about 25 days after the key date. The magnitude of the modulation is about 10% in 35% and thus is not negligible. (All the actual information is contained in the 27.5 day period following the key date. The repeat patterns emphasise the cycle but contain no additional information. In fact, they can be distorted by ''edge effects'' in short runs of data).

A further very interesting result is shown in Fig. 1(10) and Fig. 1(11). Fig. 1(10) shows that the 27.5 day cycle is far more pronounced in the winter months and accounts for a modulation of about 28% around a mean percentage of 35%. However, this modulation completely disappears in the summer. as shown in Fig. 1(11).

These results are startling and cause one to look at the basic differences between the summer and winter circulations in the troposphere. Surely the most important of these must be the change in the upper boundary condition, provided by the stratospheric winds. In the summer the stratospheric winds are easterly and wave energy is trapped in the troposphere. In winter the stratospheric winds are

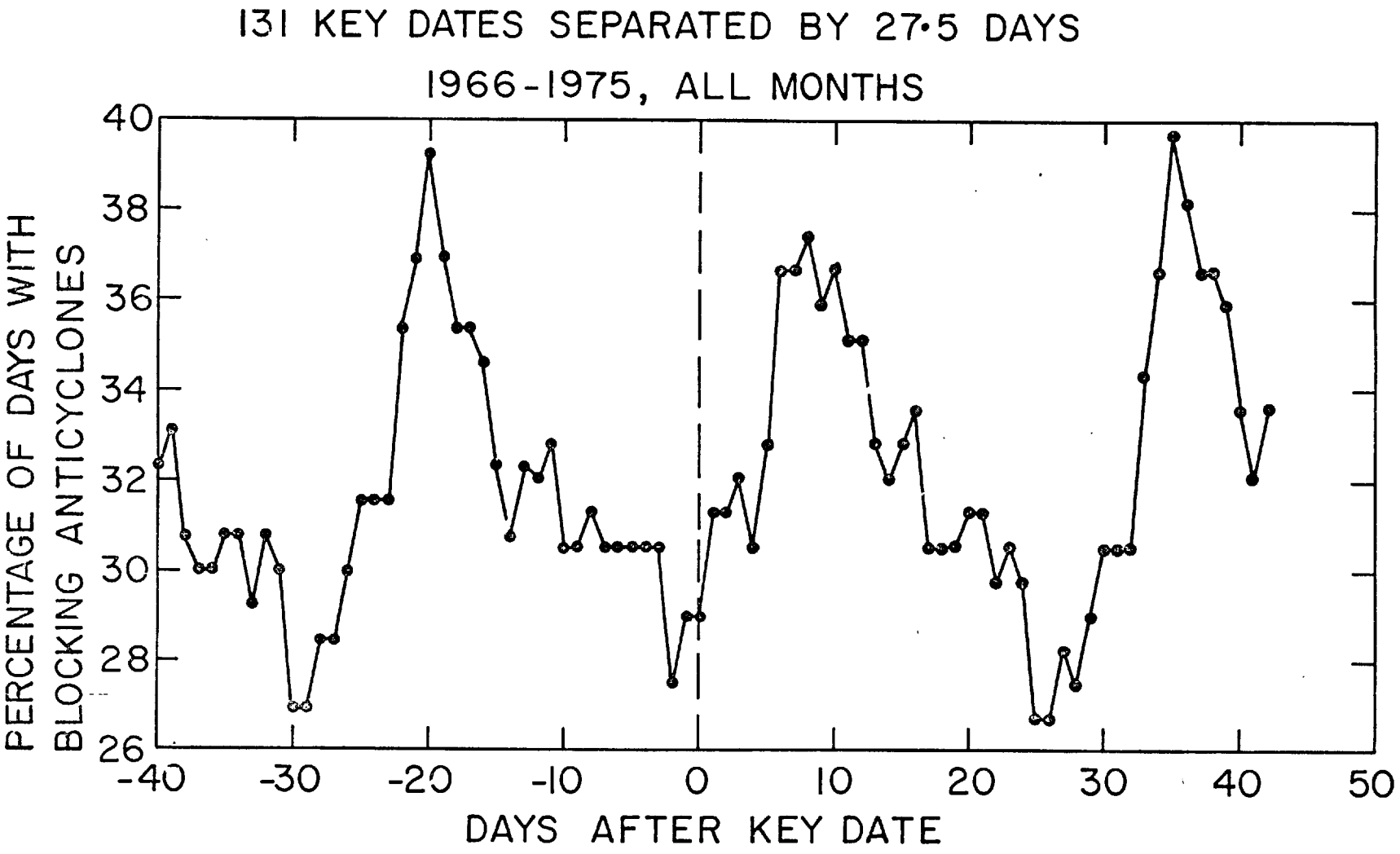

131 KEY DATES SEPARATED BY 27·5 DAYS
1966-1975, ALL MONTHS
PERCENTAGE OF DAYS WITH BLOCKING ANTICYCLONES
40
38
36
34
32
30
28
26
-40
-30
-20
-10
0
10
20
30
40
50
DAYS AFTER KEY DATE

Figure 1(9)

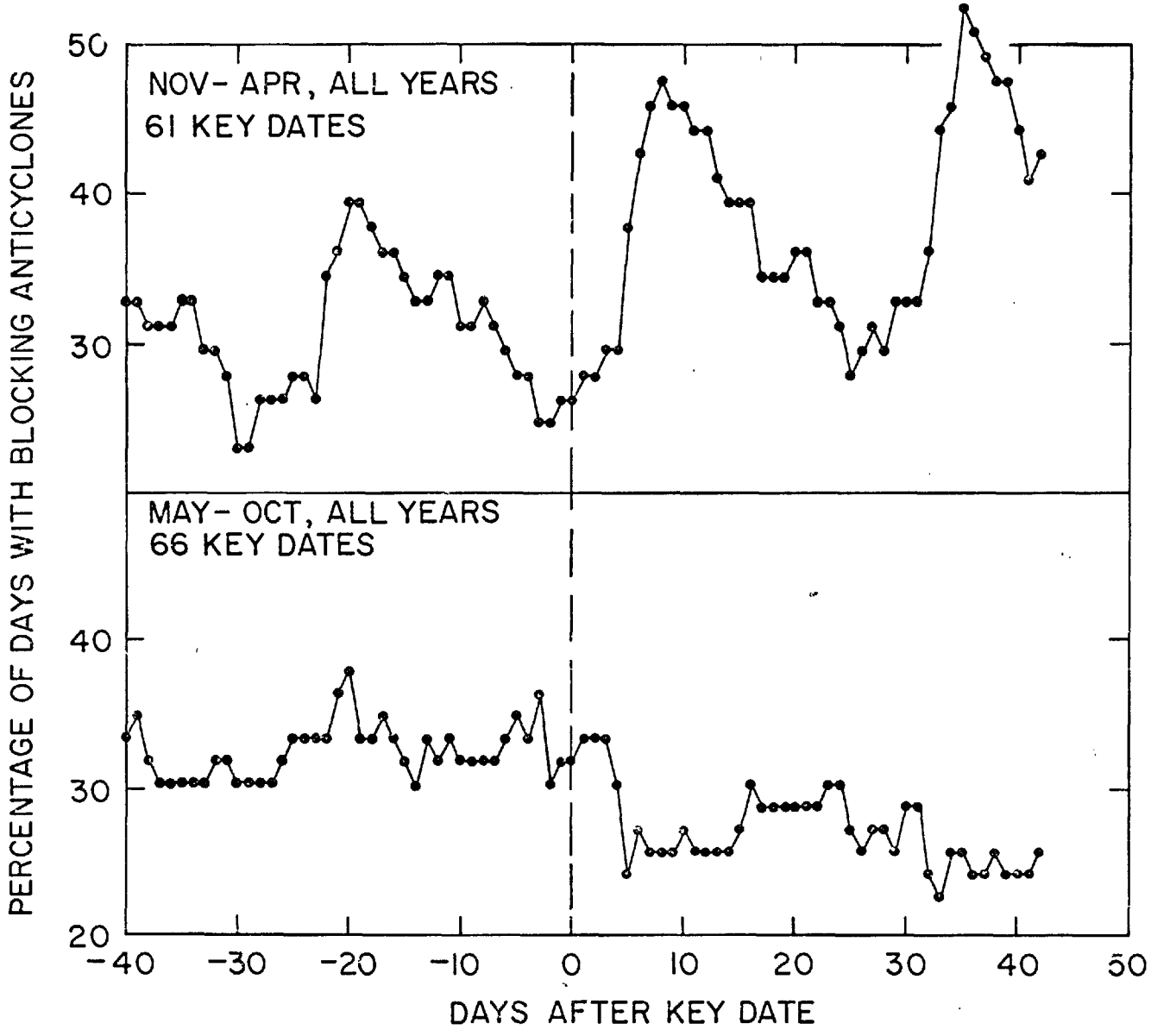



Figure 1(a)

Figure 1(b)

westerly and this allows some very long wave energy to escape, providing a critical wind speed is not exceeded. (These points will be discussed in more detail in Chapter Two). Thus fluctuations in the speed of the easterly flow in the summer will not affect the long waves in the troposphere. However, fluctuations in the speed of the winter westerly jet could have repercussions on the troposphere. A solar disturbance could cause increased ultra-violet radiation to be absorbed by the ozone in the stratosphere, thus producing significant temperature gradients due to the low atmospheric density there. This would then affect the wind speeds through the thermal wind equation. These results are strong evidence that solar events affect the tropospheric flow by acting through the upper boundary condition.

## 1.4 Summary

The main purpose of this survey was to decide on the essential features of blocking which a numerical model should be able to reproduce.

All authors are agreed upon the two preferred locations for blocking anticyclones, namely in the N.E. Pacific and N.E. Atlantic. Thus it is a plausible suggestion that the western coastlines of the continents, with their associated changes in surface temperature and surface friction, may be responsible for producing blocking. However, the fact that blocking is more common in the Atlantic sector than the Pacific sector implies that larger scale influences than just the coastlines may be at work.

It appears that a good theory of blocking should be able to answer the following questions:

1) How can a stationary warm anticyclone be produced and maintained?

2) What large scale conditions are responsible for making these warm stable anticyclones appear in the N.E. Atlantic and N.E. Pacific, and why the Atlantic more than the Pacific?

3) Why does the average position of the blocking anticyclone vary with the time of the year?

4) How can the presence of a stable, warm anticyclone feed back into the very large scales of motion and affect the whole hemispheric circulation?

The evidence is growing that blocking may be linked with, or modulated by, solar events. There is no general agreement on the mechanisms involved, but these solar influences may need to be taken

into account when trying to forecast blocking situations. In particular, a 27.5 day periodicity in blocking in the Atlantic sector appears to be present in the winter. This is probably connected with the 27.5 day rotation period of the sun.

# Chapter TWO

# THE MECHANISMS

## Chapter Two The Mechanisms

### 2.1 Introduction

In attempting to model blocking, the most important feature to reproduce is a stationary perturbation to the zonal flow. However, a good model of blocking should also be able to account for the other main observational features noted in Chapter One. Various mechanisms have been proposed and they can be roughly categorised according to whether the author considers blocking to be an isolated stationary disturbance or an amplified stationary wave.

An example of blocking treated as a localised phenomenon is the hydraulic jump analogue proposed by Rossby (1950) and further investigated by Rex (1950).

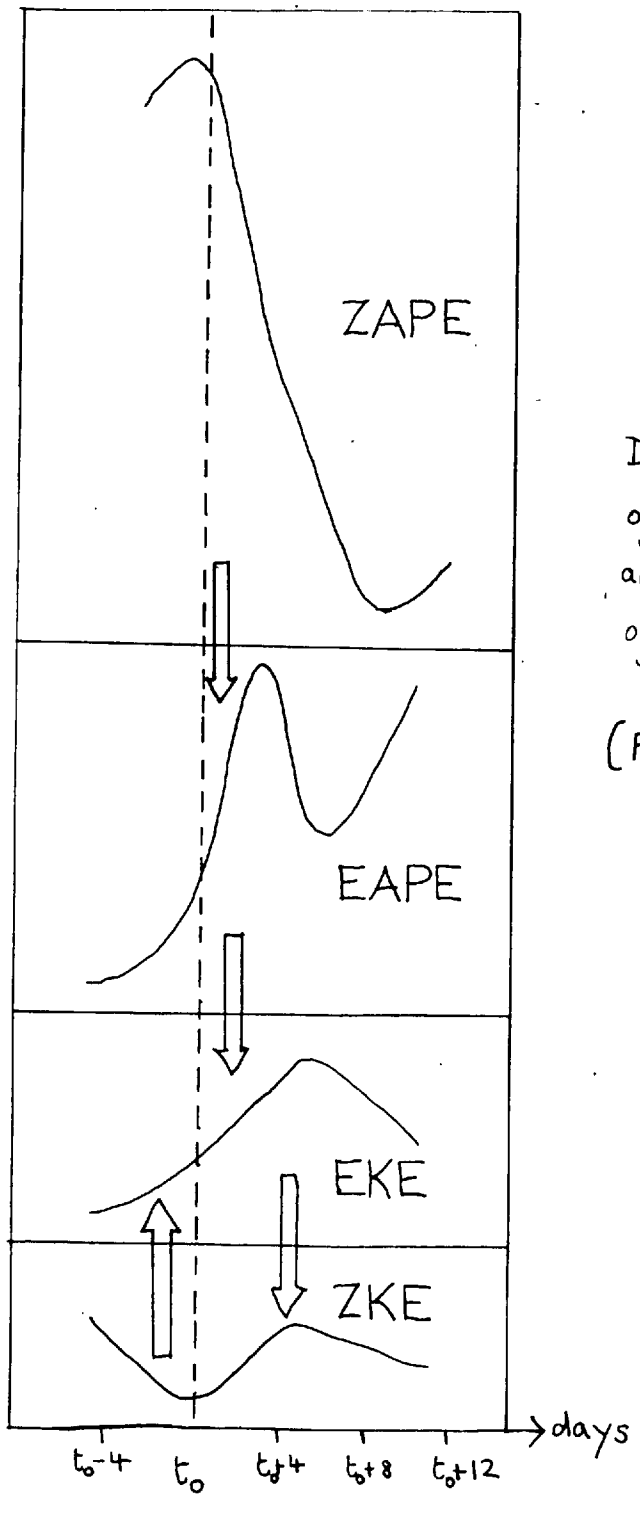
Examples of the ''wave approach'' come from looking at particular instabilities of the zonal flow. One possibility is that the momentum convergence due to baroclinic waves will intensify the jet-stream to the point where it becomes barotropically unstable. Another possibility is that certain surface conditions, such as heat transfer from the oceans, will modify the baroclinic waves themselves so that they form a stationary ''blocking wave''.

A further alternative is to study the properties of the long waves which are produced by the atmosphere flowing over mountains and heat sources and sinks. These waves are known as Rossby waves and although they are neutral in contrast to the instabilities already mentioned, they may resonate under certain conditions.

It has been suggested that a study of the energtics of a blocking situation may reveal the dominant mechanism involved. Lejenäs (1975) summarised results from Winston and Kreuger (1961) and Miyakoda (1963)

Figure 2(1)

Idealised picture of the energy changes and energy transformations during a blocking situation.




Day $t = t_o$ is the onset of the blocking. The arrows indicate the direction of the energy transformations.

(From Lejenäs, 1975)

and presented a diagram (reproduced in Fig. 2(1)) showing an idealised picture of the energy changes and energy transformations during an Atlantic blocking situation. The most striking feature is the very large value of ZAPE at the start of the blocking and its rapid reduction during the subsequent 8 days. This energy is transferred to EAPE and then to EKE during the blocking. The energy transfer ZKE to EKE prior to the blocking lends some support to the barotropic instability theory but the size of the change in ZKE is comparatively very small. Thus the energetics indicates that we should look for a reason why the poleward heat transport has been reduced to such an extent that very large values of ZAPE have built up.

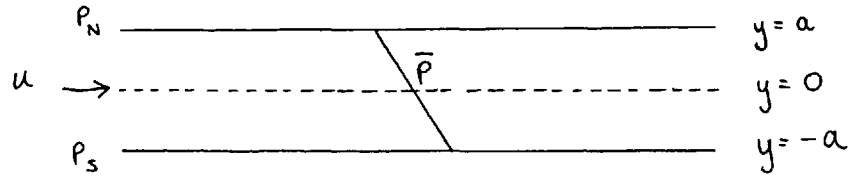
2.2 The Hydraulic Jump

A hydraulic jump can occur in open channels whenever the speed of the water exceeds $\sqrt{gH}$, which is the speed of long surface gravity waves. ($g$ = acceleration due to gravity and $H$ = local depth of the fluid). The development of stationary hydraulic jumps in streams and channels is made possible by the fact that, under steady state conditions, two states of motion are possible. One state is characterised by water speeds less than $\sqrt{gH}$. This can be shown using Bernoulli's equation, mass continuity and the hydrostatic approximation. The momentum flux differs upstream and downstream of the jump and so a pressure gradient is needed across the jump, which is provided by the change in hydrostatic pressure.

In the atmosphere $\sqrt{gH} \sim 10^5$ so the zonal winds would have to exceed about 300 m.s.$^{-1}$ before one might expect to see a hydraulic jump. However, photographs do exist showing apparent hydraulic jumps in flow over ridges; this is probably due to $H$ being significantly decreased by vertical stratification. Rossby effectively

turned the hydraulic jump problem "on its side" for the atmosphere and said that it was the width of the channel, not its depth, which was the critical quantity. His argument can be summarised as follows:

Consider a two dimensional steady current of speed $u$ in the positive $x$ direction, which is constant for $-a < y < a$ and vanishes outside this region. Taking the $x$ direction as easterly and assuming a constant Coriolis parameter $f_o$, then the pressure field $\overline{P}$ which is necessary to balance the motion geostrophically will have a linear cross-current profile.




$$p_s - p_N = \varsigma \int_{-a}^{a} f_o u \, dy$$

$$= \varsigma f_o \int_{-a}^{a} u \, dy$$

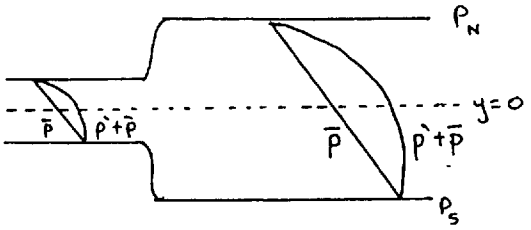
$p$= pressure
$\varsigma$= density

Now let $f = f_o + \beta_y$, where $\beta$ represents the variable part of the Coriolis parameter.

$$p(y) = p_s - \varsigma f_o \int_{-a}^{y} u \, dy - \varsigma \beta \int_{-a}^{y} yu \, dy$$

$$\therefore \hat{p} = \frac{\varsigma \beta (a^2 - y^2) u}{2}$$ where $\hat{p}$ is the additional pressure

distribution due to the presence of $\beta$, assuming the pressure on both boundaries to be unchanged. $p+\bar{p}$ exceeds $\bar{p}$ in magnitude at every point in the current away from the boundaries. Note that $p'$ reaches its maximum value at the centre of the current and that this value is a function of channel width.




$p' \sim 3$mb. from typical values

Convergence of momentum flux acts as a source term in the momentum equation so, in order to find the value of the momentum flux in the x direction, it is necessary to integrate the momentum equation with respect to x. Rossby found the total momentum flux down the channel (after integrating the east-west component of the momentum equation with respect to x and y) to be:

$$\text{Momentum flux} = \left(2au^2 + \frac{\beta u a^3}{3}\right)\rho$$

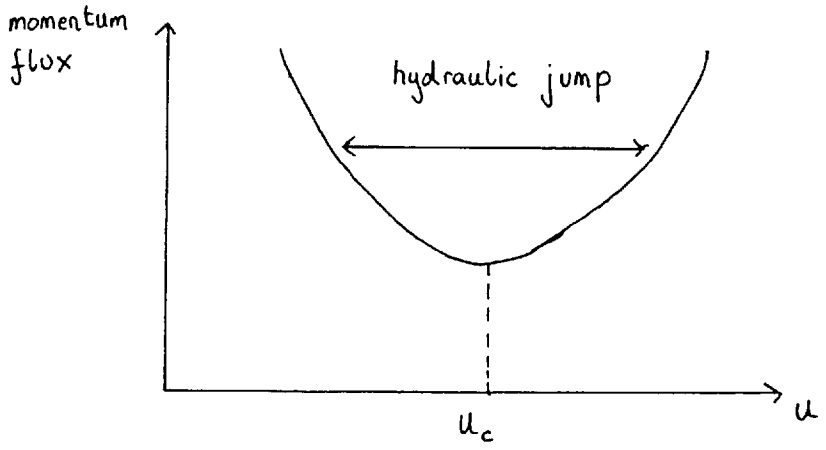
This result depends on the assumption the $\frac{Dv}{Dt}$ (v = velocity in the north-south direction) vanishes in regions of parallel flow outside the blocking zone.

Let $M = 2au\rho$ (mass transport)

$$\text{Momentum flux} = M\left(u + \frac{\beta M^2}{24u^2}\right)$$

For a given value of M, the momentum flux has a minimum value for a critical velocity $U_c$, where

$$U_c = \frac{\beta V^2}{12} \sim 7 \text{ m.s.}^{-1}$$




Thus for a fixed value of mass transport, two possible regimes of super-critical and sub-critical velocities have been established. Hence the hydraulic jump analogue.

This model does seem plausible but there are some objections which can be raised. The lateral boundary conditions seem rather arbitrary, especially as the mutual adjustment of wind and pressure fields depends on the scale of the motion involved. In addition, the usual theoretical model of hydraulic jumps relies on the surface gravity waves being long enough to depend on hydrostatic pressure. These waves are then non-dispersive and move with a velocity $\sqrt{gH}$, which corresponds to the critical velocity of the fluid. The fact that the theory "works" in real fluids implies that this is an important aspect of the flow. The atmosphere, however, is highly dispersive for long waves. It is difficult to see how a hydraulic jump, once formed, could persist in the presence of this dispersion. It may be that this point could be dealt with by extending the problem to include vertical as well as horizontal wavenumbers.

Rex (1950) made an attempt to check Rossby's theory against observations but the results were indeterminate. This was due to the difficulty which Rex experienced in identifying the boundaries of the flow and hence the stream width. It may be that some aspects of the mechanism envisaged by Rossby do exist in the atmosphere but it seems unlikely that they alone are responsible for blocking.

## 2.3 Barotropic Instability

Barotropic instability occurs when the fluid can make use of the available kinetic energy associated with the horizontal shear, as opposed to the available potential energy which is associated with a horizontal temperature gradient. These forms of energy were defined by Lorentz (1955) as follows:

Available kinetic energy is the maximum kinetic energy released when a zonal flow is adjusted so that its angular momentum is kept constant. Available potential energy is the difference between the total potential energy and the minimum achieved by an adiabatic rearrangement of the temperature field which yields a stable horizontal stratification of the potential temperature field. Barotropic instability of the zonal flow can occur when the quantity $(\beta - \frac{\partial^2 \bar{U}}{\partial y^2})$ changes sign. Here $\beta$ is the Coriolis parameter differentiated with respect to $y$ (the NS direction) and $\bar{U}$ is the zonal wind profile.

Investigations into barotropic instability have indicated that it can simulate the early stages of blocking by tending to split a narrow intense jet to form a double jet structure. Wiin-Nielsen (1961) showed in an analytic model that this process was likely to take about $1\frac{1}{2}$ days. He went on to show in a non-linear barotropic model integrated with respect to time that this phenomenon was likely to be periodic in time with a period of about 2 days for initially unstable flows.

However, the zonal flow in middle latitudes is usually barotropically stable. Kane (1973) showed that a typical tropospheric jet stream could make use of the AKE at its edges but that the centre of the jet was dominated by baroclinic processes.

The problem was extended by Lorentz (1972), who examined the

stability of a uniform zonal flow together superposed neutral Rossby waves. He found that the flow was unstable for sufficiently high wavenumber and the momentum convergence produced gave rise to bands of stronger and weaker westerlies in the originally uniform zonal flow. For the amplifying perturbations, the source of energy was the EKE of the basic flow. Lorentz suggested that this mechanism may be instrumental in favouring jets in the atmosphere but it seems unlikely that these results have any relevance to blocking.

## 2.4 Sensible Heat Exchange from the Oceans

White and Clark (1975) carried out a study on blocking in the Pacific Sector for the period 1950 to 1970. However, they only used monthly mean charts so their statistics on location and seasonal occurence of blocks is not very reliable. They did show, however, that there was a negative correlation between the anomalies in the sensible heat flux from the oceans and anomalies in the height of the 700 mb. surface. This lead them to suggest that sensible heat exchange between the ocean and the atmosphere was an important mechanisms in the formation of a blocking ridge.

The mechanism envisaged was that for representative values of the vertical wind shear, the very long waves (7,000 km. or more) would be destabilized by diabatic heating which parameterized exchange of heat with a lower boundary. These waves would normally be stable in the absence of such heat exchange. As theoretical support for this suggestion, the authors quote results from a two-layer $\beta$ plane baroclinic instability model by Haltiner (1967). Haltiner showed that the long waves were destabilised by a diabatic heating term which was essentially similar to the Newtonian cooling law and that these long waves had their phase speeds reduced until they were practically

stationary.

There are a number of objections which can be made to the conclusions of White and Clark. First of all, the anomalous heating patterns in the Pacific were on a space scale of about 2000 km. which was considerably less than the wavelength which was apparently destabilised. Secondly, the assumption that there was an infinite North-South wavelength was obviously a very poor approximation. Finally, it has been pointed out by Geisler (1977) that the destabilisation of long waves by Newtonian cooling in a two-layer baroclinic model is not a feature of baroclinic instability in a continously stratified fluid. Geisler showed that, in a continuously stratified model in the presence of realistic Newtonian cooling, the very long waves were stable and the phase speeds were virtually unchanged.

Therefore, although sea surface temperature anomalies probably do influence the general circulation of the atmosphere, it seems most unlikely that their affect on baroclinic instability is the relevant mechanism.

## 2.5 Rossby Waves (Topographic Forcing)

Long neutral waves are produced in the atmosphere due to flow over topography. It was pointed out by Rossby (1939) that these long waves are dispersive, having a phase speed $c$ in a non-divergent atmosphere.

$$c = \bar{U} - \frac{\beta}{k^2}$$

for a wave with East-West wavenumber $k$ in a constant zonal flow $\bar{U}$ on a $\beta$ plane. Thus when $\beta = \bar{U}k^2$ the wave is stationary with respect to the ground. Since the time of Rossby's formulation it has been found necessary to take divergence into account in order to predict

realistic phase speeds for the very long waves. A further examination of stationary Rossby waves is necessary to see whether they are responsible for blocking.

This approach does seem promising because results from numerical models have definitely indicated that blocking only occurs in general circulation models in the presence of mountains and/or land-sea distributions. [See Kikuchi (1968) and Lejenäs (1975)]. However, there is a problem with how blocking is defined in the various models. An example of a misleading use of the term can be found in a study by Everson and Davies (1970). They carried out some general circulation studies and stated that there was no blocking of the baroclinic flow systems when topography was absent. They then introduced a simple land/sea temperature contrast in the model and claimed that some quite realistic blocking situations were produced. However, what the model actually produced was a cold stationary anticyclone over the land - in short a Siberian anticyclone. As was pointed out in Chapter One, this is quite distinct from a warm blocking high.

The effect of topography on the zonal flow can be examined at its simplest level using the quasigeostrophic potential vorticity equation applied to flow in a channel on a β-plane. Briefly, this equation is derived as follows:

Using cartesian geometry with the x axis in an easterly direction.

$u$ = easterly component of velocity $\underset{\sim}{v}$

= northerly component of velocity $\underset{\sim}{v}$

$w$ = vertical component of veclocity $\underset{\sim}{v}$

$$\frac{D}{Dt} = \frac{\partial}{\partial t} + \underset{\sim}{v} \cdot \nabla$$

$$\frac{D}{Dt_h} = \frac{\partial}{\partial t} + u\frac{\partial}{\partial x} + v\frac{\partial}{\partial y}$$

$f$ = Coriolis parameter $= f_0 + \beta y$

$\beta = \frac{\partial f}{\partial y}$

$\zeta$ = vertical component of vorticity

$\phi$ = entropy

$\rho$ = density

$p$ = pressure

By scale analysis the vertical component of the vorticity equation is reduced to:

$$\frac{D}{Dt_h}\zeta + v\beta = \frac{f_0}{\rho}\frac{\partial}{\partial z}(\rho w)$$

where $f$ is held constant in the vortex stretching term in order that there is no spurious generation of vorticity. Vertical advection, twisting, stretching of relative vorticity and baroclinic generation of vorticity and friction are ignored.

The conservation of entropy is expressed as:

$\frac{D}{Dt}\phi = S$ where $S$ is a source term

To a very good approximation:

$\phi = \overline{\phi}(z) + \phi'(x,y,z,t)$ where $\phi'$ is a perturbation quantity and

$\frac{d\overline{\phi}}{dz} = B(z)$ (static stability)

$\therefore \frac{D}{Dt}\phi' + wB = S$ (thermodynamic equation)

For flow with the Rossby number much less than unity and the Richardson

number much greater than the inverse of the Rossby number, the horizontal wind is approximated by the non-divergent part of the real wind and a stream-function $\psi$ is defined by:

$$u = -\frac{\partial \psi}{\partial y} \quad , \quad v = \frac{\partial \psi}{\partial x}$$

$$\therefore \underset{\sim}{v}_h = \underset{\sim}{k} \wedge \nabla_h \psi$$

The thermal wind relationship is given by:

$$\frac{\partial \underset{\sim}{v}_h}{\partial z} = \frac{g}{f_o} \underset{\sim}{k} \wedge \nabla_h \phi$$

$$= \frac{g}{f_o} \underset{\sim}{k} \wedge \nabla_h \phi' \quad \text{as} \quad \phi = \bar{\phi}(z) + \phi'$$

$$\therefore \phi' = \frac{f_o}{g} \frac{\partial \psi}{\partial z} \quad \text{and} \quad \zeta = \nabla_h^2 \psi$$

Using the thermodynamic equation to eliminate W from the vorticity equation yields the quasi-geostrophic potential vorticity equation. (Q G PV equation)

$$\frac{D}{Dt_h}\left[\nabla_h^2 \psi + \beta y + \frac{f_o^2}{\varsigma} \frac{\partial}{\partial z}\left(\frac{\varsigma}{B} \frac{\partial \psi}{\partial z}\right)\right] = \frac{f_o}{\varsigma} \frac{\partial}{\partial z}\left(\frac{\varsigma S}{B}\right) \qquad \text{Equation 2(i)}$$

This is a standard equation for mid-latitude flow with constant $f_o$ and, given appropriate boundary conditions, consistent energetics. It is

convenient to linearise it about a basic state stream function $\bar{\psi}$ , where

$$\psi = \bar{\psi} + \psi'$$
$$= -\bar{u}y + \psi'$$

$\bar{U}$ is taken as a constant here so that simple analytic solutions can be obtained. The first-order equation then becomes: (B constant)

$$\left(\frac{\partial}{\partial t} + \bar{u}\frac{\partial}{\partial x}\right)\left[\nabla_h^2\psi' + \frac{f_o^2}{\rho g B}\frac{\partial}{\partial z}\left(\rho\frac{\partial\psi'}{\partial z}\right)\right] + \beta\frac{\partial\psi'}{\partial x} = \frac{f_o}{gB}\frac{\partial}{\partial z}(\rho S)$$

Equation 2(ii)

In the above equation B has been taken as a constant for algebraic simplicity but this will not seriously affect the nature of the solutions. The effect of $\rho$ decreasing with height is to amplify the motion with height so that the energy density of the wave (amplitude x $\rho^{\frac{1}{2}}$) is a constant.

Choosing stationary solutions of the form:

$$\psi' = Re\left\{F(z)\, e^{ikx} \cos\mu y\right\}$$

Re = real part

and rearranging gives an equation for the complex height structure F(z).

$$\frac{d^2F}{dz^2} - \frac{1}{H_o}\frac{dF}{dz} + \frac{gB}{f_o^2}\left(\frac{\beta}{\bar{u}} - (k^2+\mu^2)\right)F = 0$$

where $\rho$ is taken as $\rho = \rho_o e^{-z/H_o}$

This allows a solution:

$$F(z) = \left[ C_1 \exp(i\nu z) + C_2 \exp(-i\nu z) \right] \exp\left[ \frac{z}{2H_0} \right]$$

with $\nu^2 + \frac{1}{4H_0^2} = \frac{g\beta}{f_0^2} \left[ \frac{\beta}{\bar{u}} - (k^2 + \mu^2) \right]$ and $C_1$, $C_2$ are constants.

If parameters are chosen such that $\nu^2 < 0$ then

$$F(z) = \left[ C_1 \exp(-|\nu| z) + C_2 \exp(|\nu| z) \right] \exp\left[ \frac{z}{2H_0} \right]$$

and it would be natural to accept the bounded mode only (put $C_2 = 0$) in an infinite atmosphere. When $\nu^2 > 0$, the choice of wave mode is less obvious with both waves having bounded specific kinetic energy at infinity.

Setting $C_1$ to zero given an eastward tilting system with height of troughs and ridges and westward tilting wave results from putting $C_2$ equal to zero. The choice ultimately depends on the direction of energy propagation in the real atmosphere, because the component

$$C_1 \exp\left[ i(kx + \nu z) + \frac{z}{2H_0} \right]$$

corresponds to pure upward energy propagation and the other to pure downward energy propagation. This can be shown by calculating the horizontally averaged pressure work term $\overline{p' w'}^{x,y}$, since if this is positive then the atmosphere below a certain level is doing work on the atmosphere above.

The observations of large scale planetary waves show strong westward tilt with height and observations have confirmed that this corresponds to upward energy propagation. (See McNulty, 1976).

Upward energy propagation in stationary wave systems can only

occur when $\lambda^2 > 0$ and Charney and Drazin (1961) showed how this imposed a condition on the zonal wind speed $\bar{U}$ such that propagation was only possible if

$$0 < \bar{u} < \frac{\beta}{\left[(k^2+\mu^2) + \frac{f_o^2}{4gBH_o^2}\right]} = U_c \qquad \text{(critical wind speed)}$$

Equation 2(iii)

Thus stationary Rossby waves propagate wave energy upwards only when the zonal mean winds are westerly and less than some upper bound. That this should be the case is borne out to a large extent by the fact that there are large stationary wave disturbances in the wintertime stratosphere circulation, but none in the summer stratospheric easterlies. Wave energy is unable to penetrate far into the easterlies and hence the amplitude dies away rapidly with height. Charney and Drazin concluded that for typical values of $k$ and $\mu$, all waves would eventually be reflected by the strong polar night westerlies at some height by a local application of equation 2(iii).

This raises the question of what sort of upper boundary condition is appropriate when modelling large scale planetary waves. A common upper boundary condition is a ''lid'' approximation at the tropopause, which is justified in baroclinic instability studies because the fastest growing baroclinic waves are on a scale which is rapidly damped with height in the stratosphere. Shutts (1976), using the linearised QGPV equation, studied the reflective properties of the interface between two unbounded regions of different zonal winds and different static stabilities. He found that the reflection of wave

energy was much more sensitive to changes in zonal wind across the interface than to changes in static stability. He concluded that perfect energy-reflecting upper boundary conditions, such as rigid lids or free surfaces, were quite inappropriate for very long waves. These results are in accord with summarised obervations from Green (1972), which showed that the specific kinetic energy of the January mean eddy motion at $50^{o}$N remained roughly constant up to 40 or 50 km, above which it rapidly decreased. This is probably due to strong electromagnetic damping in the upper stratosphere which causes the energy to be radiated away into space.

The upper boundary condition on the flow in the real atmosphere and in numerical models is of great importance because it determines whether or not wave resonance is possible. This point can be illustrated using the linearised QGPV equation 2(ii) and orographic forcing. Ignoring compressibility for simplicity, ie $H_o = \infty$

Choose a mountain profile $z_o = \mathrm{Re}\left\{ae^{ikx} \cos \mu y\right\}$

Then the lower boundary conditions is $\frac{D}{Dt}(z - z_o) = 0.$

When linearised this becomes:

$$W\Big|_{z=o} = \mathrm{Re}\left\{\bar{U} \frac{\partial z_o}{\partial x}\right\}$$

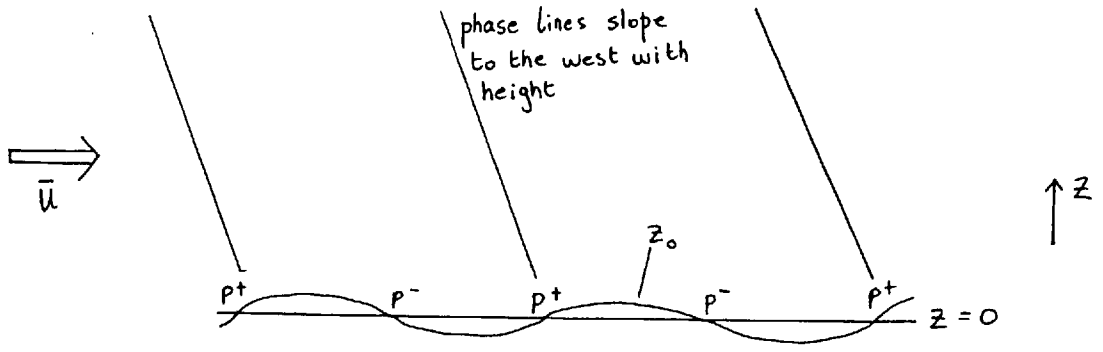
Set $S = 0$, ie pure adiabatic motion, and take the solution to equation 2(ii) which corresponds to upward energy propagation.

$$\psi' = \mathrm{Re}\left\{A \exp i(kx + \ell z)\right\} \cos \mu y$$

Using the lower boundary condition to find A yields

$$\psi' = -\frac{agB}{f_o \nu} \sin(kx + \nu z) \cos ly$$

Note that at $z = 0$, $\psi'$ and $z_o$ are $\frac{\pi}{2}$ out of phase, with $\psi'_{max}$ (and hence $p'$ max as $p' = f_o g \psi'$ from the geostrophic wind relation) on the upward slope.




Thus the waves exert a drag on the orography given by $\overline{p' \frac{\partial z_o}{\partial x}}^{x}$ which is comparable with the global average of surface friction of about 0.03 $Nm^{-2}$. (ie taking into account westerlies and easterlies).

In order to calculate various flux terms, the following typical values are used:

a ~ 200m

k ~ $2\pi/15{,}000$ km (wavenumber two)

$\bar{U}$ ~ 10 $ms^{-1}$

gB ~ $3 \times 10^{-4}$ $s^{-2}$

$\nu$ ~ $\frac{2\pi}{40 \text{ km}}$

The latitudinally averaged pressure work term is given by:

$$\overline{p' w}^{x,y} = \frac{1}{4} \frac{a^2 g \bar{u} k g B}{\nu}$$

$$\sim 0.1 \text{ watts}/m^2 \text{ of upward energy propagation}$$

Westward tilting waves in geostrophic and hydrostatic balance transport entropy polewards, as can be inferred from:

$$\overline{\rho' w'}^{x,y} = \frac{\rho f_0 \bar{u}}{B} \overline{v' \phi'}^{x,y}$$

This gives a value for the poleward heat transport

$$\overline{\rho C_v v' T'}^{x,y} = 2{\cdot}5 \times 10^{3} \ W.m^{-2}$$
$$\sim 1{\cdot}7 \ S_0$$

where $\phi' \sim \frac{T'}{\bar{T}}$ ($\bar{T} = 250$ K) and $S_0$ = solar constant. Since the total poleward heat flux required to offset the radiational imbalance of heating is about 6 solar constants, there is good reason to believe that untrapped stationary wave heat transport is an important component of the total poleward transport of heat.

The results yielded by these simple calculations are in good agreement with more realistic analysès done on a sphere with vertical wind shear by Shutts (1976) and with observations on stationary eddies (Oort and Rasmussen, (1971)).

Now consider the same problem solved with a ''rigid lid'' as an upper boundary condition. That is to say:

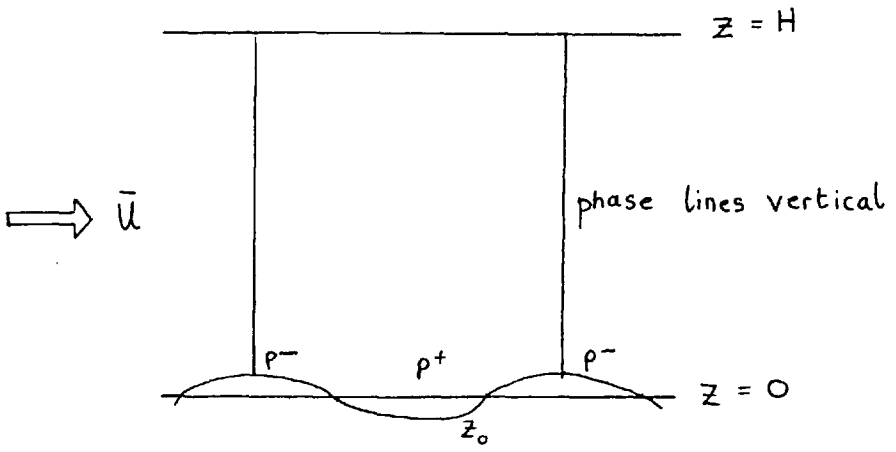
$$w = 0 \quad \text{at} \quad z = H \quad \text{and} \quad w = Re\left\{ \bar{u} \frac{\partial z_0}{\partial x} \right\} \quad \text{at} \quad z = 0$$

$$\psi' = Re\left\{ A^* e^{i(kx + \nu z)} + B^* e^{i(kx - \nu z)} \right\} \cos \mu y$$

Solving for $A^*$ and $B^*$ yields:

$$\psi' = -\frac{agB}{f\nu}\,\frac{\cos\nu(z-H)\cos kx\cos My}{\sin \nu H}$$

So, with a "lid", the phase lines are vertical and $\psi'$ (hence p') is in phase with $z_o$ at all heights.




Now $\overline{p'w}^{x} = 0$ and so there is no upward energy flux and no poleward heat transport. The surface phase of $\psi'$ has moved by $\pi/2$ with respect to the surface phase of the propagating mode and one consequence of this is that there is no longer any wave drag.

Another point to note is that in the trapped mode infinite resonances are possible for $\nu = \frac{n\pi}{H}$ for n = 0, 1, 2- - - -
It is not obvious that resonances will be possible when vertical wind shear is present because $\nu$ becomes a function of height. However, Shutts (1976) showed that trapped long waves can resonate in a vertical shear.

It has already been shown that upward energy propagation is only possible if

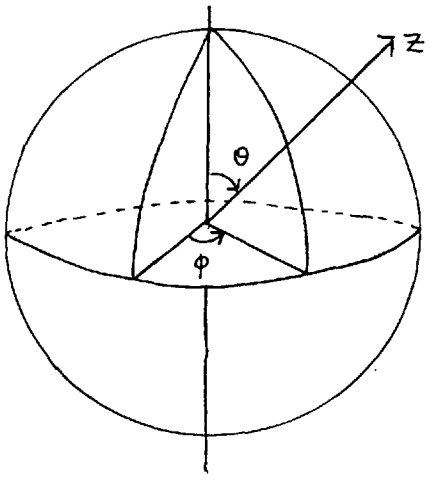
$$0 < \overline{U} < \overline{U}_c$$

Thus it is possible that if $\overline{U}$ lies outside these limits, then the upper boundary condition will effectively become a lid and the long waves will exhibit the characteristics of trapped waves, rather than vertically propagating waves. This means that the surface phase of the wave will shift with respect to the forcing and resonances may be possible.

What are the critical wind speeds for very long waves? It is unrealistic to use a $\beta$-plane approximation to calculate these so a transformation to spherical geometry is needed first.

Transformation to Spherical Geometry

The transformation from the rectangular cartesian coordinate system $(x,y,z)$ to the spherical coordinate system $(\phi, \theta, z)$ is made.




In contrast to the $\beta$ plane analysis the full variation of the Coriolis parameter is permitted in the absolute vorticity, though again a mid-latitude value is assumed in association with the stretching term and to derive the pressure from the geostrophic wind equation.

The QGPV equation is found to be:

$$\frac{D}{Dt_h}\left[\nabla_h^2\psi + 2\Omega\cos\theta + \frac{f_0}{S}\frac{\partial}{\partial z}\left(\frac{\rho}{B}\phi'\right)\right] = \frac{f_0}{S}\frac{\partial}{\partial z}\left(\frac{\rho}{B}S\right) \qquad \text{Equation 2(iv)}$$

where S is a thermodynamic source term. All symbols have the same meaning as before and $\Omega$ is the angular rotation rate of the earth. The gradient operator for scalars in spherical curvilinear coordinates is given by:

$$\underset{\sim}{\nabla} = \frac{\hat{\phi}}{R\sin\theta}\frac{\partial}{\partial\phi} + \frac{\hat{\theta}}{R}\frac{\partial}{\partial\theta} + \hat{k}\frac{\partial}{\partial z}$$

where $\hat{\phi}$, $\hat{\theta}$, and $\hat{k}$ form an orthonormal triad pointing eastward, southward and upward respectively and R = radius of the earth. Linearising Equation 2(iv) about an atmosphere in differential solid rotation for small stationary perturbations so that:

$$\psi = -\bar{\psi}(z)\cos\theta + \psi'(\theta,\phi,z)$$

and $$\bar{u}(\theta,z) = \frac{\sin\theta}{R}\bar{\psi}(z)$$

gives after algebraic manipulation

$$\frac{\bar{\psi}}{R^2}\frac{\partial}{\partial\phi}\left\{\frac{1}{R^2\sin\theta}\left[\frac{\partial}{\partial\theta}\left(\sin\theta\frac{\partial\psi'}{\partial\theta}\right)+\frac{1}{\sin\theta}\frac{\partial^2\psi'}{\partial\phi^2}\right] + \frac{f_0^2}{g\rho}\frac{\partial}{\partial z}\left(\frac{\rho_0}{B}\frac{\partial\psi'}{\partial z}\right)\right\}$$

$$+\frac{1}{R^2}\frac{\partial\psi'}{\partial\phi}\left\{\frac{2\bar{\psi}}{R^2} + 2\Omega - \frac{f_0^2}{g\rho}\frac{d}{dz}\left(\frac{\rho}{B}\frac{d\bar{\psi}}{dz}\right)\right\} = \frac{f_0}{S}\frac{\partial}{\partial z}\left(\frac{\rho S}{B}\right)$$

Assuming a separation of variables by writing:

$$\psi' = Re\left\{ F(z)\,\Theta(\theta)\,\exp(im\phi)\right\}$$

$$S = Re\left\{-i\,S_0(z)\,\Theta(\theta)\,\exp(im\phi)\right\}$$

and substitution in the linearised potential vorticity equation leads to:

$$\frac{\left\{\frac{d}{d\theta}\left(\sin\theta\,\frac{d\Theta}{d\theta}\right)-\frac{m^2}{\sin\theta}\,\Theta\right\}}{R^4\,\Theta\sin\theta} = \frac{f_0^2}{g\,R^2\varsigma}\frac{d}{dz}\left(\frac{\varsigma}{B}\frac{dF}{dz}\right)\frac{1}{F}$$

$$-\frac{1}{\bar\psi R^2}\left\{2\left(\Omega+\frac{\bar\psi}{R^2}\right)-\frac{f_0^2}{g\varsigma}\frac{d}{dz}\left(\frac{\varsigma}{B}\frac{d\bar\psi}{dz}\right)\right\}-\frac{f_0}{mg\,\bar\psi F}\frac{d}{dz}\left(\frac{\varsigma}{B}\,S_0\right)$$

The left hand side of the equation is a function of $\theta$ alone and the right hand side of $z$ alone, therefore:

$$\frac{1}{R^4\Theta\sin\theta}\left\{\frac{d}{d\theta}\left(\sin\theta\frac{d\Theta}{d\theta}\right)-\frac{m^2}{\sin\theta}\,\Theta\right\} = \alpha \quad \text{(a constant)}$$

Using the transformation $P = \cos\theta$ we obtain:

$$\frac{d}{dP}\left\{(1-P^2)\frac{d\Theta}{dP}\right\}+\left\{n(n+1)-\frac{m^2}{1-P^2}\right\}\Theta = 0$$

if $\quad \alpha R^4 = -n(n+1)$

This equation has solutions $\Theta(\cos\theta) = P_n^m(\cos\theta)$ which are associated Legendre polynomials and exist only for $n \geq m$, when $\Theta$ is non-singular at $P = \pm 1$.

The equation for the complex vertical structure F(z) becomes:

$$\frac{d^2F}{dz^2} + \frac{B}{\rho}\frac{d}{dz}\left(\frac{\rho}{B}\right)\frac{dF}{dz} + \frac{gB}{f_o^2}\left[\frac{2\Omega}{\bar{\psi}} - \frac{f_o^2}{\rho g}\frac{1}{\bar{\psi}}\frac{d}{dz}\left(\frac{\rho}{B}\frac{d\bar{\psi}}{dz}\right) - \frac{(n-1)(n+2)}{R^2}\right]F$$

$$= -\frac{gBR^2}{fm\bar{\psi}\rho}\frac{d}{dz}\left(\frac{\rho S_o}{B}\right) \qquad \text{Equation 2(v)}$$

For adiabatic motion of an atmosphere in solid rotation which is uniformly stratified, equation 2(v) reduces to:

$$\frac{d^2F}{dz^2} - \frac{1}{H_o}\frac{dF}{dz} + \frac{gB}{f_o^2}\left[\frac{2\Omega}{\bar{\psi}} - \frac{(n-1)(n+2)}{R^2}\right]F = 0 \qquad \text{Equation 2(vi)}$$

Comparing this vertical structure equation with the corresponding one for constant zonal flow in cartesian geometry shows that the only change is the replacement of the total horizontal wavenumber squared $(k^2 + \mu^2)$ by $\frac{(n-1)(n+1)}{R^2}$.

Shutts (1976) pointed out that the Charney-Drazin derivation of this equation omits the term $\frac{2\bar{\psi}}{R^4}\frac{\partial\psi'}{\partial\phi}$, which represents the eddy poleward advection of the potential vorticity of the mean flow. Consequently, their interpretation of $(k^2 + \mu^2)$ in the transformation to spherical geometry becomes $\frac{n(n+1)}{R^2}$ which is significantly larger only for very small n (n = 1, 2 and 3). Although the horizontal structure is represented by Legendre functions of global extent, the arguments are only strictly valid for one hemisphere because of the mid-latitude value of the Coriolis parameter. Therefore only wave modes which vanish at the equator will be considered for further study. This is true for all modes satisfying the condition (n-m) = an odd integer, e.g. $P_2^1$,

$P_3^2$, $P_4^3$ for the first three zonal wavenumbers. Typical values used by Charney and Drazin for $(k^2 + \mu^2)$ were $10^{-12}$ and $4 \times 10^{-13}$ m.$^{-2}$ and these lead to critical zonal wind speeds $\bar{U}_c$ of 15 and 32 m.s.$^{-1}$. For spherical harmonic modes $n = 2$ and $n = 3$, the equivalent total square wavenumbers from Shutt's derivation are $10^{-13}$ and $2.5 \times 10^{-13}$ m.$^{-2}$ which lead to average critical zonal wind speeds of 80m.s.$^{-1}$ and 46 m.s.$^{-1}$. Hence the largest scale waves associated with $n = 2$ and $n = 3$ can propagate up into much stronger zonal westerlies than the Charney–Drazin analysis suggested. Thus the $P_2^1(\cos\theta)$ mode should be able to penetrate the whole depth of the mesosphere up to the region where energy dissipation takes place; this may be due to electromagnetic damping and/or wave–mean flow interactions.

Thus it does seem likely that unrealistic modelling of the general circulation may be due to an incorrect, energy-reflecting upper boundary condition. Shutts (1976) made this point as follows: "Evidence of this type of modelling deficiency can be inferred from the results of numerical simulations of the stratosphere. The 11 - level model of the circulation of the stratosphere used by Mahlam and Manabe (1972) was unsuccessful in the description of the mean zonal wind and temperature structure, with winds too strong by a factor of two and polar night temperatures colder than observed by 25 - 30 K. Planetary wave transfer of heat is the dominant mechanism offsetting th polar cooling of the stratosphere in winter (Green 1972) and the absence of this transport process (through the forced reflection of energy at 10 mb.) could account for the coldness there. Thermal wind balance demands that the shear should be greater there and hence excessive zonal wind speeds result. The effect of spurious energy reflection could also seriously upset the troposheric circulation through the reduced stationary wave

transport of heat and build-up of wave energy. Numerical modellers frequently complain of ''excessive blocking'' in weather prediction schemes and it is quite possible for this to be a manifestation of the forced trapping of waves and their resonant behaviour. The treatment of large scale forced waves in climate models presents a formidable problem to the modeller with the tropospheric wave motion suffering considerable distortion in the absence of a realistic stratosphere.''

Notice again the loose usage of ther term blocking when applied to numerical models. It has yet to be proved that wave-trapping in numerical models has anything to do with blocking as described by the observations in Chapter One.

Bypassing for the moment the question of whether blocking is due to wave-trapping or not, a definite advantage in looking at stationary Rossby waves is that one can consider the interference patterns between waves as well as the isolated waves themselves. This approach can then account for the apparently isolated nature of blocking highs, while allowing for the existence of planetary scale waves.

In Fig 2(2) the positions of the long waves at 500 mb, as a function of latitude on a normal January chart are shown (Eliasen 1958). Eliasen's harmonic analyses of normal charts are listed in Appendix Three. A normal January chart means the average of a number of mean January flow charts and it seems reasonable to identify the waves on it with the mean position of stationary Rossby waves in the January circulation. Note that between $50^{\circ}N$ and $60^{\circ}N$ wavenumbers one and two tend to interfere constructively in the sector $0^{\circ}$ to $40^{\circ}E$ and that wavenumbers two and three interfere constructively at about $140^{\circ}W$. These regions

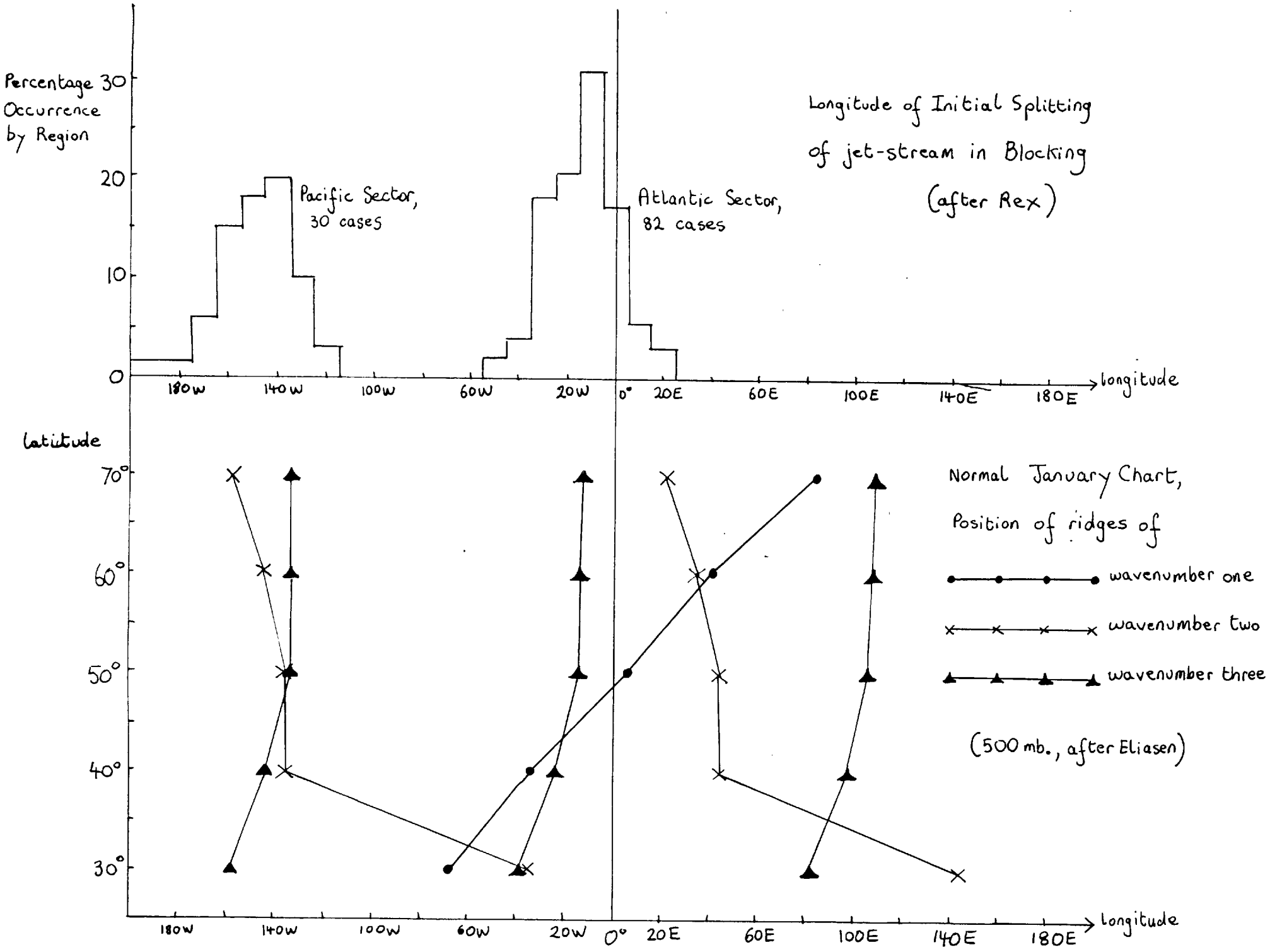

Percentage Occurrence by Region
30
20
10
0
Pacific Sector, 30 cases
Atlantic Sector, 82 cases
180W
140W
100W
60W
20W
0°
20E
60E
100E
140E
180E
longitude
Longitude of Initial Splitting of jet-stream in Blocking (after Rex)
latitude
70°
60°
50°
40°
30°
Normal January Chart, Position of ridges of
wavenumber one
wavenumber two
wavenumber three
(500 mb., after Eliasen)

Figure 2(2)

are compared with Rex's data on the geographical distribution of blocking in Fig2(2) and it is clearly seen that the two main areas for the initial splitting of the jet stream lie just upstream from the two main areas of constructive interference. Note that there is significantly more blocking in the Atlantic than in the Pacific. It can be seen that when wavenumbers one and two are large then blocking in the Atlantic is probable, but the large wavenumber one is also tending to wipe out the reinforcement pattern in the Pacific due to wavenumbers two and three. However, when wavenumber one is small the interference between wavenumbers two and three should show up. As wavenumber one is usually of large amplitude in the wintertime circulation, then one would expect to see more Atlantic than Pacific blocking. In this respect the spectral analyses are consistent with Rex's results. The spectral analyses are also consistent with the observed seasonal longitudinal movement of blocking in the Atlantic sector. All the phases of the long waves on a 500 mb. normal July chart are moved slightly to the east with respect to the normal January phases. This gives rise to the main areas of constructive interference moving towards the east by about $20^{\circ}$ longitude in the summer. This is illustrated in Fig. 2(3), which shows the addition of wavenumbers one and two (each having an arbitrary amplitude of 3 units) with phases taken from normal January and July charts. The eastward shift of the area of constructive interference over Western Europe is consistent with the ''continental'' nature of summer blocking situations illustrated in Fig. 1(6). To look at interference patterns at 500 mb. rather than some other height may seem rather arbitrary. However, 500 mb. is very close to steering level of the baroclinic waves and this point will be expanded in later chapters.

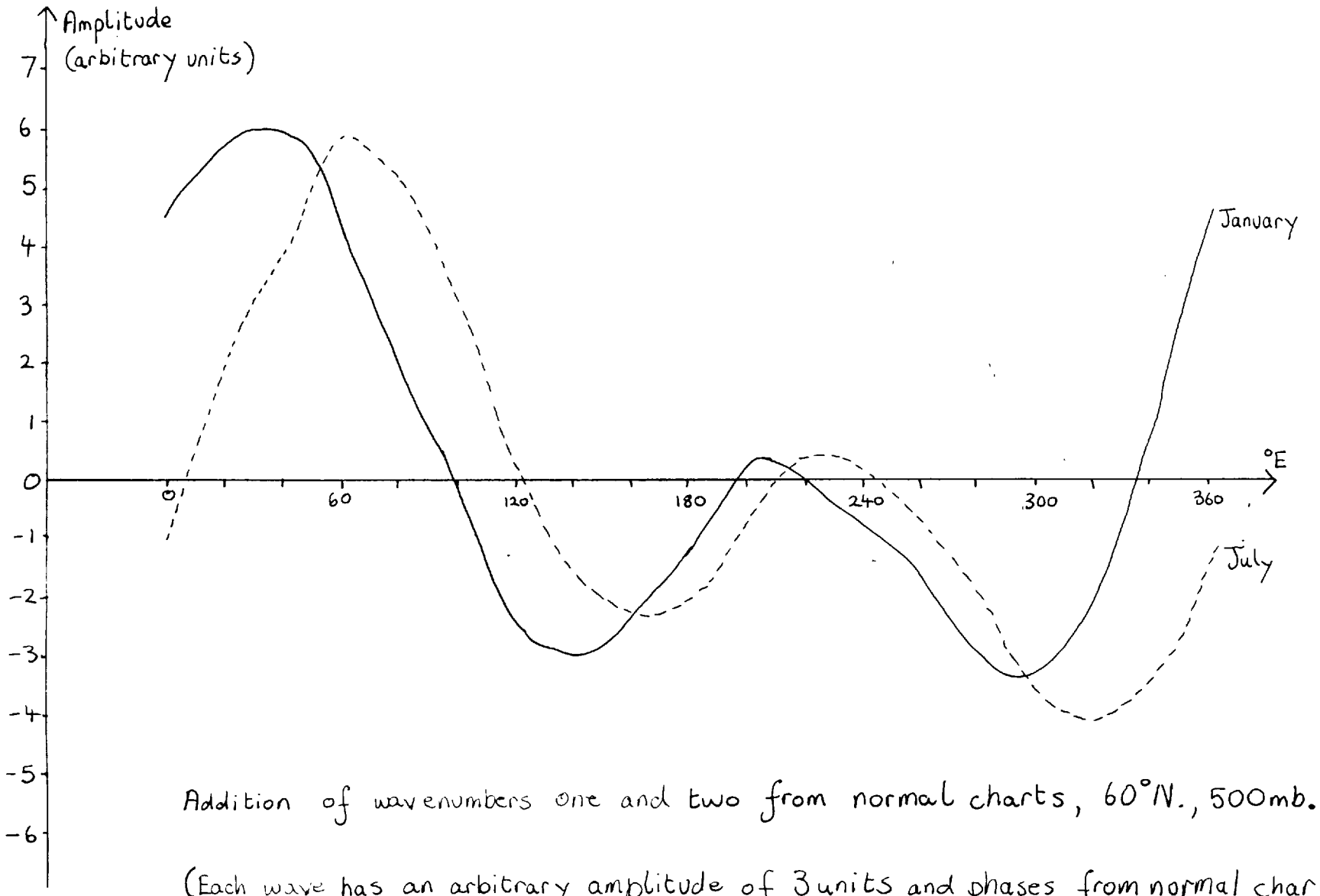



Figure 2 (3)

Addition of wavenumbers one and two from normal charts, 60°N., 500mb.

(Each wave has an arbitrary amplitude of 3 units and phases from normal charts)

## 2.6 Summary

Of all the mechanisms investigated, the forcing of Rossby waves by topography is the most successful in accounting for the observed features of blocking. This is because long stationary Rossby waves are possible and, on normal charts, these interfere to produce ridges at 500 mb. in the Atlantic and Pacific sectors. However, these simple interference patterns do not account for the observed temperature structure of blocking. Nevertheless, Rossby waves can be trapped under strong westerlies with a resultant loss of poleward heattransport. This could account for the build up of ZAPE prior to the blocking. Finally, resonances of trapped Rossby waves are possible.

In the next two chapters the behaviour of the long waves will be examined in case studies on blocking in different regions.

# Chapter THREE

## CASE STUDIES - PART ONE

## PACIFIC BLOCKING

Part One

## Chapter Three Case Studies Pacific Blocking

### 3.1 Introduction

In the following chapters the results of case studies on Northern Hemisphere winter-time flow are presented. The case studies cover periods of zonal flow and blocking and test some of the hypotheses concerning Rossby waves, which were mentioned in Chapter Two. As was stated in Chapter One, various types of blocking situations can be identified synoptically as follows:

i) Atlantic blocking alone

ii) Pacific blocking alone

iii) Double blocking, ie. blocking in the Atlantic and Pacific regions simultaneously.

Rex's catalogue of blocking dates (1950) for the period 1932 to 1950 indicates 68 cases of Atlantic blocking, 18 cases of Pacific blocking and 13 cases of double blocking. For these purposes double blocking has been defined as simultaneous blocking in both regions for six days or more. As was previously stated, Atlantic blocking is the most common type observed and will be investigated in the next chapter. This chapter is concerned with the comparatively uncommon event of Pacific blocking alone. The definition of blocking used is the same as that given in Appendix One.

### 3.2 Wintertime Pacific Blocking - JANUARY 1968

A good example of this mode of blocking occurred in January 1968.

The circulation was characterised by two periods of blocking, both in the North East Pacific, on the following dates:

January 6 → 16 (strong)

January 25 → 30 (weak)

The terms ''strong'' and ''weak'' blocking are used very subjectively here. They refer mainly to the central height of the anticyclone at 500 mb. and to a lesser extent on the presence of a split jet-stream.

Figs 3(1) to 3(6) are U.S. Daily Synoptic Weather Maps at 500 mb. for selected dates in January 1968 and they illustrate the main features of the flow during the month.

Fig. 3(1), Jan. 5th — The flow is nearly zonal.

Fig. 3(2), Jan. 6th — There is a warm anticyclone in the North East Pacific, with a central height of 564 dm.

Fig. 3(3), Jan. 12th — There is still a warm anticyclone in the North East Pacific, which is now about 7°C warmer than it was on the 6th Jan. Note that the zonal flow is now very distorted with a wavenumber four disturbance. A depression is passing to the south of the blocking high in the Pacific.

Fig. 3(4), Jan. 17th — The anticyclone in the Pacific is retrogressing and weakening. The blocking is breaking down.

Fig. 3(5), Jan. 25th — A stationary warm ridge establishes itself in the Eastern Pacific.

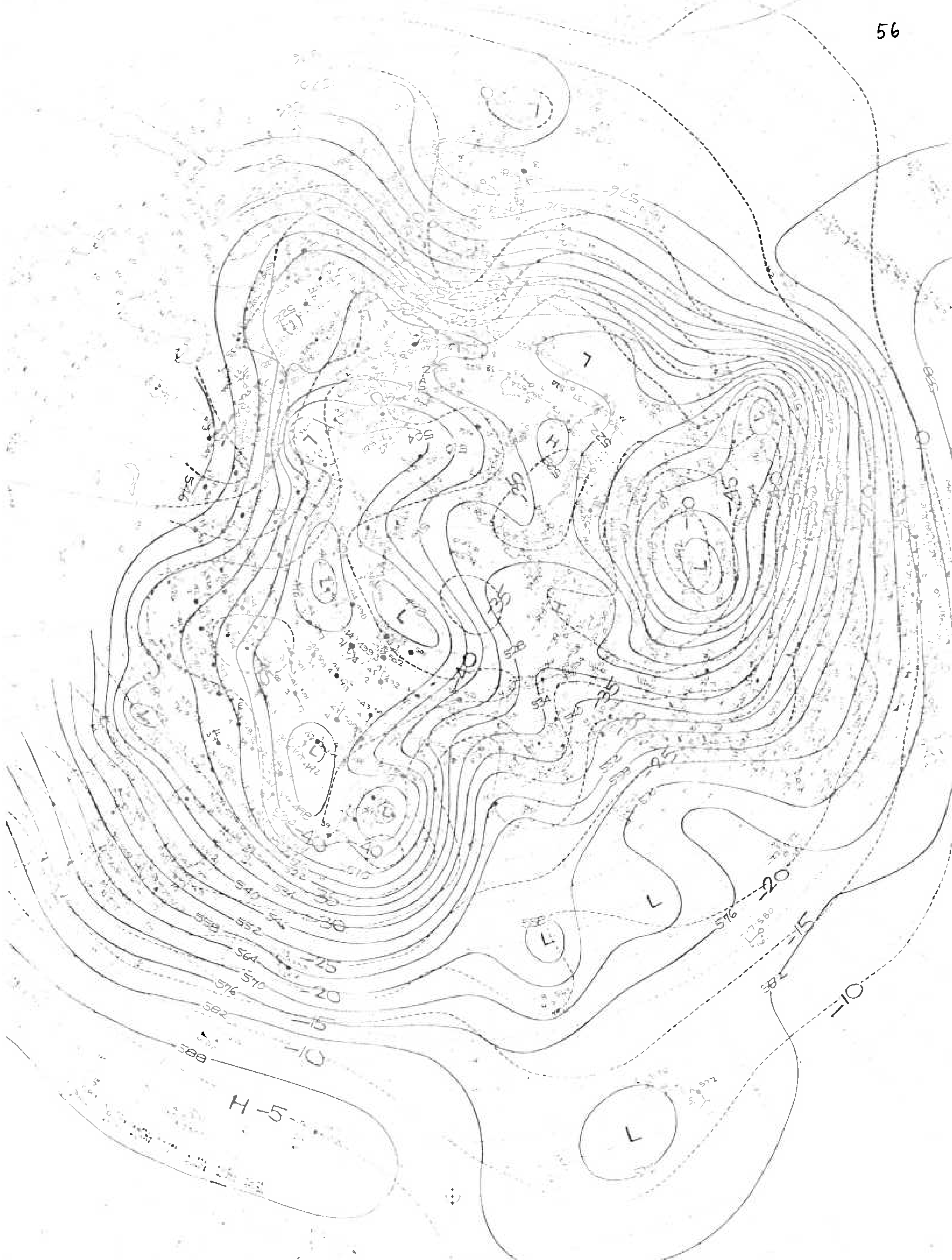



Figure 3(1) 5 January 1968
(500 mb)



Figure 3(z) 6 January 1968
(500 mb)

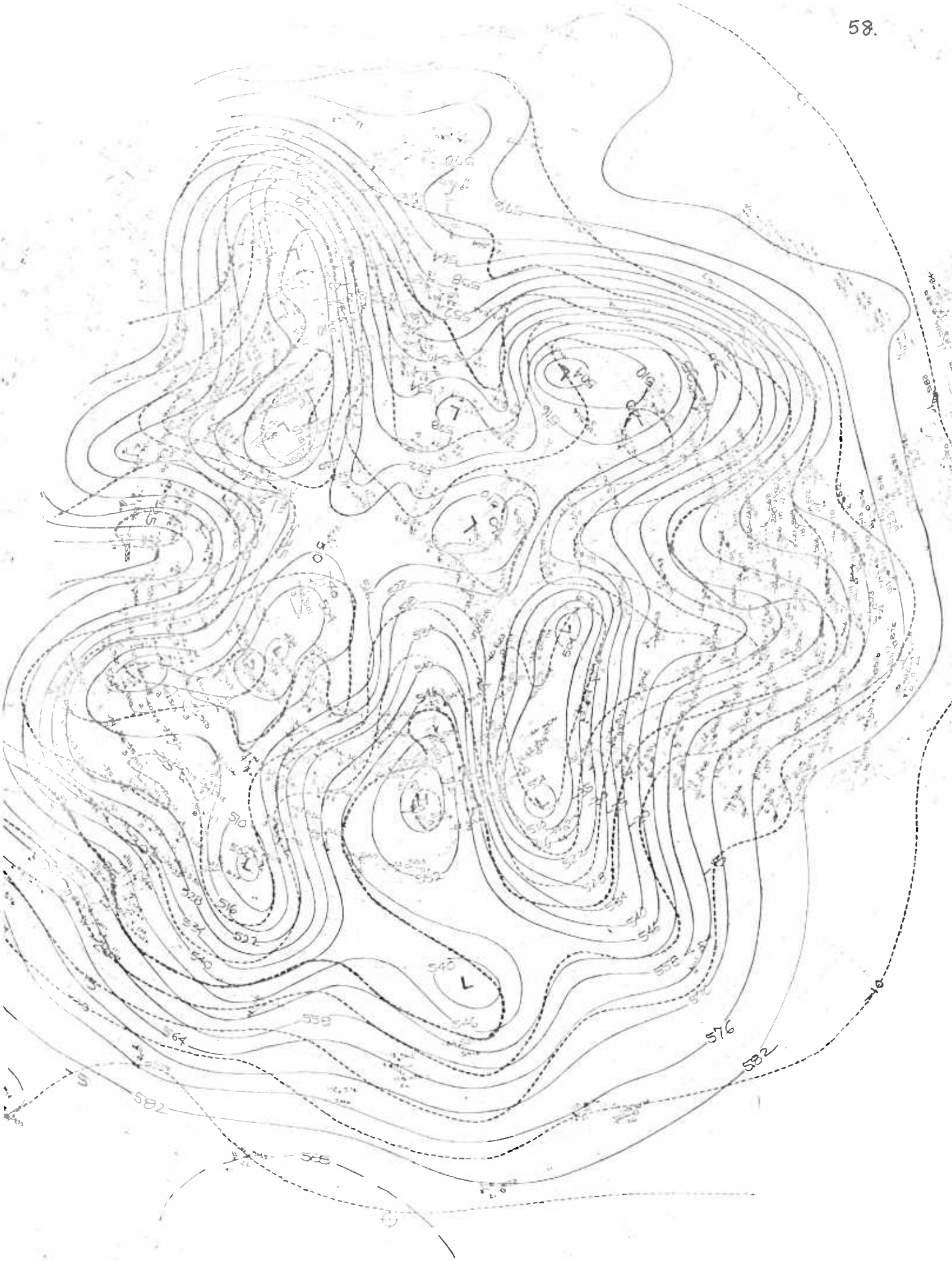



Figure 3(3) 12 January 1968
(500 mb)

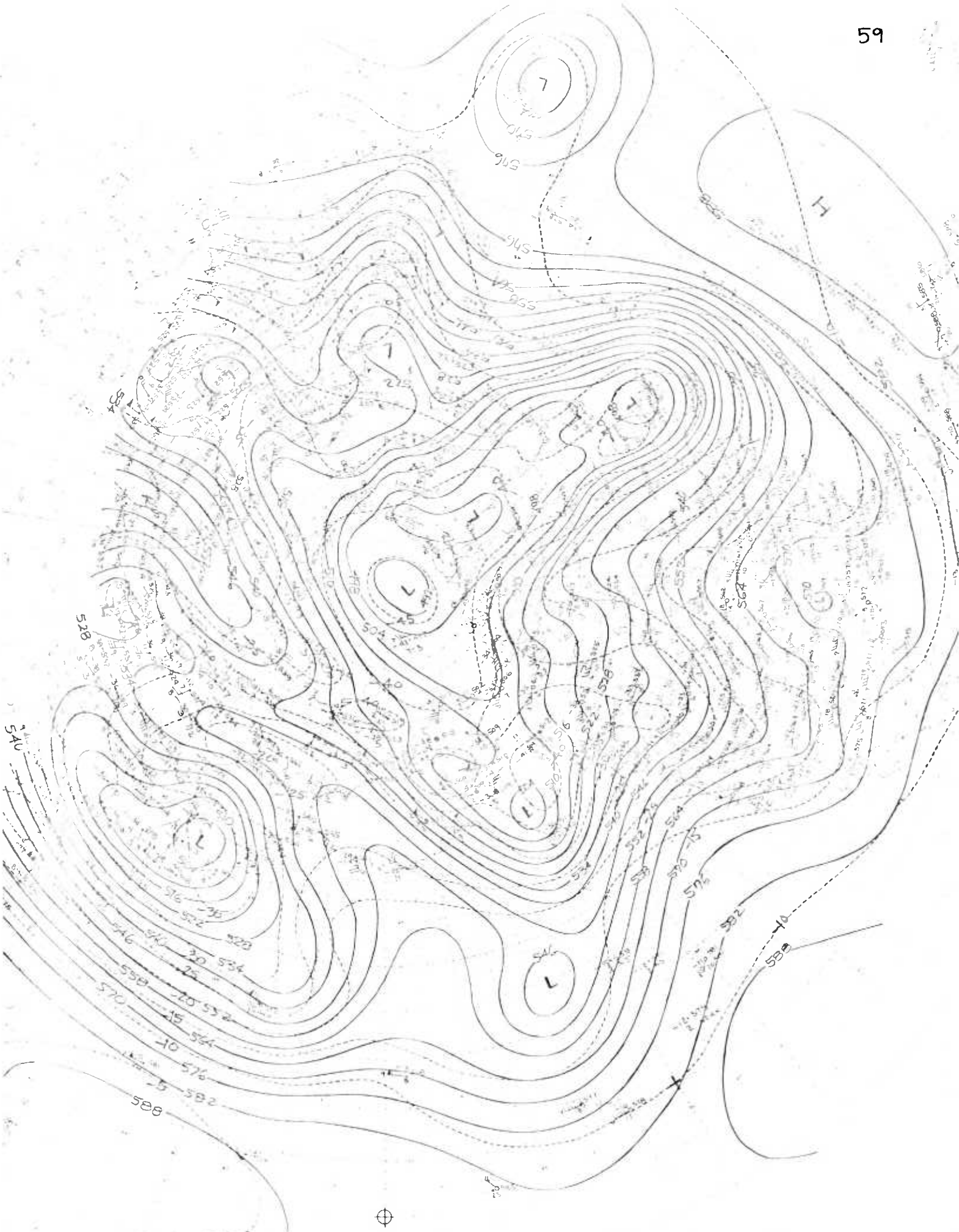


Figure 3(4) 17 January 1968
(500 mb)




Figure 3(5) 25 January 1968
(500 mb)

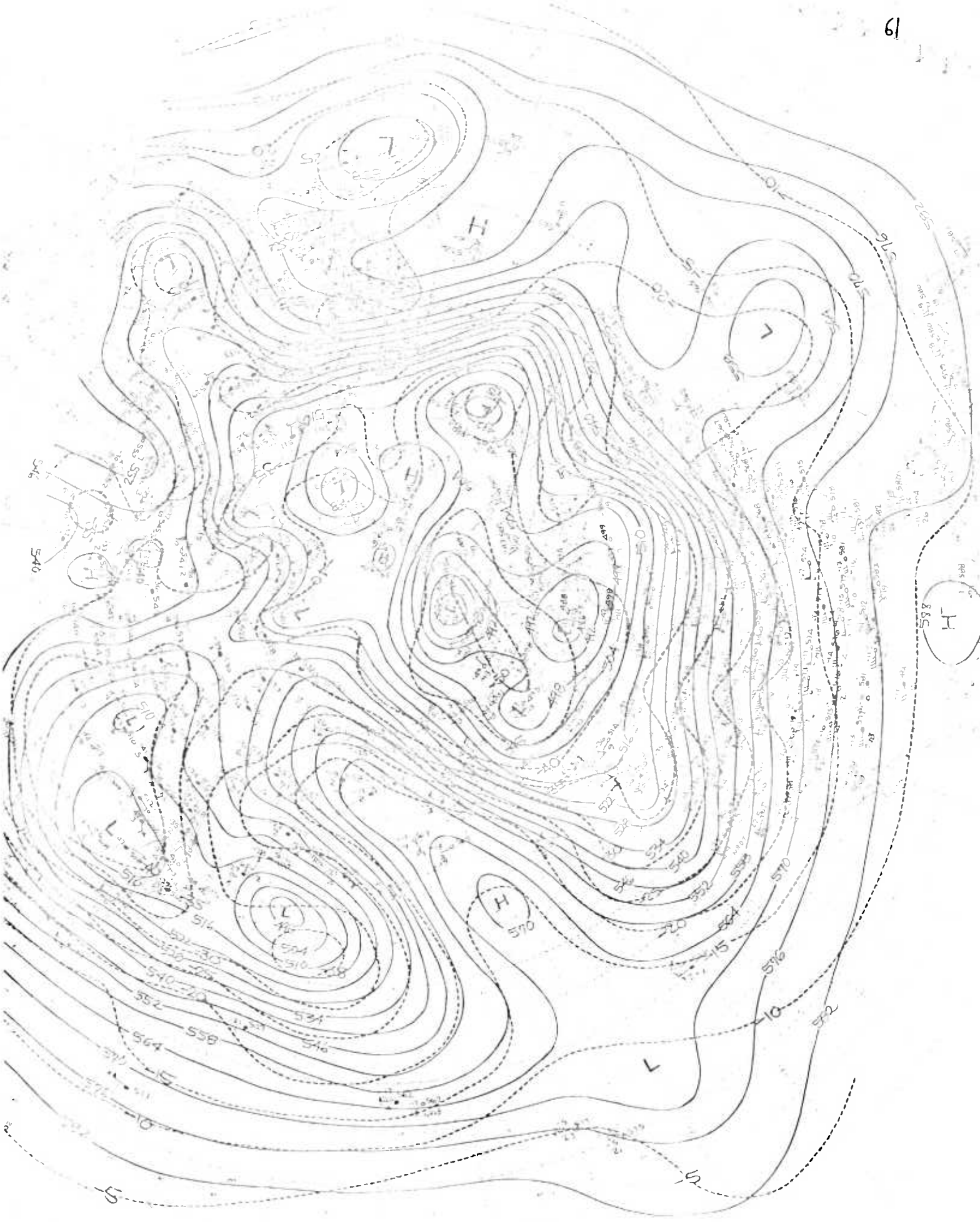


Figure 3(6) 30 January 1968
(500 mb)

Fig. 3(6), Jan. 30th — This ridge is weakening and retrogressing in a manner very similar to the breakdown on Jan. 17th.

A day-by-day Fourier analysis was made of the 500 mb. height and the sea-level pressure around latitudes $60^{\circ}N$ and $40^{\circ}N$ ; $60^{\circ}N$ was the latitude of the centre of the blocking high while $40^{\circ}N$ was to the south of the ''blocking zone''. The data was obtained from the U.S. Daily Synoptic Weather Maps and readings were taken at every $10^{\circ}$ longitude. A recursive technique was used to calculate the Fourier Series. This technique is described in Chapter 24 of ''Mathematical Methods for Digital Computers'' by A. Ralston and H. Wilf.

Fig. 3(7) shows the amplitudes of wavenumbers one and four at $60^{\circ}N$ as a function of time throughout the month. Note that the amplitude of wavenumber one is small during both periods of blocking and that the breakdown of both of the blocks is associated with strong growth of wavenumber one. Wavenumber four is of small amplitude at the beginning of the first block but grows strongly so that it is of large amplitude during the latter half of the first block. It then dies away quickly and its amplification is not a feature of the second block.

Fig. 3(8) shows the amplitudes of wavenumbers two and three at $60^{\circ}N$ throughout the month. Note that wavenumbers two and three are large at the start of the month and during the initiation of the first blocking period. The commencement of the second blocking period is again characterised by large amplitudes of wavenumbers two and particularly three.

These features of the very long waves are discernible at 500 mb.

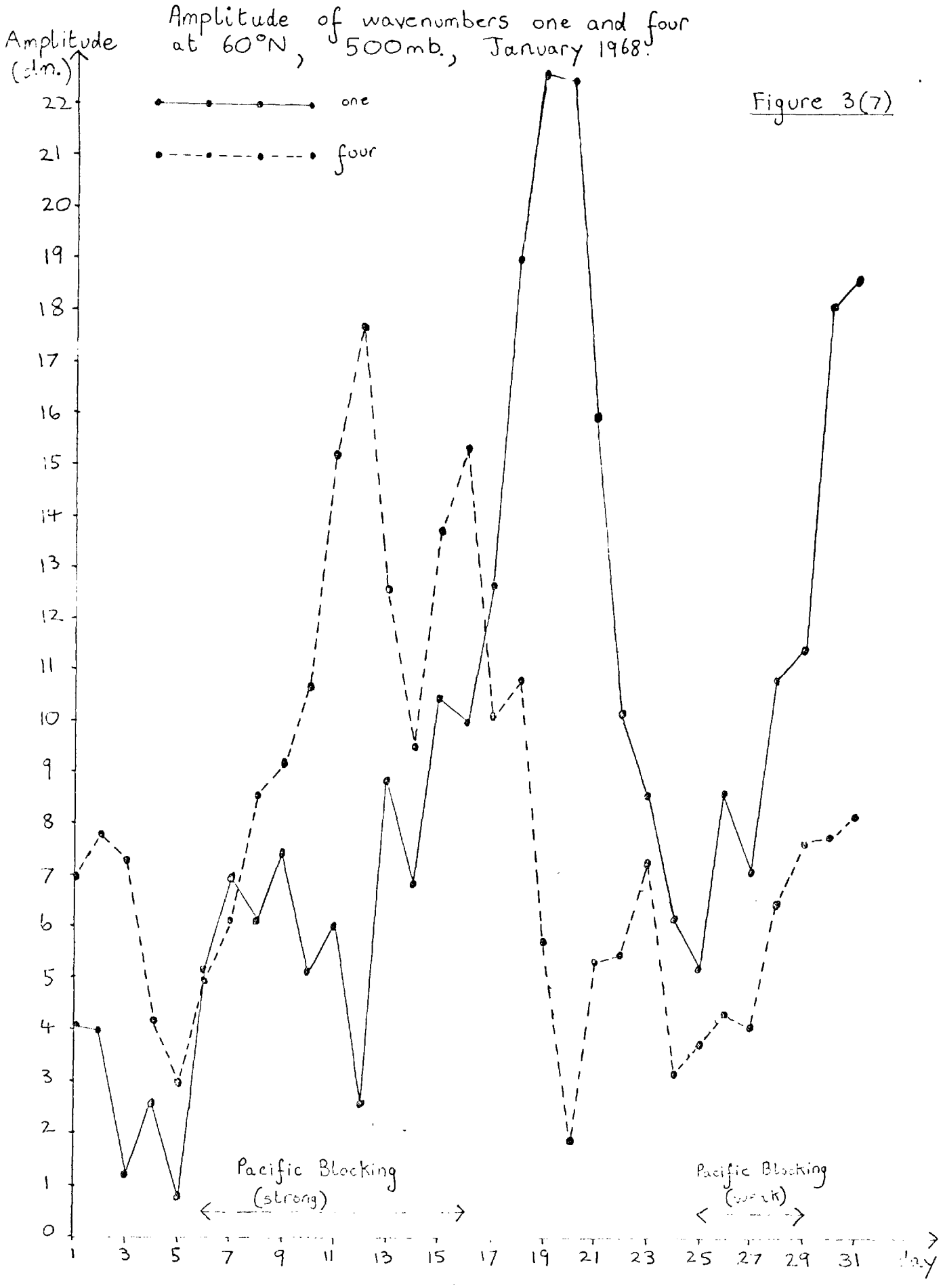
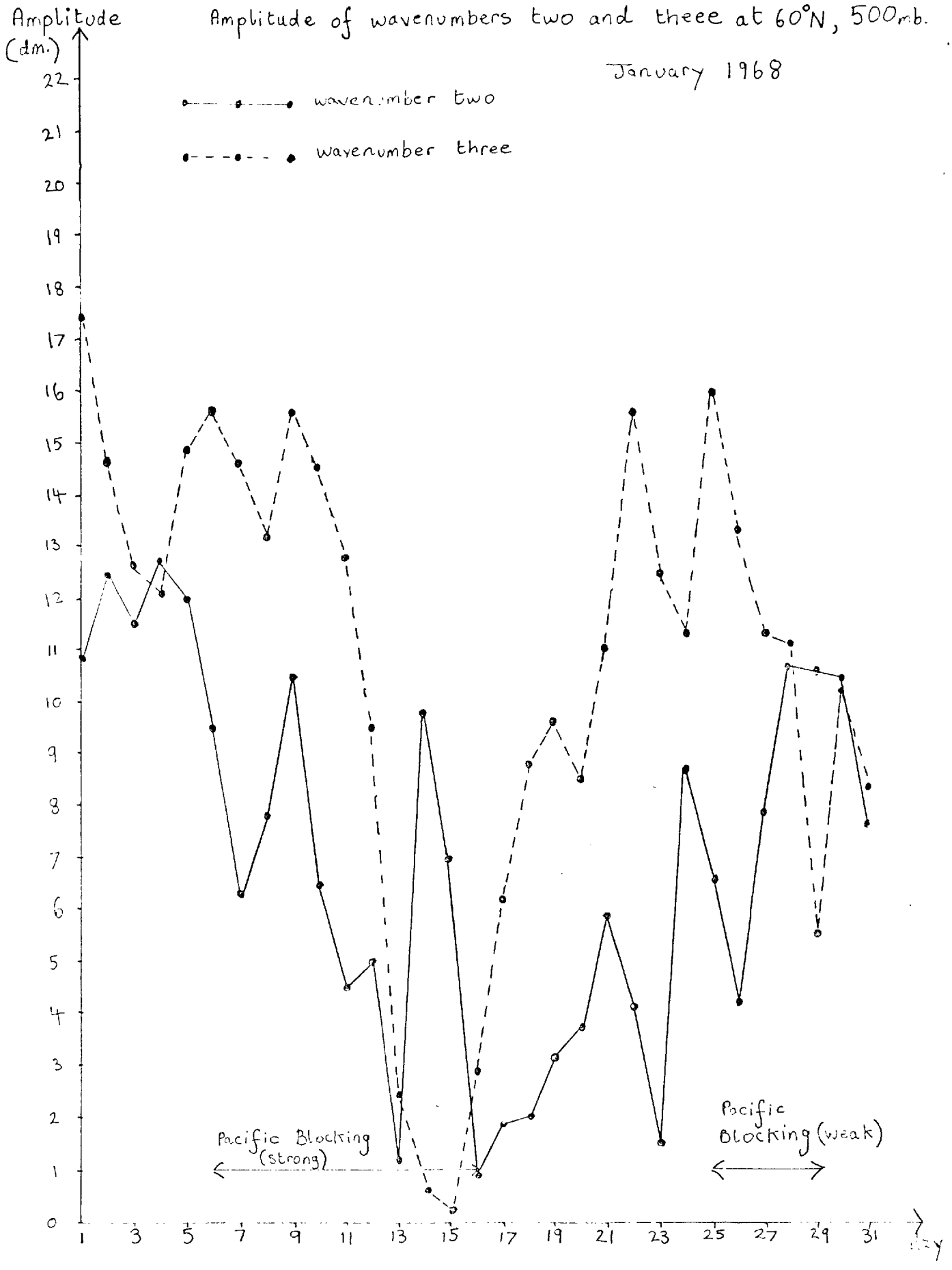

Amplitude of wavenumbers one and four at 60°N, 500mb., January 1968.
Amplitude (d.m.)
one
four
Pacific Blocking (strong)
Pacific Blocking
Day

Figure 3(7)

Figure 3(8)


Amplitude (dm.)
Amplitude of wavenumbers two and theee at 60°N, 500mb.
January 1968
wavenumber two
wavenumber three
Pacific Blocking (strong)
Pacific Blocking (weak)
0
1
2
3
4
5
6
7
8
9
10
11
12
13
14
15
16
17
18
19
20
21
22
1
3
5
7
9
11
13
15
17
19
21
23
25
27
29
31
DAY

at 40°N, but in a much less striking fashion than at 60°N.

A comparison of wave activity on the main baroclinic scale at both latitudes is interesting. Fig. 3(9) shows the amplitudes of wavenumbers six, seven and eight at 40°N and Fig. 3(10) shows these amplitudes at 60°N. The values at 60°N are fairly constant throughout the month, but large amplitudes of wavenumbers six and eight are seen to occur at 40°N in the latter half of the first blocking period. This is true to a lesser extent for wavenumber six during the second blocking period.

In Chapter Two it was pointed out that wavenumbers two and three on normal charts interfere to produce a ridge over the Eastern Pacific at 500 mb. This ridge is normally eliminated by the trough of the normal wave number one. It was suggested that wavenumbers two and three with near normal phases and amplitudes would produce a ridge in the Pacific provided wavenumber one was of small amplitude or not of normal phase. An investigation of the phases of the long waves in January 1968 did show this to be the case.

The positions of the ridges of wavenumbers two and three in the Eastern Pacific at 60°N leading up to the first block were as follows:

Figure 3(9)

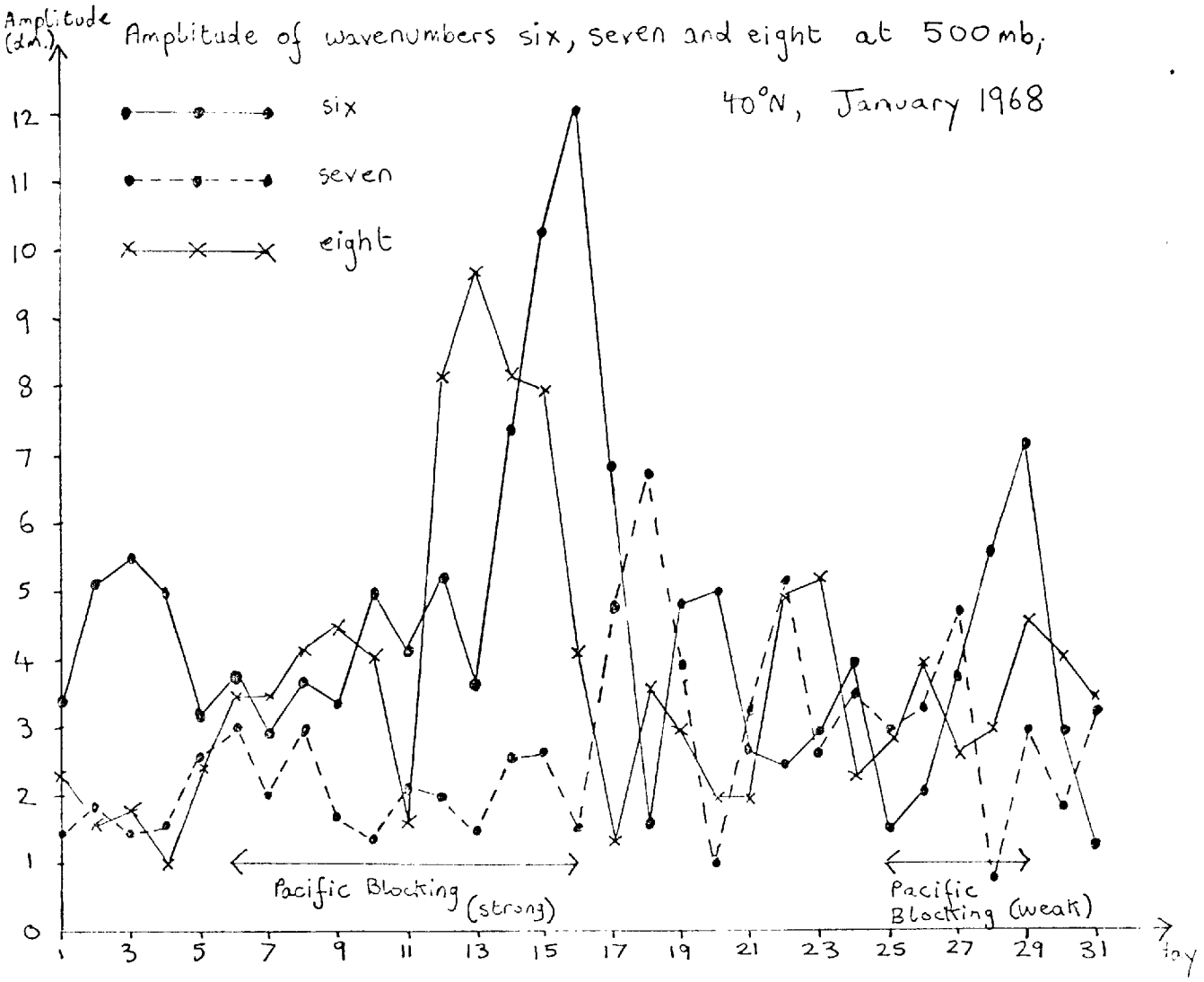
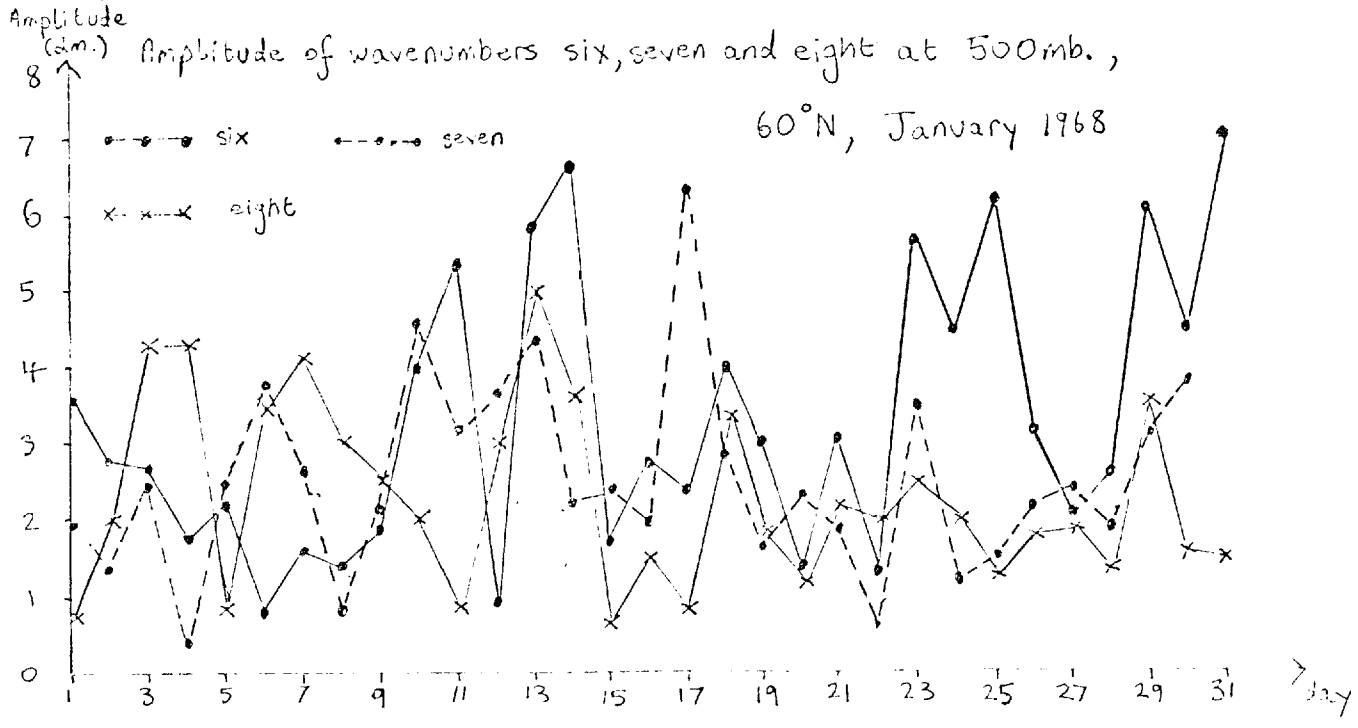



Figure 3(10)



| Date | Wavenumber Two 500mb (°E) | Wavenumber Two Sea level (°E) | Wavenumber Three 500mb (°E) | Wavenumber Three Sea level (°E) |
|---|---|---|---|---|
| 1 | 207 | 257 | 202 | 221 |
| 2 | 203 | 253 | 207 | 233 |
| 3 | 200 | 252 | 203 | 234 |
| 4 | 205 | 253 | 204 | 228 |
| 5 | 205 | 250 | 202 | 229 |
| 6 Blocking commences | 203 | 237 | 200 | 237 |
| 7 | 194 | 224 | 206 | 238 |
| 8 | 191 | 226 | 203 | 244 |
| Normal (Eliasen) | 213 | 259 | 228 | 252 |

The phase coincidence is in general more marked at 500mb. than at sea level and this is consistent with the synoptic charts, which show a much more clearly defined anticyclone at 500mb than at sea level.

A large amplitude stationary wavenumber four then grew up which ''maintained'' the blocking in the Pacific, but distorted the whole zonal flow. The positions of the ridge of wavenumber four in the Eastern Pacific at 60°N during the first block were as follows:

| Date | Wavenumber Four 500 mb (°E) | Wavenumber Four Sea level (°E) |
|---|---|---|
| 6 Blocking Commences | 187 | 199 |
| 7 | 193 | 163 |
| 8 | 181 | 174 |
| 9 | 177 | 179 |
| 10 | 173 | 174 |
| 11 | 171 | 153 |
| 12 | 172 | 185 |
| 13 | 175 | 185 |
| 14 | 162 | 175 |
| 15 | 163 | 175 |
| 16 Blocking Ends | 167 | 180 |

Thus at 500 mb the ridge of wavenumber four was about 30° longitude upstream from the original ridge due to the interference of wavenumbers two and three. This could be important and will be referred to in later chapters.

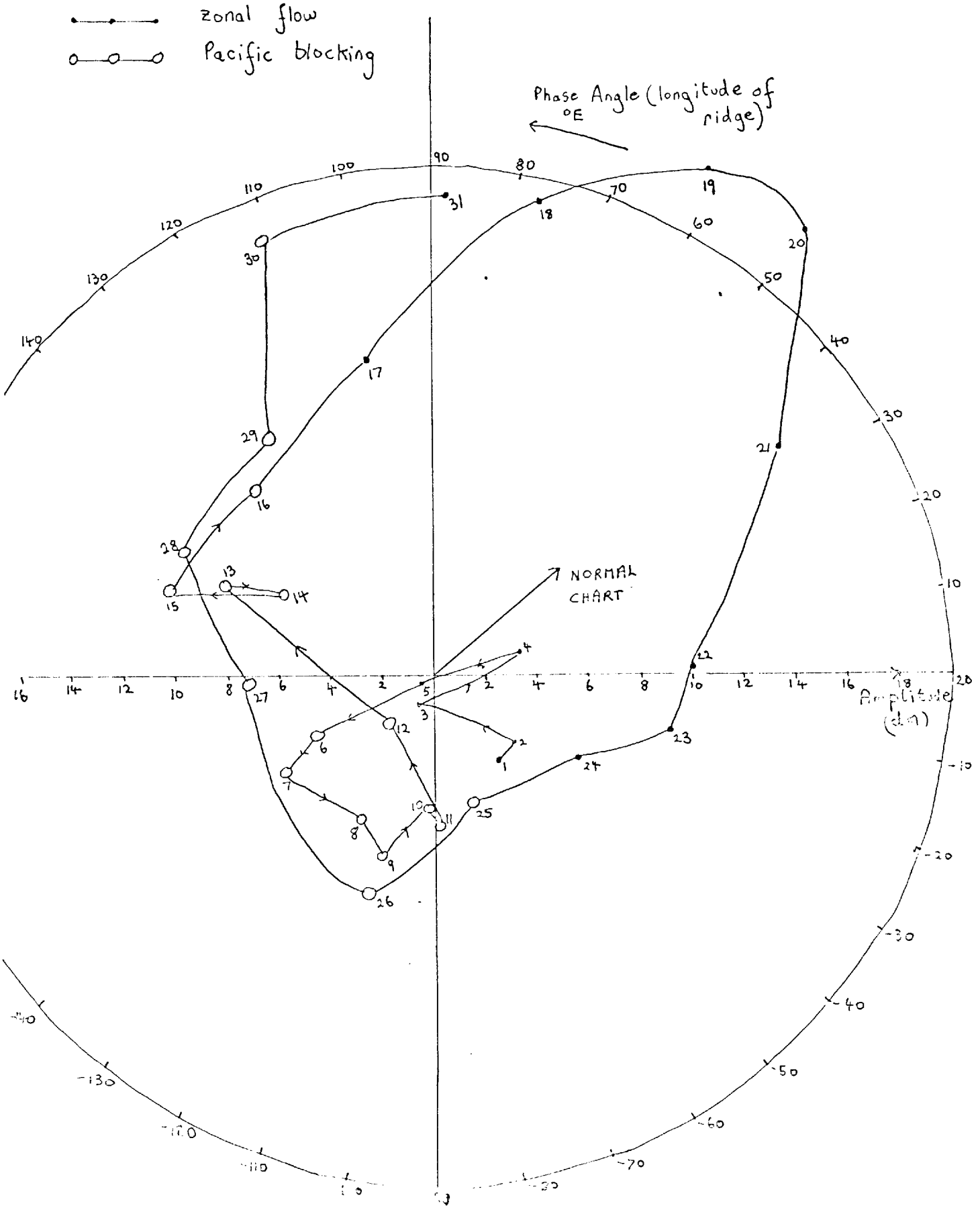
Very strong growth of wavenumber one accompanied by a collapse of wavenumber four occurred at the end of this block. Fig 3(ii) is an amplitude-phase polar plot for wavenumber one throughout the month. This also shows the amplitude and phase of wavenumber one at 500 mb and 60°N on a normal January chart (Eliasen, 1958). It can be seen that the two periods of Pacific blocking occurred when wavenumber one was of small amplitude and with a phase angle 180° different from that of the normal wave. The breakdown of both blocks occurred when wavenumber one grew strongly and propagated towards the west. The largest amplitudes of wavenumber one occurred when its phase was nearly that of the normal wave.

During the second period of blocking wavenumbers two and three, in the absence of wavenumber one, again interfered to produce a high pressure ridge in the Eastern Pacific. The positions of the ridges at 500 mb during this period at 60°N were as follows:

| Date | Wavenumber Two | | Wavenumber Three | |
|---|---|---|---|---|
| | 500mb (°E) | Sea level (°E) | 500mb (°E) | Sea level (°E) |
| 25 Blocking commences | 169 | 268 | 207 | 267 |
| 26 | 198 | 262 | 210 | 220 |
| 27 | 197 | 260 | 198 | 224 |
| 28 | 198 | 263 | 192 | 233 |
| 29 | 195 | 266 | 192 | 203 |
| 30 Blocking ends | 195 | 261 | 182 | 212 |
| 31 | 173 | 263 | 183 | 209 |
| Normal (Eliasen) | 213 | 259 | 228 | 252 |

Figure 3 (11)

Amplitude - Phase Polar Plot of wavenumber one at 500 mb., 60°N
January 1968



Note again the phase coincidence at 500 mb rather than sea level. There was no amplification of wavenumber four and this second block was short lived. Strong growth and westward propagation of wavenumber one produced a trough which eliminated the local reinforcement of wavenumbers two and three in the Pacific.

Thus it does seem that the initiation and crutial maintenance of blocks in the Pacific is due to a simple interference pattern. However, there may be an additional maintenance mechanism at work in long-lived blocks which was responsible for the production of wavenumber four during the blocking which lasted from 6th to 16th January. Indeed, if one wants to use the term ''blocking wave'', then it seems most appropriate to use it to describe this wavenumber four. Possible maintenance mechanisms will be investigated in Chapters Five and Six.

3.3 Behaviour of Wavenumber One

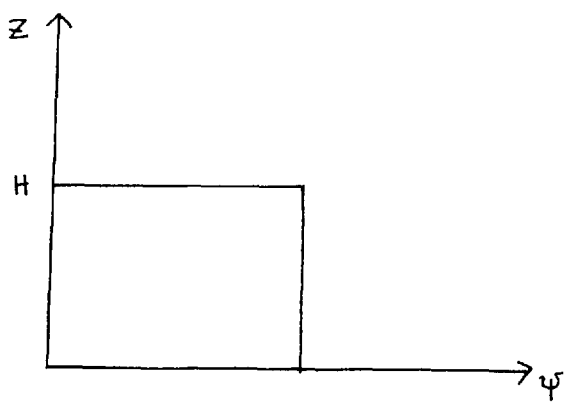
Wavenumber one was obviously important in initiating and destroying blocking situations in the Pacific so its behaviour throughout the month was further examined. The amplitude-phase polar plot in Fig 3(11) showed a wave propagating towards the west with large changes of amplitude.

A reasonable conclusion to draw from this data is that there was a stationary wavenumber one present, with phase and amplitude similar to that of the normal wave, and a travelling wavenumber one of slightly larger amplitude. Together these waves produced the observed interference pattern. It was deduced that the travelling wave was moving at a speed of between $10ms^{-1}$ and $20ms^{-1}$ towards the west. Thus blocking in the Pacific occurred when the travelling wave was $180^{o}$ out of phase with the stationary wave. For this to

have been the case the two wavenumber one waves would have had different total wavenumbers in order to account for their different propagation speeds.

What mechanisms are likely to produce a retrogressive wavenumber one? Very long baroclinically unstable waves were first identified by Green (1960) and further investigated by Geisler and Garcia (1977). However, these waves are progressive and so do not explain the data. In Chapter Two it was shown how the behaviour of long waves in the troposphere is affected by wind conditions in the stratosphere. Stratospheric conditions in January 1968 were investigated and it was found that a major stratospheric warming had commenced on December 17th 1967; it reached its peak on January 1st 1968 and lasted until January 14th 1968. The air at 10 mb. over the pole was warmed by $56^{\circ}C$ and the strongest easterly winds measured at 10 mb. were 60 $m.s.^{-1}$ Thus it seems likely that wavenumber one was affected by this change in vertical propagation conditions in early January 1968. What would be seen in the troposphere if wavenumber one changed from a vertically trapped mode to a vertically propagating mode?

Consider first a trapped stationary wave with zero vertical wavenumber. There is a "lid" at $z = H$.




From equation 2(iii)

$$c = \bar{u} - \frac{\beta R^2}{(n-1)(n+2)} = 0$$

When the ''lid'' is removed there is a wave packet with a spread of vertical wavenumber $\lambda$ of the form $\frac{\sin 2\lambda H}{2\lambda H}$. This packet is highly dispersive; there will be a stationary wave ( $\lambda = 0$ ) and a spread of progressive waves with their propagation speeds depending on their vertical wavenumbers.

$$c = \bar{u} - \frac{\beta R^2}{(n-1)(n+2) + \frac{f_0^2}{gB}\lambda^2}$$

However, if the stationary trapped wave already has a vertical wavenumber $\lambda_s$ associated with it, then removing the ''lid'' will introduce a range of values of $\lambda$, both greater and smaller than $\lambda_s$. This is because the spread of vertical wavenumber in the packet will be of the form $\frac{\sin 2(\lambda_s + \lambda) H}{2(\lambda_s + \lambda) H} + \frac{\sin 2(\lambda_s - \lambda) H}{2(\lambda_s - \lambda) H}$

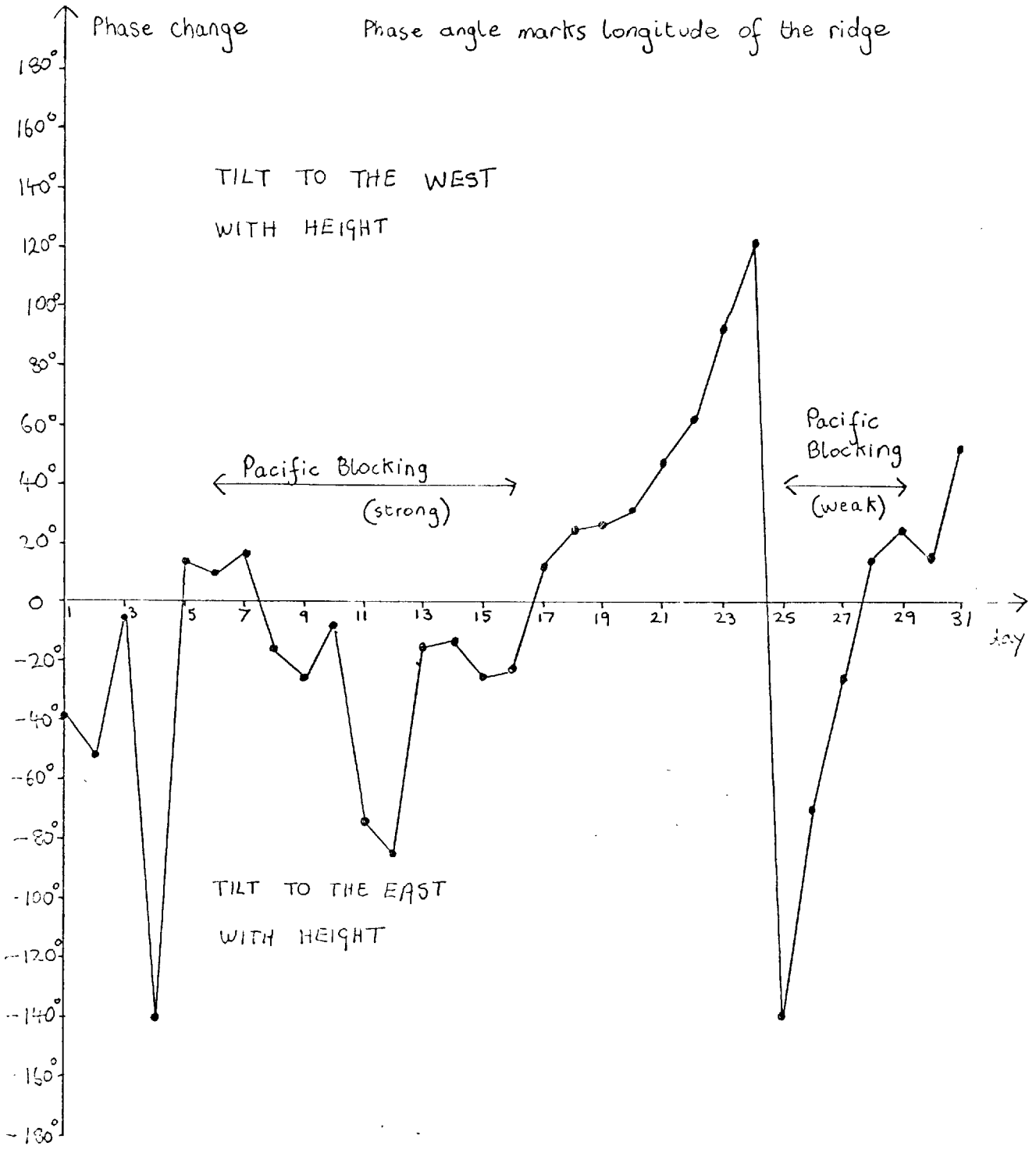
This will give rise to both progressive and retrogressive waves as well as the original stationary wave. Hence travelling waves should be expected when a stratospheric warming finishes but the observed direction of propagation will depend on the initial conditions.

Fig 3(12) shows the phase change with height of wavenumber one between sea level and 500 mb. This is a slightly unreliable quantity to calculate from only two levels because, for very large phase changes, the sign of the change is ambiguous. This was not too much of a problem with wavenumber one but there were many uncertainties in the data for higher wavenumbers. Hence this data for higher wavenumbers was not used. At the beginning of the month and during the first block there was a tilt to the east with height of wavenumber one,

Figure 3(12)

Phase difference with height of wavenumber one, 60°N, January 1968.

(Surface phase − 500mb. phase)



consistent with it being trapped under the easterly winds in the stratosphere. The phase tilt then alternated between the east and the west which is consistent with there being interference between two waves with different vertical wavenumbers. It is interesting to note that there was no blocking in the Atlantic when wavenumber one was of very large amplitude. This was because of the very strong tilt to the west with height of wavenumber one plus the fact that the wave was not stationary. It is part of the synoptic definition of blocking that the surface anticyclone should be directly, or nearly directly beneath the upper level anticyclone and this requires that the waves involved should not have large phase changes with height. This was the case with wavenumbers two and three during the Pacific blocking, but even so the surface anticyclone was not very well defined. During the two periods of large amplitude of wavenumber one the 500 mb ridge of this wave was over the Atlantic but the sea level ridge was over Siberia. This point can be reinforced by the synoptic charts shown in Figs 3(13) and 3(14). The charts contrast the strength and position of the Siberian anticyclone on January 10th (small amplitude wavenumber one) and January 19th (large amplitude wavenumber one). On the 10th the anticyclone is weak and centred at about $40^{\circ}N$ but on the 19th the anticyclone is intense and centred at $60^{\circ}N$. Thus to identify a large amplitude wave in Fourier space is not necessarily sufficient to identify a blocking situation in physical space.

The vertical phase changes with height of wavenumber one can be used to calculate the poleward heat transport due to wavenumber one. It is necessary to calculate $\overline{v^{*}T^{*}}^{x}$ from a stream function $\psi^{*}$, where the prime denotes deviations from a ''large'' mean state.

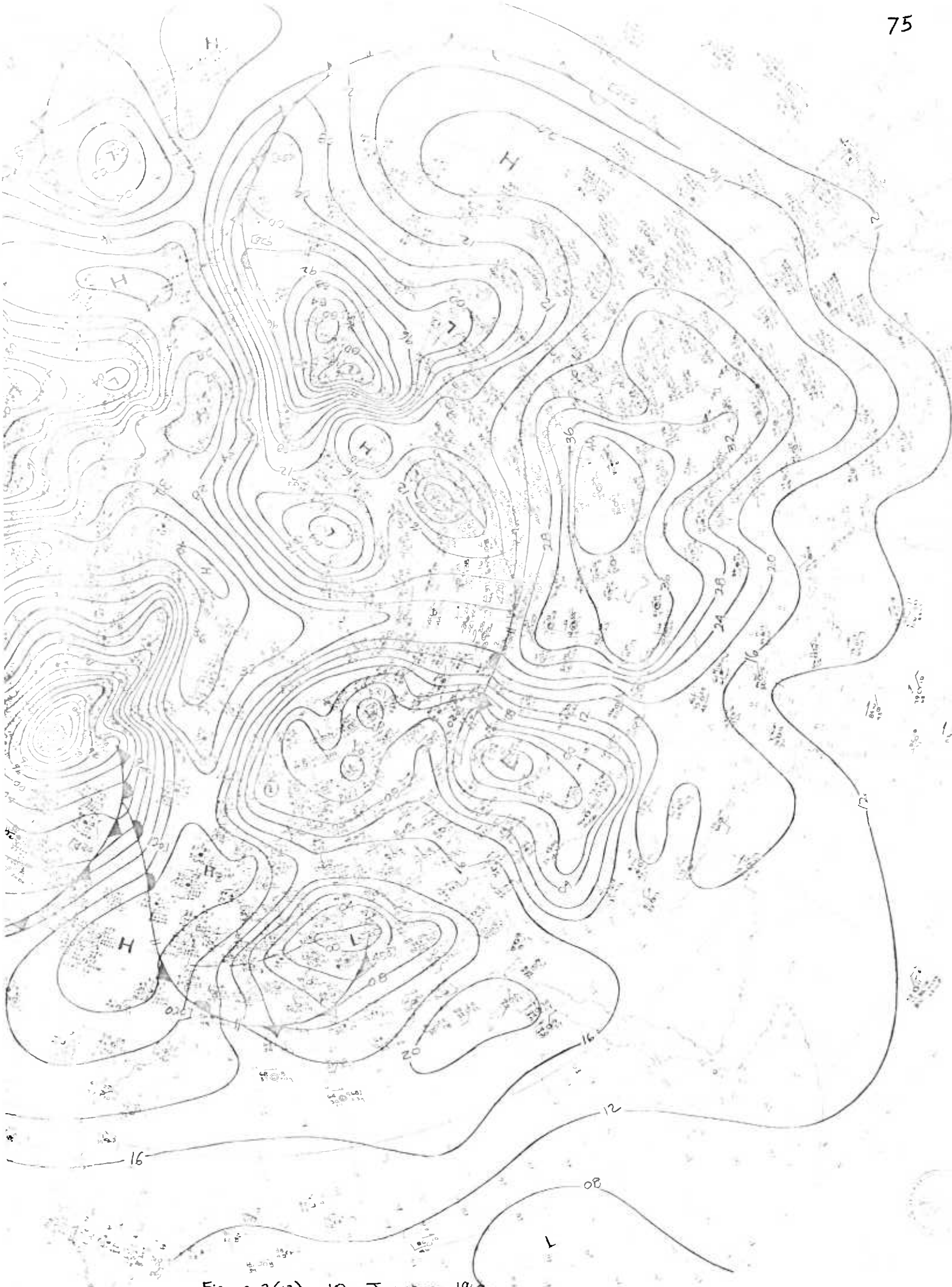



Figure 3(13) 10 January 1968
(sea level)

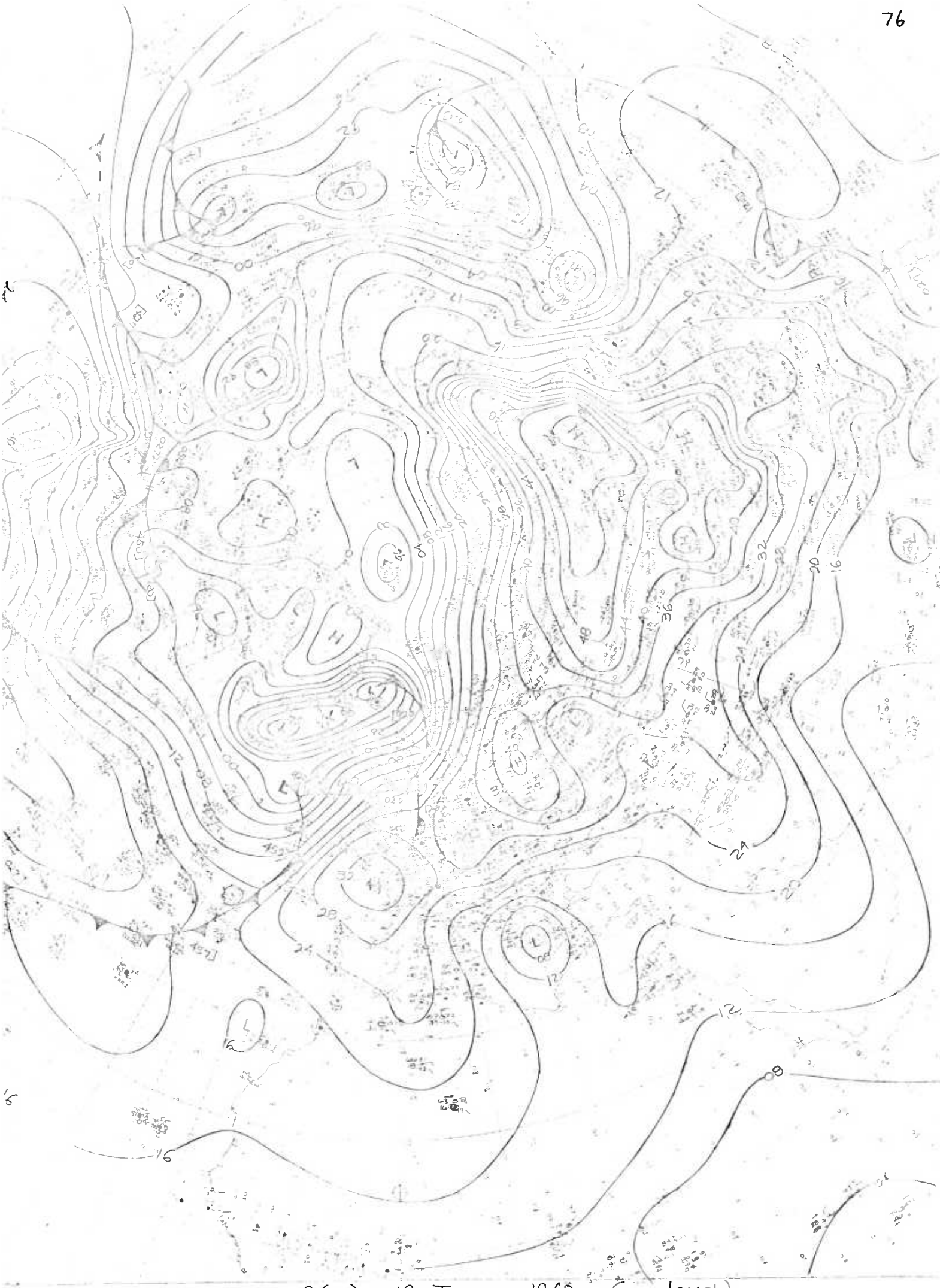


Figure 3(14) 19 January 1968 (sea level)

Using standard notation,

$$\psi' = A\cos(kx + \nu z)$$

$v' = \dfrac{\partial \psi'}{\partial x}$ by definition

$$\phi' = \frac{T'}{\bar{T}} - \frac{R}{C_p}\frac{p'}{\bar{p}}$$ to first order

but $\overline{v'p'}^{x} = 0$ for geostrophic motion

$$\therefore \quad \overline{v'\phi'}^{x} = \overline{\frac{v'T'}{\bar{T}}}^{x} \quad " \qquad "$$

$$\phi' = \frac{f_0}{g}\frac{\partial \psi'}{\partial z} \quad \text{(thermal wind)}$$

$$\therefore \quad \overline{v'T'}^{x} = \frac{\bar{T} f_0 A^2 k \nu}{2g}$$

$p' = \rho f_0 \psi' = -\rho g z'$ where $z'$ is the height perturbation on a constant pressure surface

$$\therefore \psi' = -g/f_0 \, z'$$

$$\therefore \overline{v'T'}^{x} = \frac{\bar{T} g (z')^2 \nu k}{2f_0} \quad \text{——} \quad \text{Equation 3(i)}$$

The vertical wavenumber was estimated from the phase change between the ground and 500 mb., the height of which was taken to be 5.2 km. The value of $\overline{T}$ used was 270 K.

Fig 3(15) shows the mean of the sea level and 500 mb. northward heat transport by wavenumber one in January 1968. [The value for $z'$ used was the mean of the sea level and 500 mb amplitudes.] It can be seen that nearly all the northward heat transfer due to wavenumber one took place after the breakdown of the two Pacific blocks. For comparison the heat transport calculated in the same way from wavenumber one on a normal January chart is $4.48\ ^{o}C\ m.s.^{-1}$ The importance of the poleward heat transport by the very long waves in winter in the lower troposphere is well known. One of the early observational studies on this was carried out by Wiin-Nielsen et. al (1964). The variation of this heat transport during periods of zonal flow and blocking obviously needs closer investigation, but these results indicate that the poleward heat transport due to wavenumber one during Pacific blocking is small compared with the normal.

3.4 Zonal Winds

Fig. 3(16) shows the calculated zonal mean of the geostrophic zonal wind at $50^{o}N$ at 500 mb. and the sea level. At the beginning of the month the wind speed was about 25 $m.s.^{-1}$ at 500 mb. and 4 $m.s.^{-1}$ at sea level. However, the wind speeds decreased at both levels during the first period of blocking and on one day the sea level wind actually went easterly. The zonal wind at 500 mb. recovered after the breakdown of the first block but again decreased during the second block. The sea level wind never seemed to recover and went easterly on two more occasions.

The maintenance of surface winds against friction is due to the

Figure 3(15)

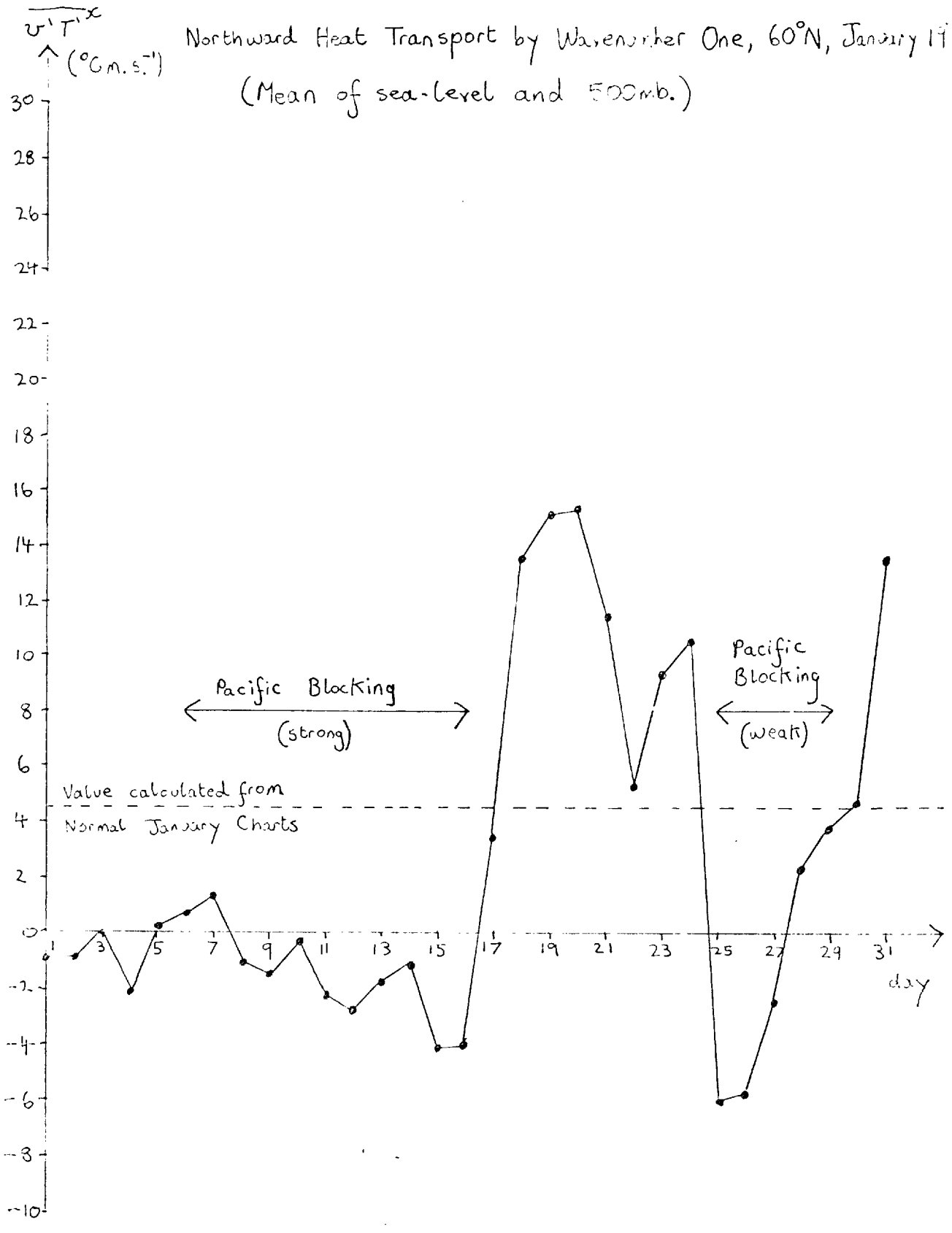
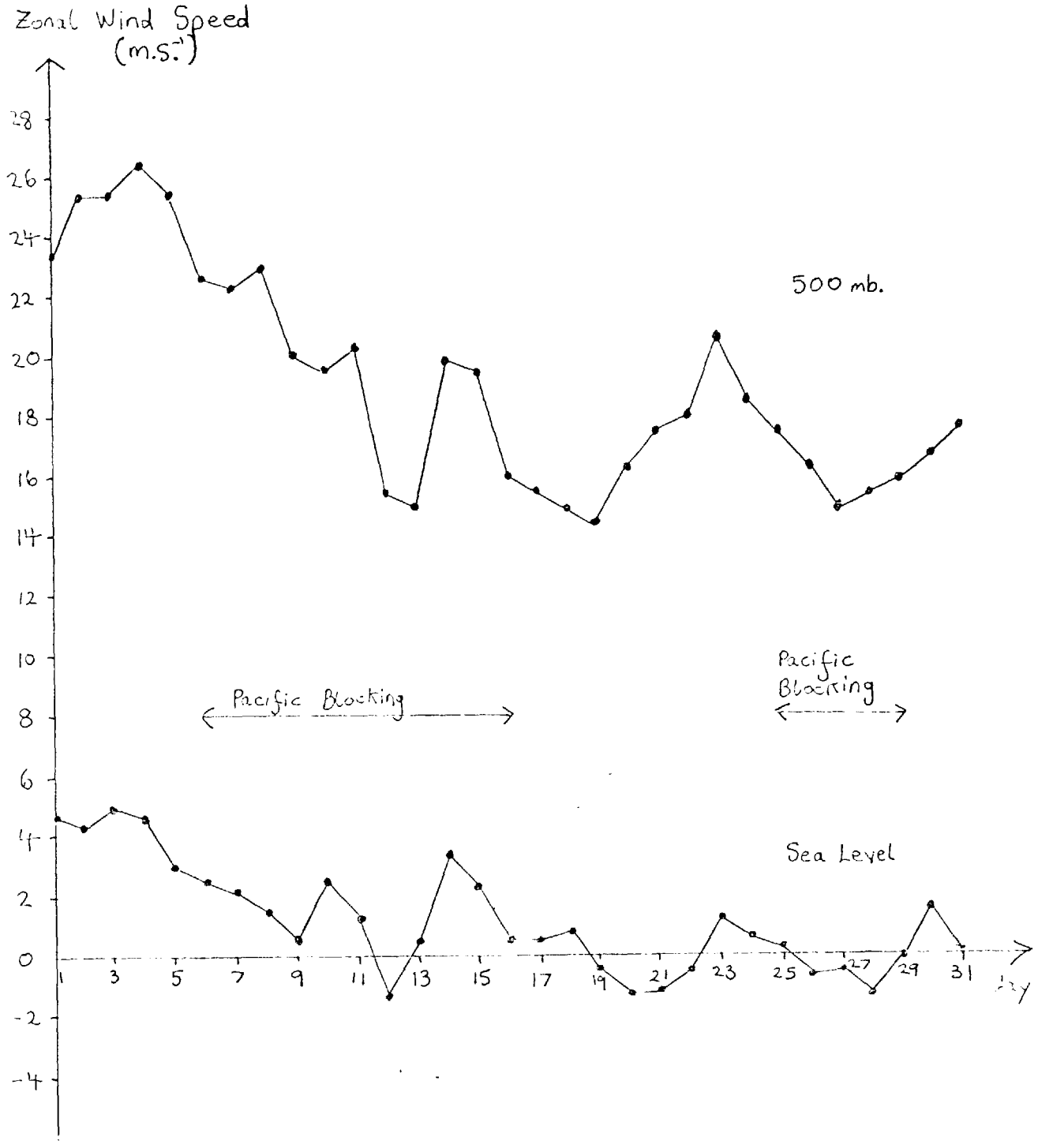

$\overline{v'T'}^x$
(°C m. s.⁻¹)
Northward Heat Transport by Wavenumber One, 60°N, January 1968
(Mean of sea-level and 500mb.)
30
28
26
24
22
20
18
16
14
12
10
8
6
4
2
0
-2
-4
-6
-8
-10
Pacific Blocking
(strong)
Pacific Blocking
(weak)
Value calculated from
Normal January Charts
1
3
5
7
9
11
13
15
17
19
21
23
25
27
29
31
day

Figure 3(16)

Zonal Geostrophic Winds at 50°N, January 1968
(zonal mean)



transport of westerly momentum into mid-latitudes by baroclinic waves. These baroclinic waves are growing in the main baroclinic zone which lies in mid-latitudes. The fact that winds at the surface go easterly from time to time implies that, not only is there an absence of the mechanism which normally drives the mid-latitude surface westerlies, but that westerly momentum is actually being transported out of this region. This could reflect the formation of two baroclinic zones at different latitudes (i.e. a split jet-stream) and is consistent with increased wave activity on the baroclinic scale at $40^{\circ}N$ observed during the fist block. This mechanism will be discussed in greater detail in Chapter Six.

The reduction of surface winds in mid-latitudes could have serious consequences for the thermally forced long waves because reduced low level flow over heat sources and sinks increases the amplitude of the response.

From equation 2(i) the response of zonal flow to thermal forcing can be calculated. For thermal forcing of the type $S = a e^{-bz} \cos kx \cos \mu y$ and assuming $\varsigma$ constant with height for simplicity:

$$\psi = -\frac{a g \cos \mu y}{f_0 \bar{u} k (\nu^2 + b^2)} \left[ \nu \cos(\nu z + kx) + b e^{-bz} \sin kx \right]$$

is the steady state solution where

$$\nu^2 = \frac{g\beta}{f_0^2} \left[ \frac{\beta}{\bar{u}} - (k^2 + \mu^2) \right]$$

It can be seen that in this simple case with the zonal wind constant with height the amplitude of the stream function is inversely proportional to the zonal wind speed. In the equivalent simple case for mountain forcing the amplitude of the stream function does not depend on the zonal wind speed.

Thus the main features of Pacific blocking during January 1968 have been outlined; they will be summarised at the end of the chapter. However, as it was suggested that Pacific blocking may have been indirectly due to the breakdown of a stratospheric warming, an attempt was made to see whether other major stratospheric warmings had affected the tropospheric flow in a similar fashion.

## 3.5 Stratospheric Warmings

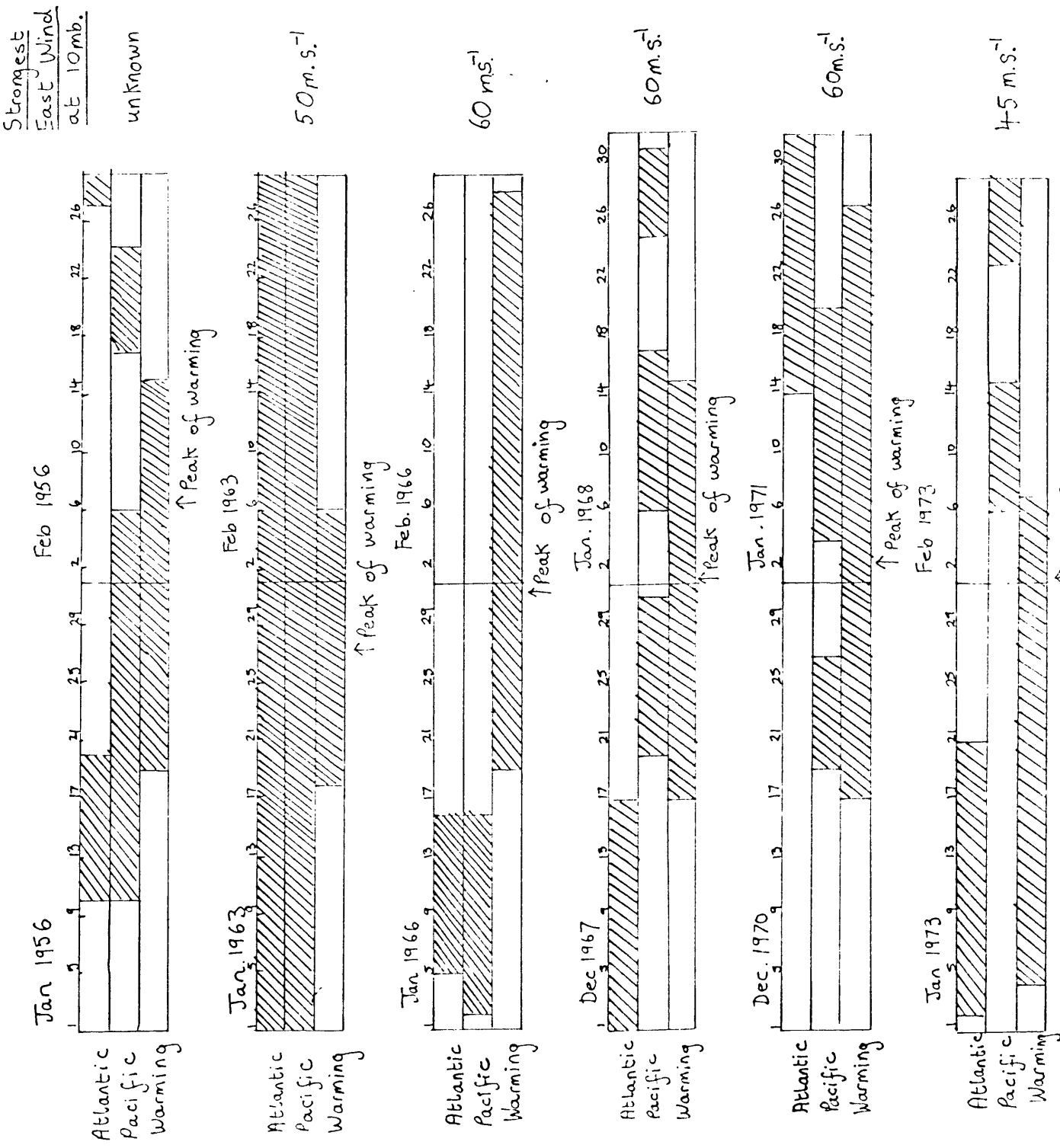
The cause of stratospheric warmings is still under active study and there have been suggestions in the literature that warmings and tropospheric blocking are linked. Labitzke (1965) produced very convincing evidence that Atlantic blocks occur about ten days after the commencement of minor stratospheric warmings. [In minor warmings the stratospheric polar vortex does not actually break down.] The hypothesis to be tested here is that Pacific blocking is likely during the breakdown of a major stratospheric warming. The mechanism envisaged is that the removal of the upper ''lid'' will produce a travelling wavenumber one. This will interfere with a stationary wavenumber one and Pacific blocking will occur during the periods of destructive interference.

Six cases of major stratospheric warmings were investigated and the results are shown in Fig. 3(17). The stratospheric data was kindly supplied by Brian Taylor of the Meteorological Office, Bracknell.

In the cases of January 1956, December 1967, December 1970 and January 1973 Pacific blocking did occur at the end of the warmings. This was not the case for the major warmings of January 1963 and 1966. However, January 1963 was an extremely anomalous month because the flow in the troposphere was dominated by very

Figure 3(17)

Major Warmings and their relationship to tropospheric Blocking



large amplitude wavenumbers two and three. Perhaps it is not surprising that January 1963 does not confrom with the suggested pattern. Many studies of the energetics of the flow in January 1963 have been carried out, for example by Perry (1967), and however interesting and vitally important these results may be, there seems to be a danger in generalising them to cover less spectacular periods of blocking.

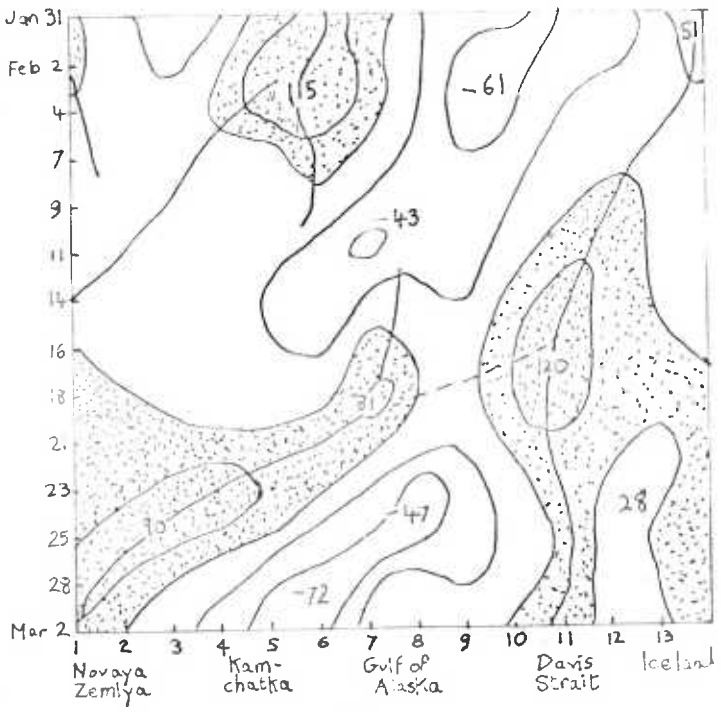
There is an additional piece of information in the literature relevant to the breakdown of the major stratospheric warming of January 1956. This appears in a paper on Pacific blocking by Woffinden (1960). He discusses the ''westward dispacement of a minimum zonal index'' and gives an example of this as February 1957. His figures are reproduced in Fig 3(18) and the following quote is from the paper.

''A positive anomaly band can be followed westward around the Pole. The axis of positive anomaly can be traced from the 510 ft. centre at position 1 (Novaya Zemla) near the end of January, first westward to strongly influence the Davis Strait about mid-February, thence to the Gulf of Alaska and finally on around to Novaya Zemla. In this instance strong blocking highs did appear over North America on the 5 day mean 700 mb. charts centred on February 13th, 16th, 19th, 21st, 24th.'' Thus, from this description, it really does seem as though a travelling wavenumber one occurred towards the end of the warming period. When the phase of this travelling wave was $180^{o}$ different from that of the normal wave Pacific blocking was observed. Note however that the travelling wave was progressive; this is consistent with the earlier suggestion that the travelling waves oberved after the breakdown of a warming could be either progressive or retrogressive.

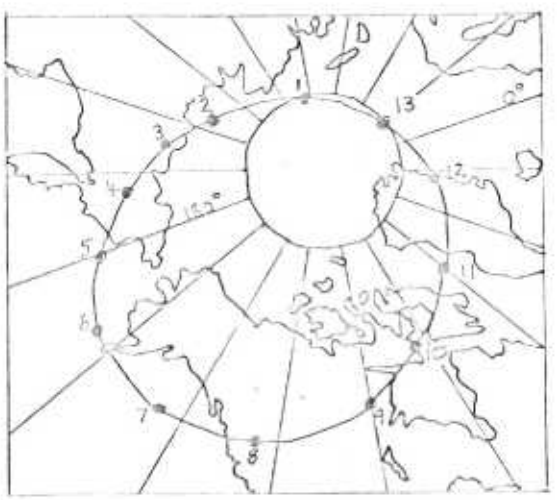
Figure 3(18), from Woffinden (1960)

Time Variation of 700mb. 5-day mean height departure from Normal along the line shown in (b).

[The numbers forming the abscissa of (a) refer to the positions shown in (b) and the ordinate is the central day of the 5 day mean period. Values greater than 400ft. are stippled.]




(a)



(b)

These results on stratospheric warmings are far from conclusive but they may be of some use as a forcasting tool. It is interesting to note that there does not seem to be a typical tropospheric blocking pattern prior to the onset of the major warmings; indeed in December 1970 there was no blocking at all in the fortnight preceeding the warming. This implies that blocking, as distinct from large amplitude long waves, is not cause of stratospheric warmings.

## 3.6 Summary

Pacific blocking was characterised by a local reinforcement of wavenumbers two and three at 500 mb. in the absence of wavenumber one. In the first case (6th to 16th January 1968) this lead to an amplification of wavenumber four which''maintained'' the Pacific block and distorted the whole hemispheric flow. In the second case (25th to 30th January 1968) there was no amplification of wavenumber four and the block was short-lived.

Poleward heat transport by wavenumber one was very small during Pacific blocking as wavenumber one was small in amplitude during these periods. The zonal mean winds decreased at $50^{\circ}N$ during blocking and the sea-level winds went easterly on several occasions. This was accompanied by increased baroclinic activity to the south.

# Chapter FOUR

## CASE STUDIES - PART TWO

## ATLANTIC AND DOUBLE BLOCKING

## Chapter Four Case Studies PART TWO Atlantic and Double Blocking

### 4.1 Introduction

In this chapter further results from case studies are presented. The studies cover the months January 1966 and December 1963; Atlantic and Double blocking were features of both these months.

### 4.2 JANUARY 1966 - Pacific Blocking and Double Blocking

Blocking in this month was classified as follows:

| | | |
|---|---|---|
| Pacific Blocking: | 2 → 6 | (moderate) |
| | 7 → 16 | (weak, with surface anticyclone ill defined) |
| Atlantic Blocking: | 5 → 16 | (strong) |

In the second half of this month the zonal flow looked rather distorted but no periods of blocking were clearly identifiable.

Figs. 4(1) and 4(2) are U.S. Daily Synoptic Weather maps at 500 mb. which illustrate the main features of the blocking.

| | |
|---|---|
| Fig. 4(1), 4th Jan | There is a warm anticyclone in the N.E. Pacific with a central height of 540 dm. |
| Fig. 4(2), 11th Jan, | There is now a warm anticyclone in the N.E. Atlantic with a central height of 564 dm. There is still a warm anticyclone in the N.E. Pacific but this has declined and its central height is 528 dm. |

A day-by-day Fourier analysis was carried out at latitudes $40^{\circ}N$ and $60^{\circ}N$ by the method described in Chapter Three.

Fig 4(3) shows the amplitudes of wavenumbers one, two and three throughout the month. The most striking feature was the amplification of wavenumbers one and two during the first five days of the Atlantic block. Wavenumber two then died away and wavenumber one remained large in amplitude




Figure 4(1) 4 January 1966 (500 mb)

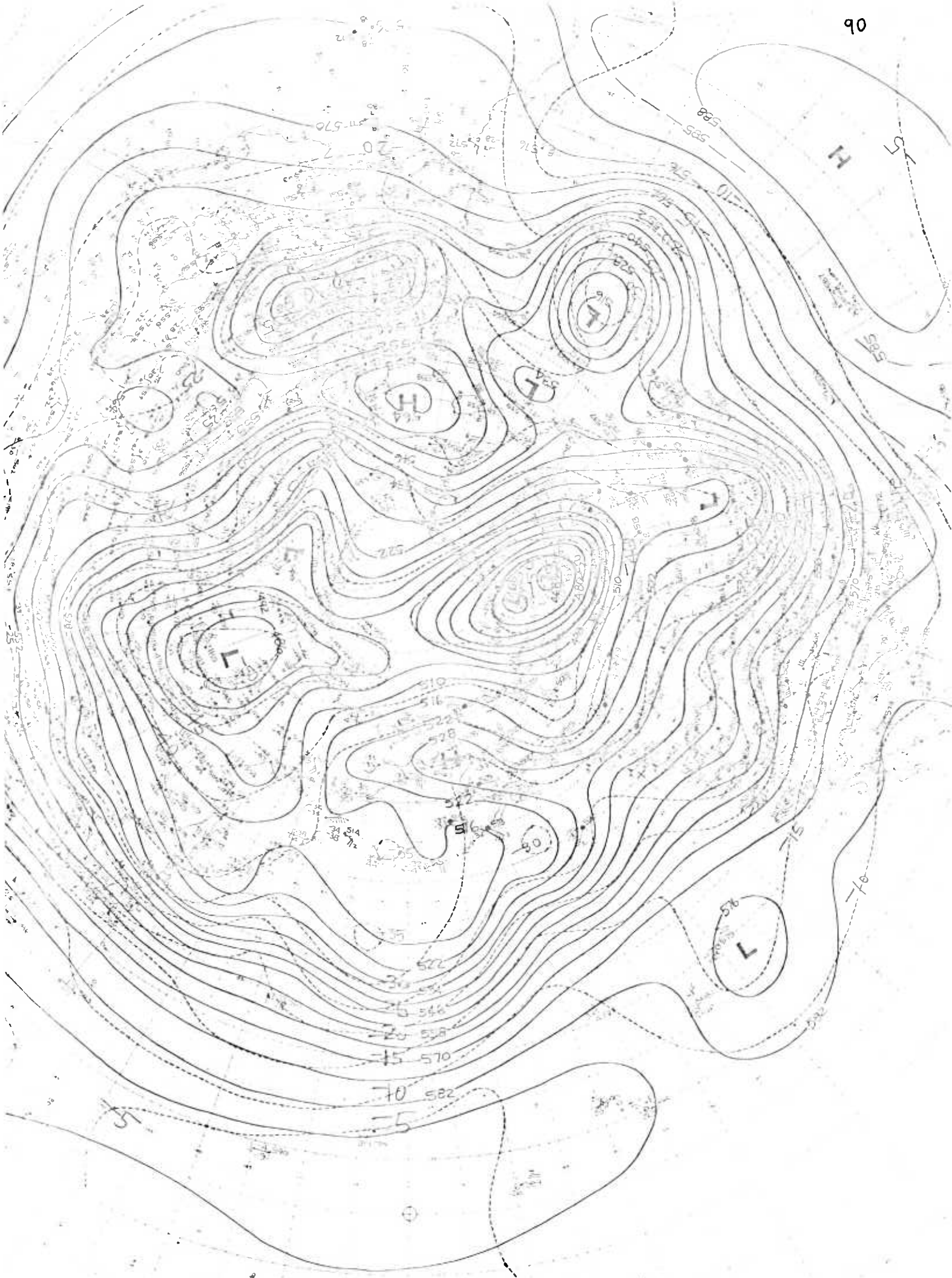
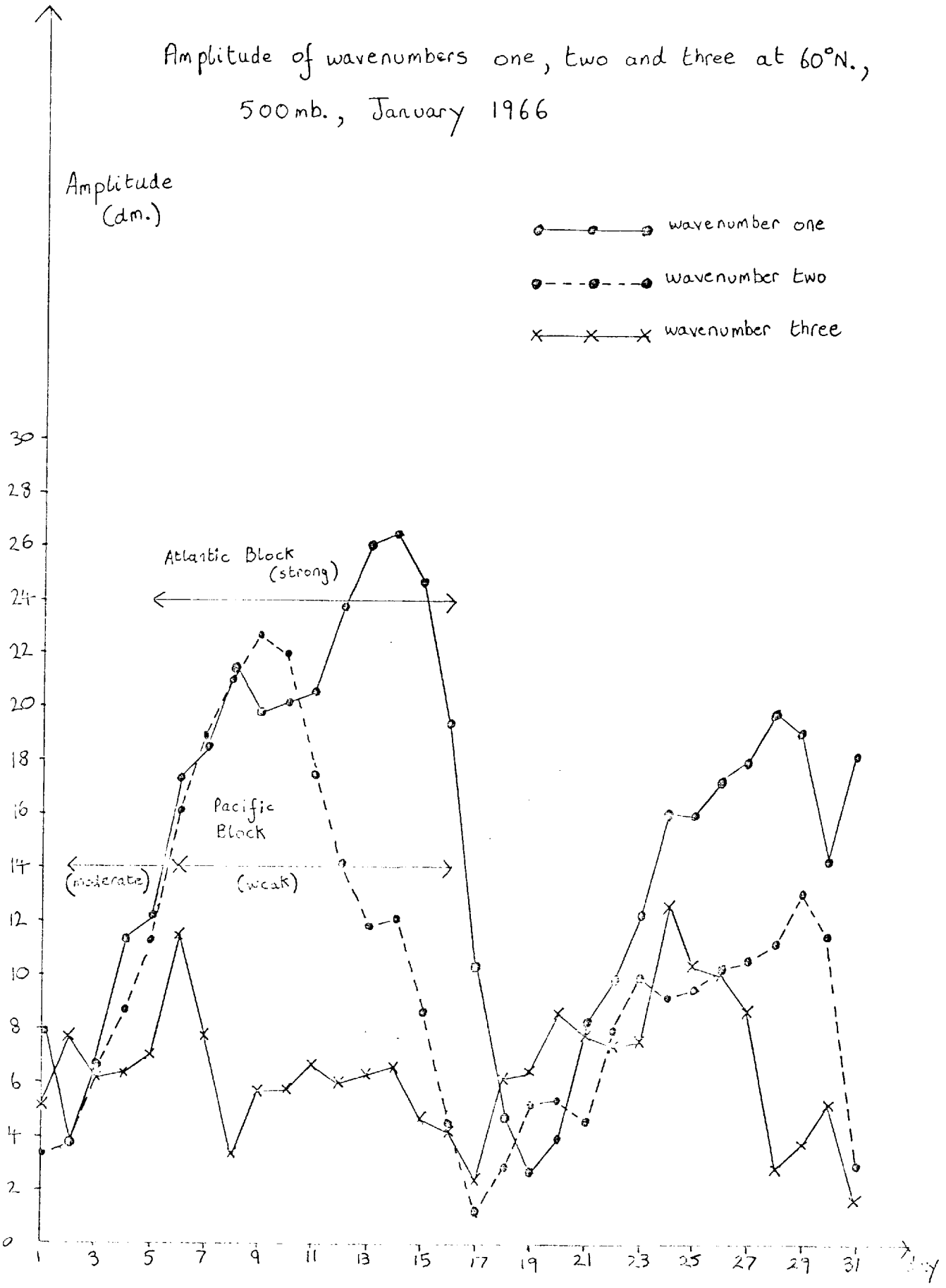


Figure 4(z) 11 January 1966 (500mb)

FIGURE 4(3)


Amplitude of wavenumbers one, two and three at 60°N., 500mb., January 1966
Amplitude (dm.)
wavenumber one
wavenumber two
wavenumber three
Atlantic Block (strong)
Pacific Block
(moderate)
(weak)
0
2
4
6
8
10
12
14
16
18
20
22
24
26
28
30
1
3
5
7
9
11
13
15
17
19
21
23
25
27
29
31
day

until the end of the Atlantic block. The initial Pacific block was associated with the growth of wavenumbers one, two and three but wavenumber three never reached a large amplitude. However, note that the vertical scale in Fig. 4(3) is double that used in Fig. 3(7) and Fig 4(12) in order to allow for the very large amplitude waves in January 1966.

The amplitude of wavenumber four was generally below 10 dm. throughout the month and its amplification was not a feature of the blocking period. Increased wave activity on the baroclinic scale at $40^{o}$N was also not a feature of the blocking.

When the phases of the waves were examined it was found the Atlantic blocking commenced with an almost exact phase coincidence of the ridges of wavenumbers one and two at 500 mb; both waves then amplified rapidly. The breakdown of the block really began on the 11th January, when wavenumber two remained stationary and decayed in amplitude while wavenumber one, although still growing, began to retrogress.

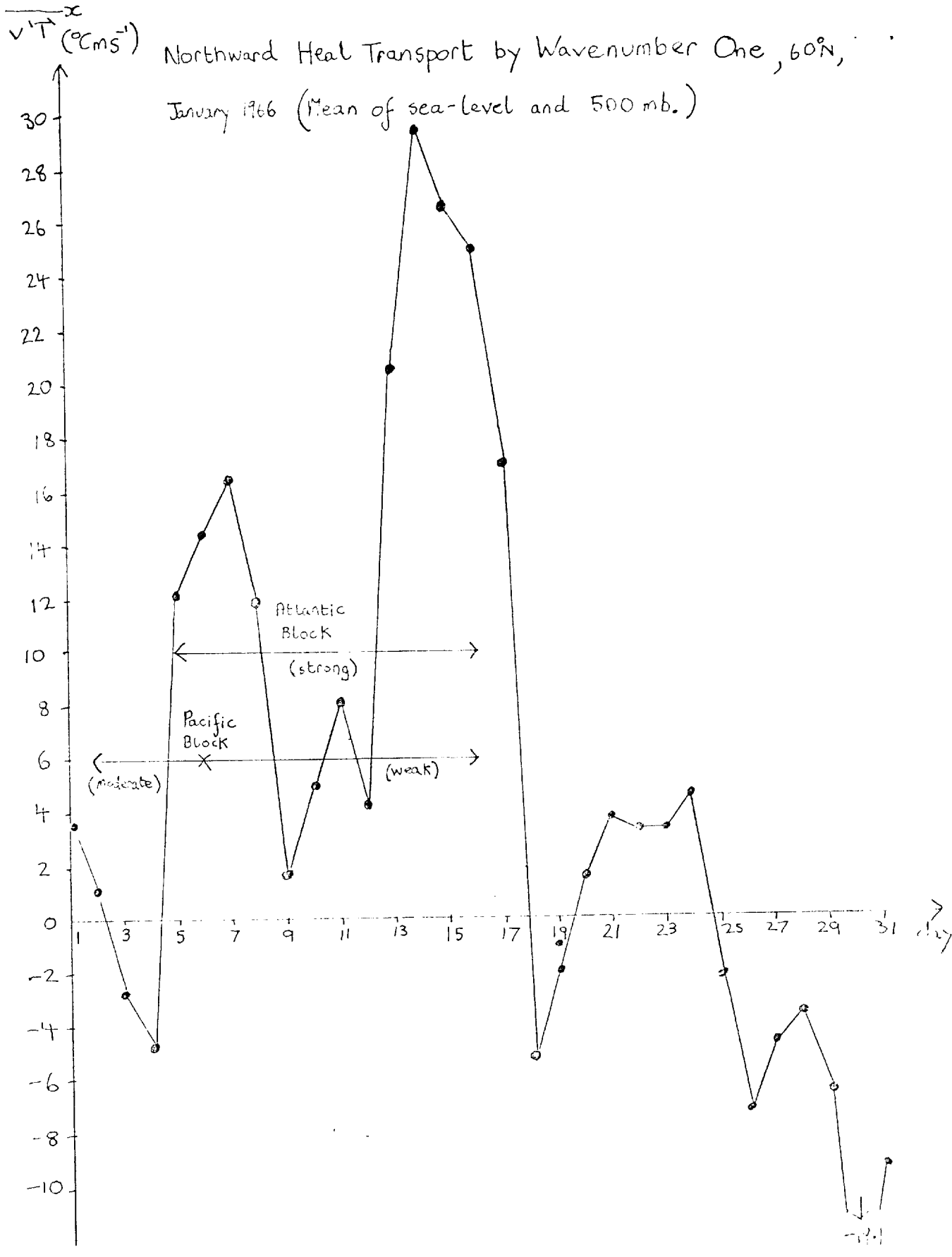
The longitude of the ridges of wavenumbers one and two in this area during the blocking were as follows:

| Date | Wavenumber One | | Wavenumber Two | |
|---|---|---|---|---|
| | 500 mb.(°E) | Sea Level(°E) | 500 mb.(°E) | Sea Level(°E) |
| 4 | -18 | -86 | 20 | 59 |
| 5 Atlantic Blocking starts | 30 | 142 | 27 | 60 |
| 6 | 22 | 86 | 26 | 60 |
| 7 | 19 | 76 | 30 | 58 |
| 8 | 26 | 61 | 23 | 49 |
| 9 | 15 | 23 | 22 | 42 |
| 10 | -1 | 19 | 19 | 51 |
| 11 | -6 | 23 | 18 | 63 |
| 12 | -19 | -7 | 9 | 72 |
| 13 | -29 | 13 | 7 | 72 |
| 14 | -27 | 27 | 11 | 71 |
| 15 | -46 | 31 | 15 | 76 |
| 16 Atlantic Blocking ends | -53 | 80 | 20 | 90 |
| Normal (Eliasen) | 40 | 114 | 33 | 79 |

Again the phase coincidence was more marked at 500 mb. than at sea level. Wavenumber two exhibited a fairly constant slope to the west with height throughout the blocking. Wavenumber one also tilted to the west with height at the start of the blocking. However, this phase slope was considerably reduced during the block but increased again as the block broke down.

The phase changes with height of wavenumber one were used to calculate thepoleward heat transfer by wavenumber one, using equation 3(i). These results are shown in Fig 4(4). The poleward heat transfer

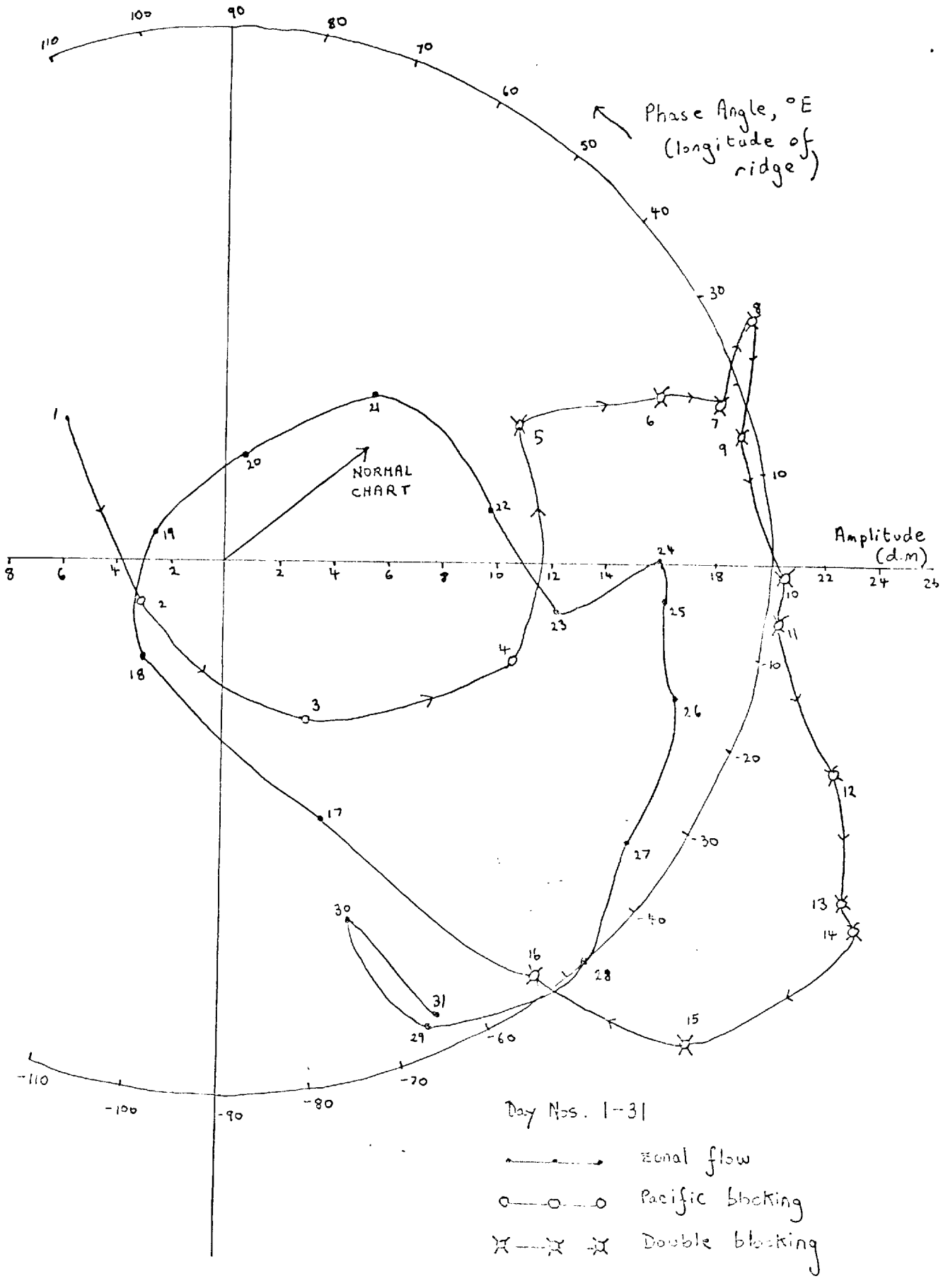
FIGURE 4(4)


$\overline{v'T'}^x$ (°Cms⁻¹)
Northward Heat Transport by Wavenumber One, 60°N,
January 1966 (Mean of sea-level and 500 mb.)
30
28
26
24
22
20
18
16
14
12
10
8
6
4
2
0
-2
-4
-6
-8
-10
1
3
5
7
9
11
13
15
17
19
21
23
25
27
29
31
Atlantic Block
(strong)
Pacific Block
(moderate)
(weak)

by wavenumber one was very large at the beginning and end of the block, reflecting the large wave amplitudes and the tilt of the wave to the west with height. However, in the middle of the block the heat transport fell to nearly zero despite the large wave amplitudes. This was due to the phase lines of wavenumber one becoming nearly vertical. The very large negative value for the heat transport at the end of the month was surprising but does not correspond to an obvious synoptic feature.

Fig 4(5) shows an amplitude - phase polar plot of wavenumber one at 60°N, 500 mb. for January 1966. Initially wavenumber one was of small amplitude and progressive. When the phase was nearly that of the normal wave it became stationary, amplified and then retrogressed. This indicates an increase in either the vertical or meridional wavenumber. This retrogression continued until the end of the month. In the second half of the month the data could be interpreted as being the interference pattern produced by a stationary and travelling wavenumberone. It therefore seems surprising that there was no Atlantic blocking in the period 23rd to 28th January when the amplitude of wavenumber one was large. However, during this period there was at no time a marked coincidence of the phases of wavenumbers one and two. This suggests that the local reinforcement of wavenumbers one and two could be important in initiating Atlantic blocking.

In Chapter Three it was found that in January 1968 Pacific blocking was due to the interference of wavenumbers two and three. This was again the case in January 1966. The longitude of the ridges of these waves at 60°N in the N.E. Pacific were as follows:



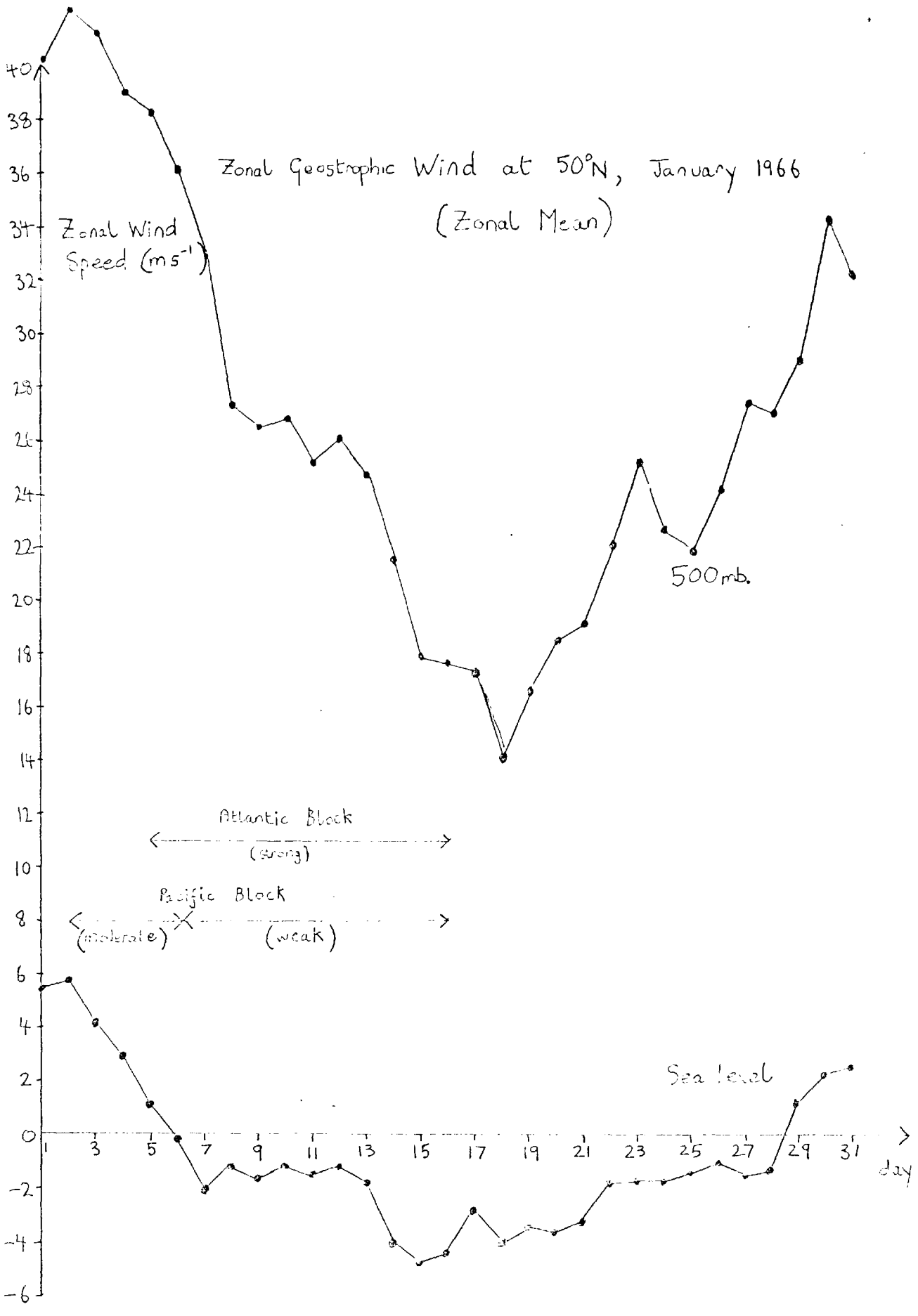

Amplitude - Phase Polar Plot of wavenumber one at 500mb, 60°N, January 1966

| Date | Wavenumber Two | | Wavenumber Three | |
|---|---|---|---|---|
| | 500 mb.(°E) | Sea Level(°E) | 500 mb.(°E) | Sea Level(°E) |
| 1 | 184 | 256 | 194 | 248 |
| 2 Pacific Blocking starts | 199 | 254 | 201 | 227 |
| 3 | 198 | 231 | 203 | 232 |
| 4 | 200 | 239 | 207 | 243 |
| 5 Atlantic Blocking starts | 207 | 240 | 238 | 251 |
| 6 | 206 | 240 | 247 | 254 |
| Normal (Eliasen) | 213 | 259 | 228 | 252 |

This local reinforcement between wavenumbers two and three continued during the Double blocking but it was almost eliminated by the trough of wavenumber one. This is consistent with the fact that the central height of the Pacific block at 500 mb. was about 40 dm. lower than that of the Atlantic block. Before leaving this discussion of the wave phases, it is interesting to note that it was only the phase of wavenumber one which showed significant departures from its normal phase during the blocking.

The geostrophic zonal wind speeds during January 1966 at 50°N were calculated; these are shown in Fig. 4(6). The zonal westerly winds were very strong at the beginning of the month but decreased rapidly during the blocking; the sea level winds went easterly during the blocking. The westerly winds at 500 mb. increased after the breakdown of the blocking but the sea level winds did not go westerly again until 29th January. As in Chapter Three, the implication of these results is that westerly momentum was being tansported out

FIGURE 4(6)


Zonal Geostrophic Wind at 50°N, January 1966
(Zonal Mean)
Zonal Wind Speed ($m s^{-1}$)
500mb.
Atlantic Block
(strong)
Pacific Block
(moderate)
(weak)
Sea level
day

of mid-latitudes during the blocking.

Summary

Strong Atlantic blocking was characterised by an initial phase coincidence of the ridges of wavenumbers one and two, followed by strong amplification of both these waves. Blocking in the Pacific was characterised by a local reinforcement of wavenumbers two and three, although this was practically eliminated by the trough of wavenumber one during the Double blocking. Poleward heat transport by wavenumber one was large at the beginning and end of the Atlantic blocking, but small in the middle of this blocking. The zonal mean of the zonal wind speed at 500 mb. at 50°N decreased during the blocking and the sea-level winds went easterly. The zonal wind speeds returned to more normal values about a week after the blocking had broken down.

## 4.3 DECEMBER 1963 - Atlantic, Pacific and Double Blocking

Blocking this month was classified as follows:

| | | |
|---|---|---|
| Atlantic Blocking: | 1 - 8 | (strong) |
| | 11 - 17 | (strong) |
| Pacific Blocking: | 8 - 13 | (weak) |

The main features of the flow throughout the month are shown in Figs. 4(7) to 4(10), which are taken from U.S. Daily Synoptic Weather Maps at 500 mb.

| | | |
|---|---|---|
| Fig. 4(7) | 1st Dec. | There is a warm anticyclone with a central height of 564 dm. over Europe. |
| Fig. 4(8) | 3rd Dec. | The anticyclone has moved to the east so that it is now centred over Iceland, with a central height of 570 dm. It has warmed by about 10°C. |

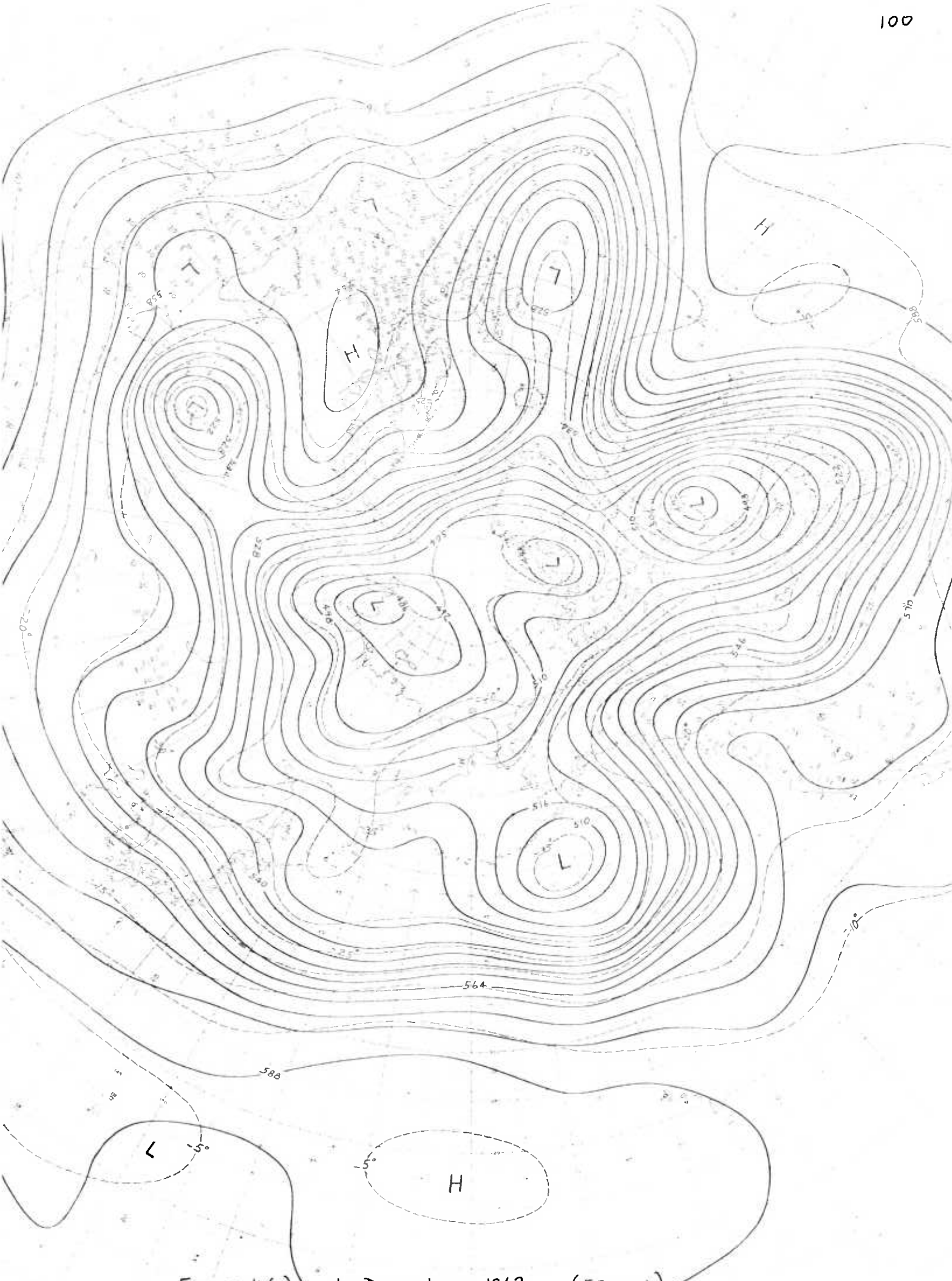



Figure 4(7) 1 December 1963 (500 mb)




Figure 4(8) 3 December 1963 (500mb)

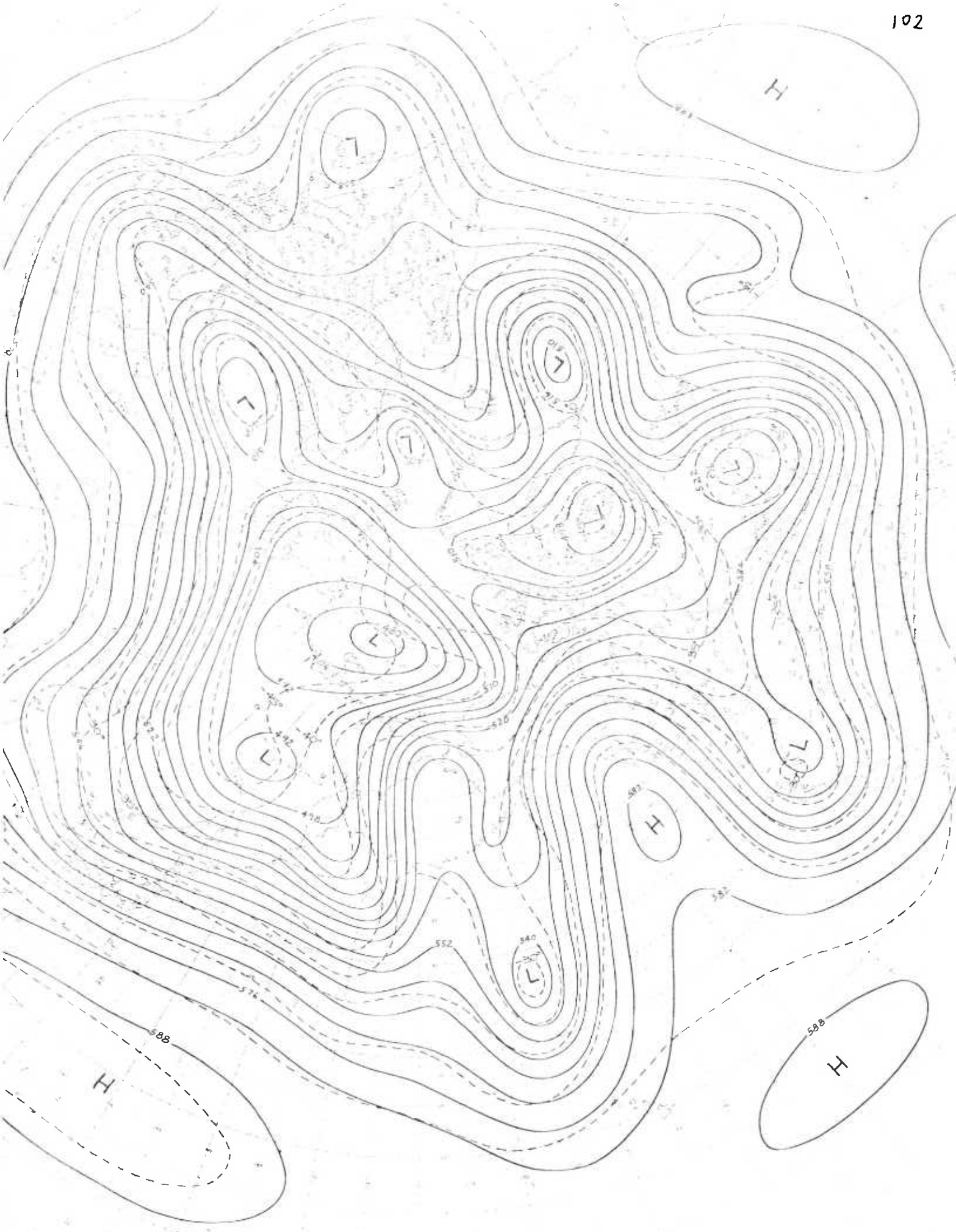



Figure 4(9) 10 December 1963 (500mb)

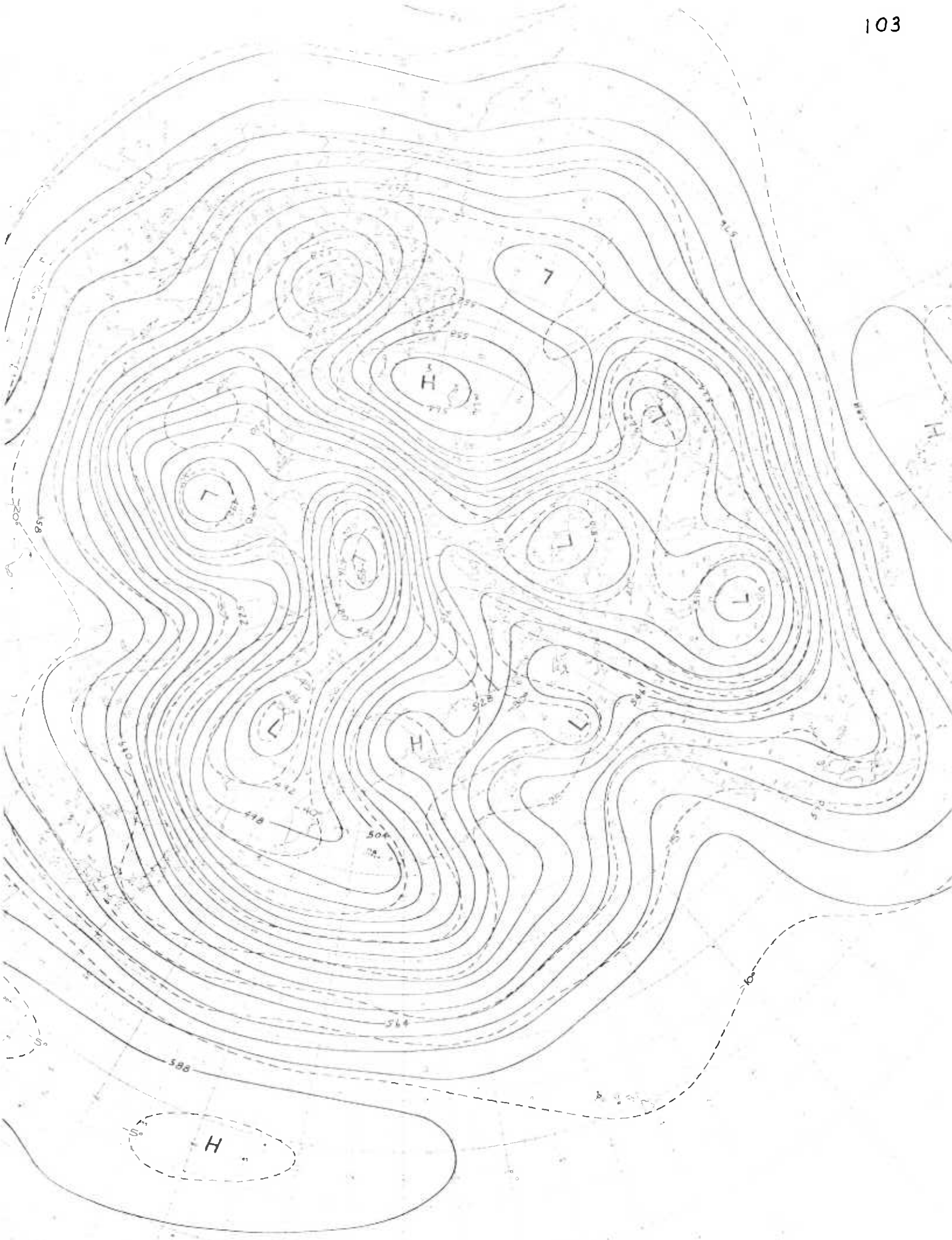



Figure 4(10) 13 December 1963 (500 mb)




Figure 4(11) 30 December 1963. (500 mb)

| | | |
|---|---|---|
| Fig. 4(9) | 10th Dec. | Blocking in the Atlantic sector has temporarily broken down and a warm ridge is established in the Pacific sector. |
| Fig. 4(10) | 13th Dec. | Atlantic blocking is well established with a central height of 564 dm. The high is centred over Iceland but extends well to the east to affect the coast of Canada. Blocking in the Pacific is breaking down. |
| Fig. 4(11) | 30th Dec. | Zonal flow is well established at the end of the month. |

A day-by-day Fourier analysis was carried out at latitudes $40^{\circ}$N and $60^{\circ}$N by the method described in Chapter Three.

Fig. 4(12) shows the amplitude of wavenumbers one and four throughout the month. The main feature was the amplification of wavenumber one, and to a lesser extent wavenumber four, during both periods of Atlantic blocking. Wavenumber one was not of large amplitude during the first four days of the Pacific blocking. Fig 4(13) shows the amplitudes of wavenumbers two and three throughout the month. The main feature to note here was the strong growth in wavenumbers two and three during the Pacific blocking. Wavenumber three was of large amplitude during the second period of Atlantic blocking.

An examination of the phases of the long waves showed that the Atlantic blocking was due mainly to an interferencebetween wavenumbers one and three, not one and two as was the case in January 1966. At the beginning of the month the block was already established over Europe and wavenumber one was the main component of this pattern. However, as the block shifted to the Atlantic wavenumbers one and three together produced the high, while at the end of the blocking wavenumber three alone was ''maintaining'' the blocking in the Atlantic sector. In both cases of Atlantic blocking the ridge of wavenumber four was about $30^{\circ}$ long. upstream from the longitude of of maximum reinforcement of wavenumbers one and three.

FIGURE 4(12)

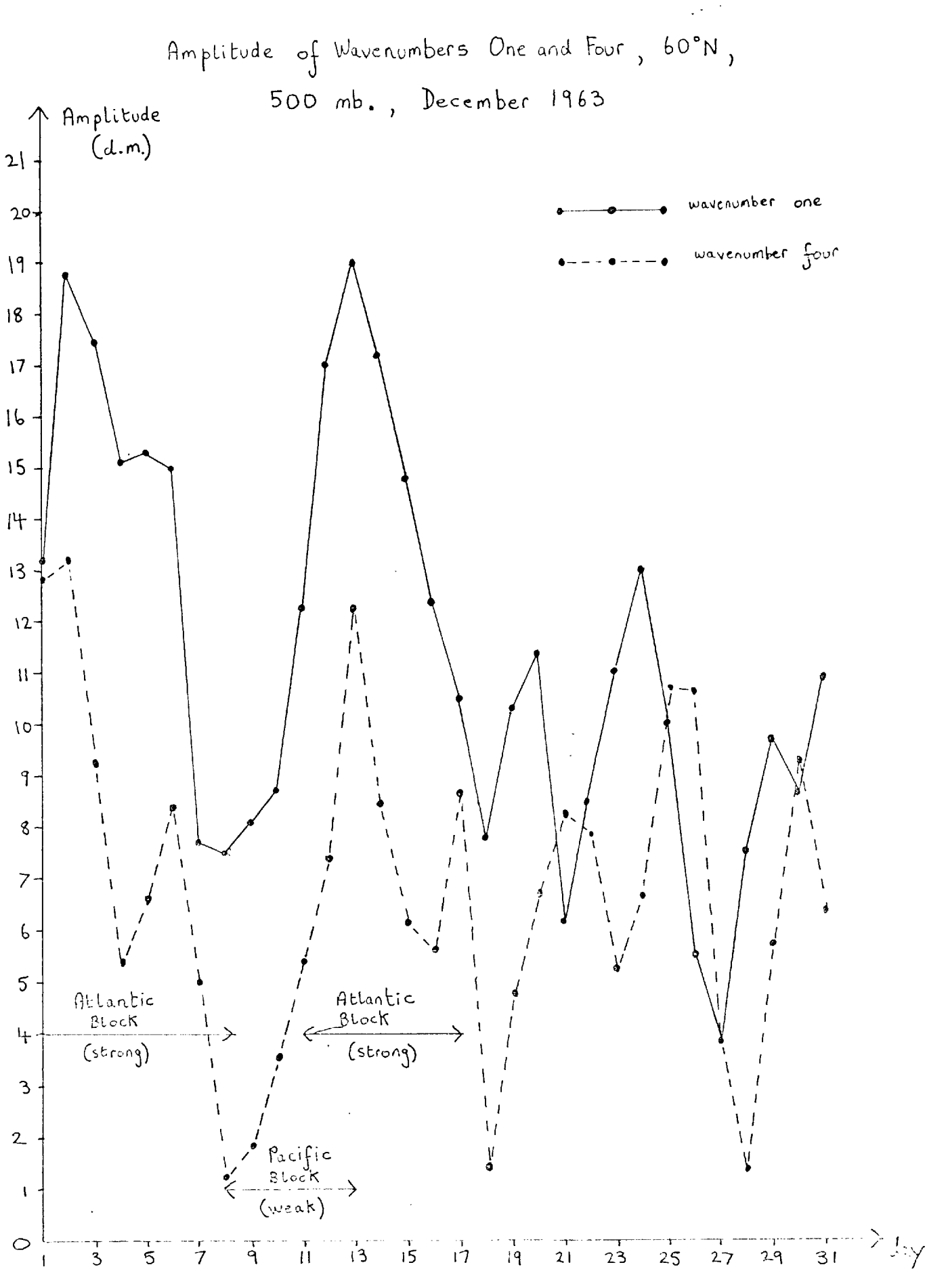
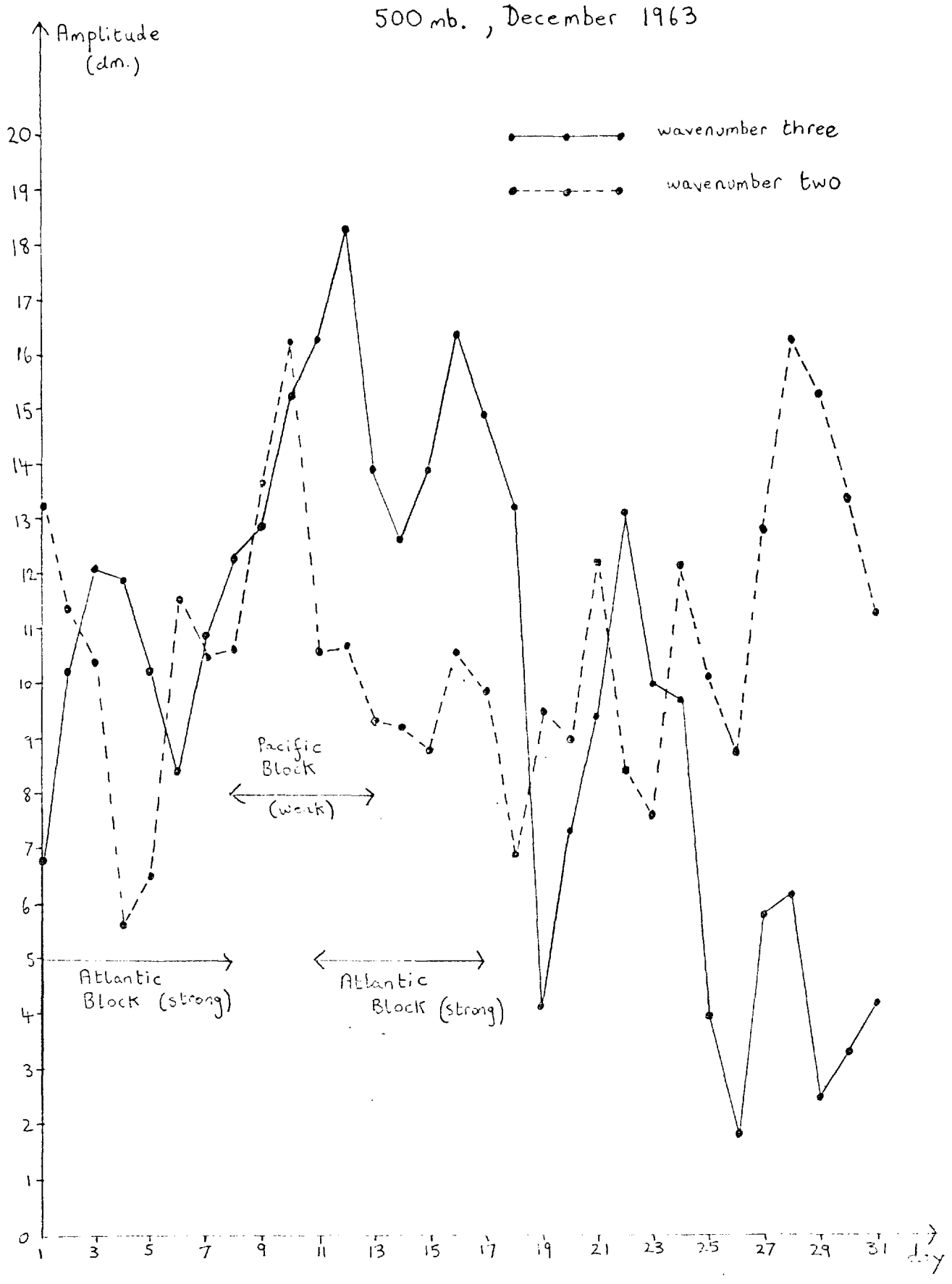

Amplitude of Wavenumbers One and Four, 60°N, 500 mb., December 1963
Amplitude (d.m.)
wavenumber one
wavenumber four
Atlantic Block (strong)
Atlantic Block (strong)
Pacific Block (weak)
Day

FIGURE 4(13)

Amplitude of Wavenumbers Two and Three, 60°N, 500 mb., December 1963



The longitude of the ridges in the Atlantic sector of wavenumbers one, three and four were as follows:

| Date | Wavenumber One | | Wavenumber Three | | Wavenumber Four | |
|---|---|---|---|---|---|---|
| | 500 mb(°E) | Sea Level(°E) | 500 mb.(°E) | Sea Level(°E) | 500 mb.(°E) | Sea Level(°E) |
| 1 Atlantic Blocking | 18 | 53 | 316 | 355 | 306 | 324 |
| 2 | 344 | 24 | 319 | 352 | 309 | 329 |
| 3 | 341 | 359 | 333 | 360 | 314 | 339 |
| 4 | 341 | 355 | 338 | 357 | 313 | 349 |
| 5 | 341 | 18 | 341 | 355 | 303 | 318 |
| 6 | 335 | 20 | 341 | 347 | 307 | 313 |
| 7 | 314 | 265 | 338 | 351 | 315 | 346 |
| 8 Atlantic Blocking breaks down | 314 | 270 | 335 | 357 | 327 | 329 |
| 9 | 280 | 222 | 329 | 1 | 278 | 360 |
| 10 | 288 | 256 | 330 | 1 | 278 | 281 |
| 11 Atlantic Blocking recommences | 299 | 345 | 324 | 351 | 293 | 301 |
| 12 | 307 | 333 | 326 | 355 | 297 | 314 |
| 13 | 304 | 320 | 330 | 353 | 289 | 285 |
| 14 | 292 | 296 | 332 | 353 | 295 | 326 |
| 15 | 294 | 316 | 332 | 349 | 297 | 334 |
| 16 | 266 | 212 | 330 | 347 | 292 | 333 |
| 17 Atlantic Blocking breaks down | 253 | 188 | 313 | 346 | 293 | 308 |
| 18 | 232 | 176 | 315 | 349 | 293 | 334 |

The phases coincidence of wavenumbers one and three was not very marked during the second period of Atlantic blocking; this is consistent with Fig. 4(10) which shows a rather large lateral extent of the anti-cyclone in the Atlantic.

Pacific blocking was again due to contructive interference between wavenumbers two and three when wavenumber one was not of large amplitude. The longitude of the ridges of wavenumbers two and three in the Pacific sector were as follows.

| Date | Wavenumber Two | | Wavenumber Three | |
|---|---|---|---|---|
| | 500 mb.(°E) | Sea Level(°E) | 500 mb.(°E) | Sea Level(°E) |
| 7 | 184 | 251 | 218 | 231 |
| 8 Pacific Blocking commences | 200 | 257 | 215 | 237 |
| 9 | 206 | 300 | 209 | 241 |
| 10 | 204 | 237 | 210 | 241 |
| 11 | 203 | 235 | 204 | 231 |
| 12 | 189 | 232 | 206 | 235 |
| 13 Pacific Blocking breaks down | 176 | 166 | 210 | 233 |

It can be seen from the above tables that the phase lines of all the long waves leaned to the west with height all of the time, with the exception of wavenumber one during the breakdown of both blocking periods in the Atlantic. During these two periods of easterly phase tilt with height the amplitude of wavenumber one was small. Fig. 4(14) shows the poleward heat transport by wavenumber one at 60°N, calculated using equation 3(i). The poleward heat transport during the two periods of Atlantic blocking was positive but not large; it was small and negative at the end of both these blocking periods. Fig. 4(14) should be compared with Fig. 4(4), which shows large values for the

FIGURE 4(14)

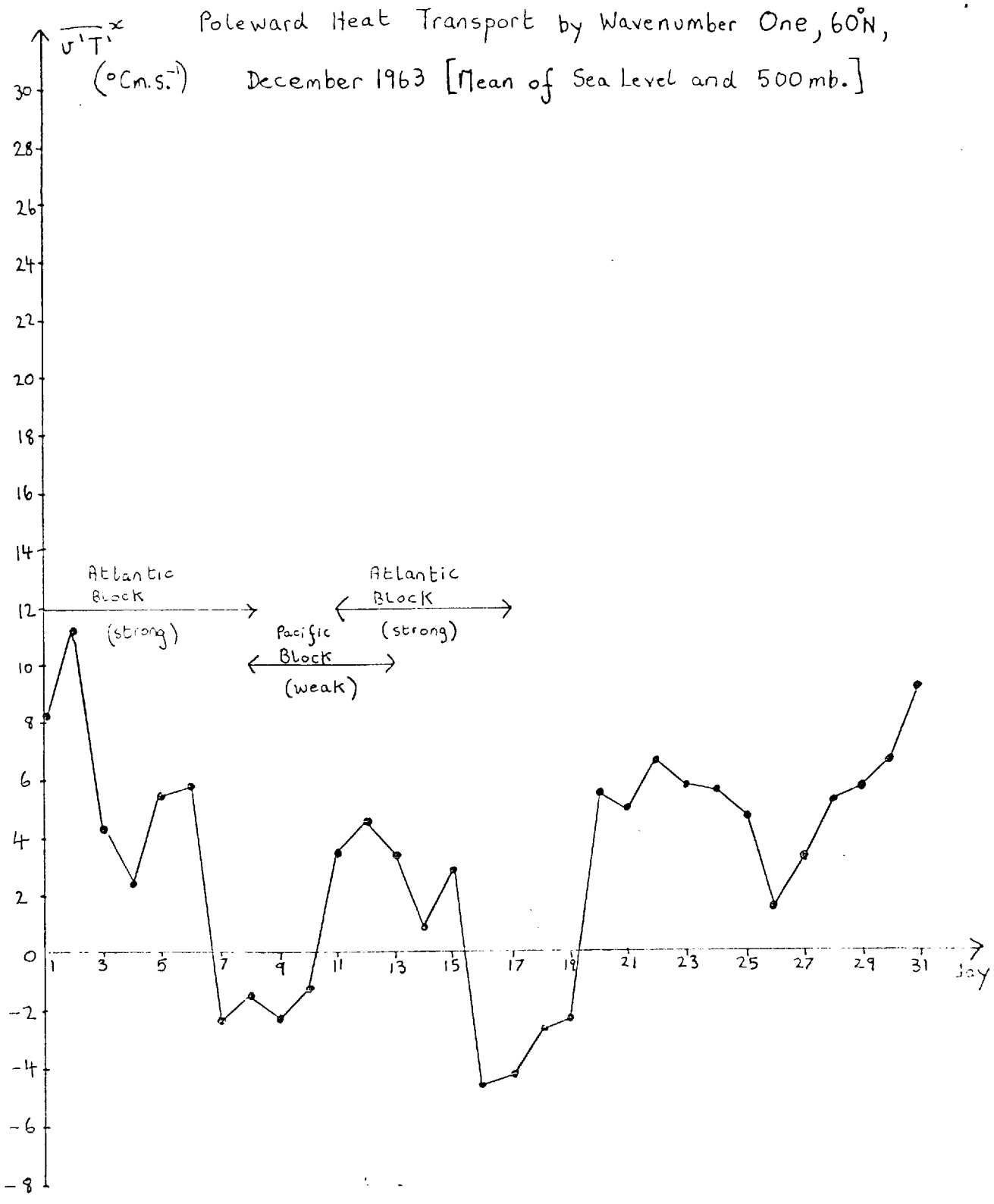
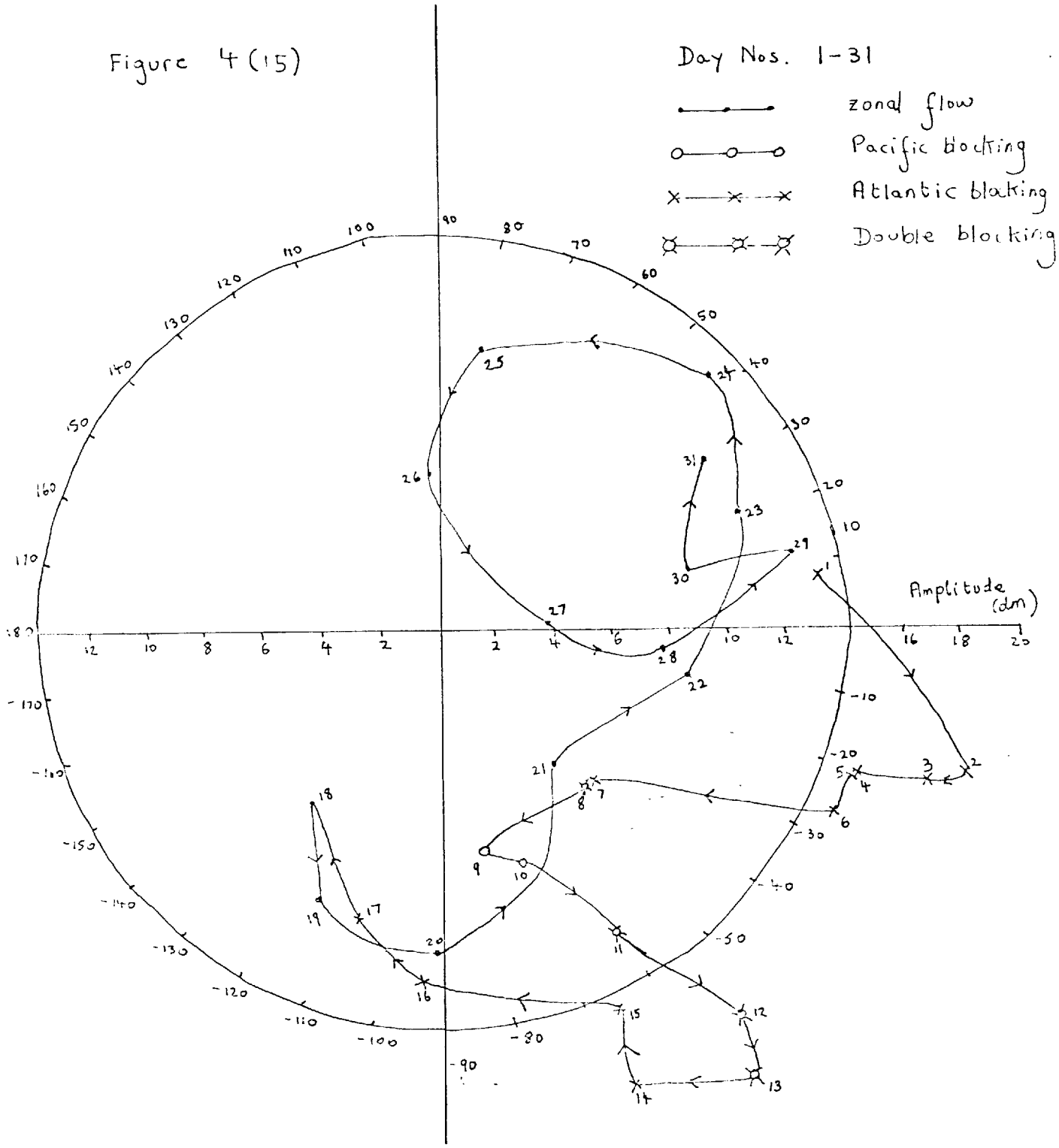

$\overline{v'T'}^x$ (°Cm.s.$^{-1}$)
Poleward Heat Transport by Wavenumber One, 60°N,
December 1963 [Mean of Sea Level and 500 mb.]
30
28
26
24
22
20
18
16
14
12
10
8
6
4
2
0
-2
-4
-6
-8
Atlantic Block (strong)
Pacific Block (weak)
Atlantic Block (strong)
1
3
5
7
9
11
13
15
17
19
21
23
25
27
29
31
day

Figure 4 (15)

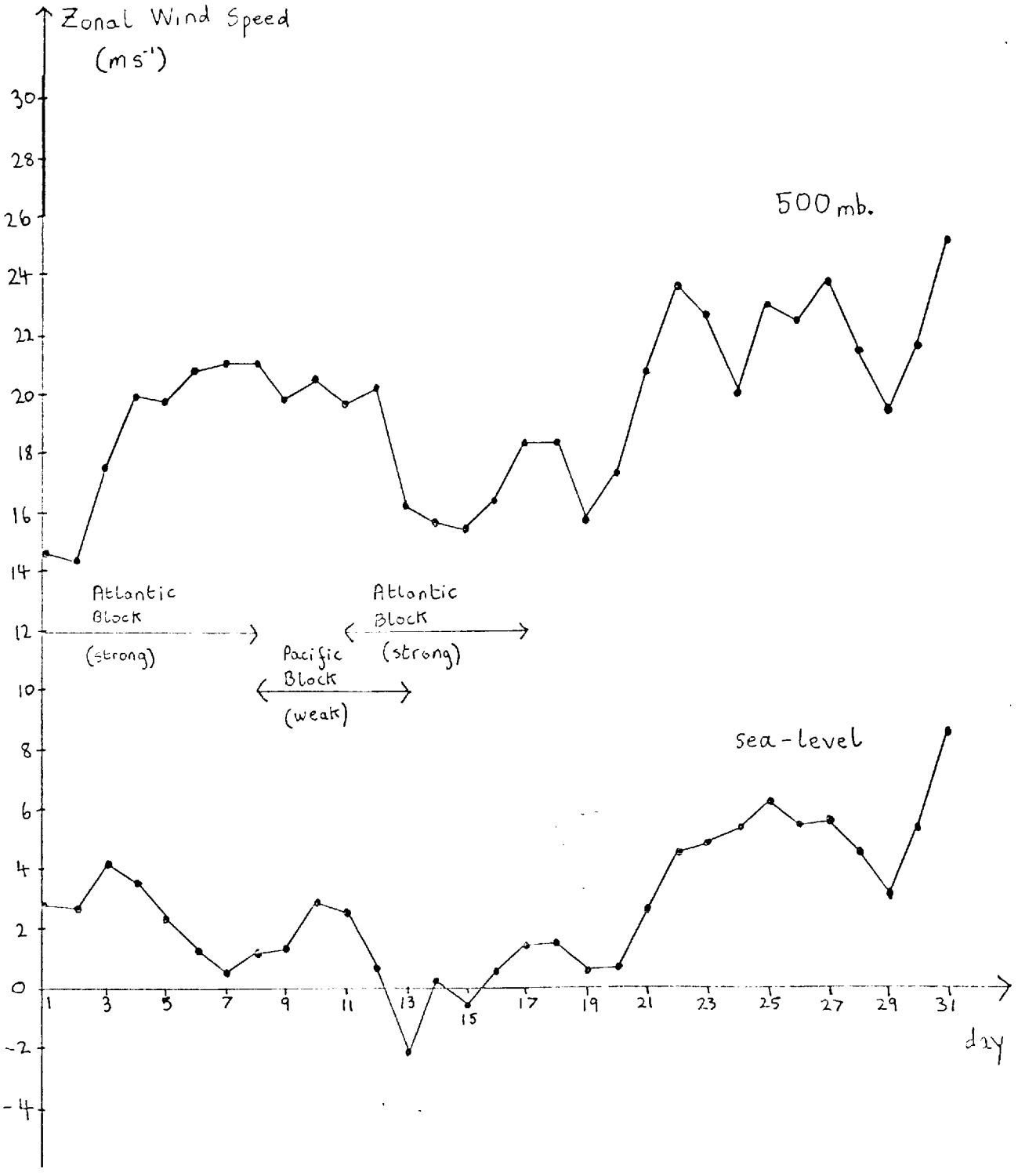



Amplitude - Phase Polar Plot of Wavenumber One at 500mb, 60°N, December 1963

FIGURE 4(16)

Zonal Geostrophic Winds at 50°N, December 1963

(Zonal Mean)



poleward heat transport by wavenumber one during Atlantic blocking in January 1966. This difference was due to the amplitude of wavenumber one being much larger in January 1966 than December 1963, and the magnitude of the heat transfer depends on the square of the amplitude of the wave. However, it is clear that Atlantic blocking broke down in different fashions in the two months. In January 1966 the large amplitude wavenumber one retrogressed and then decreased in amplitude, while the opposite sequence of events happened in December 1963. Thus the heat transfer by wavenumber one was large during the breakdown of the Atlantic blocking in January 1966, and small during the breakdown of the Atlantic blocking in December 1963. Fig. 4(15) shows an amplitude-phase polar plot of wavenumber one during December 1963. The behaviour of the wave was rather unstructured and cannot be interpreted as containing stationary and travelling waves. There was a clear phase difference between the two positions of Atlantic blocking and the reason for this is not obvious.

Fig. 4(16) shows the zonal-mean geostrophic zonal winds at 500 mb. and sea level. The month commenced with a low wind speed at 500 mb., this increased until the second Atlantic blocking period, when it decreased again. The zonal wind speeds at 500 mb. were greatest in the second half of the month when there was no blocking. The sea level wind speeds decreased during the first half of the month when there was blocking and these winds went easterly on two occasions. The sea level winds returned to being westerly again in the second half of the month when there was no blocking. Again the implication was that westerly momentum was being transported out of mid-latitudes during the blocking.

Summary

The two periods of Atlantic blocking were characterised by a local reinforcement of wavenumbers one and three. Wavenumber four did amplify during these two blocking periods, with the phase of its ridge about $30^{o}$ long. upstream from the main anticyclone. However, at no time did wavenumber four dominate the flow in the way that it did in January 1968. The one period of Pacific blocking was associated with the strong growth of wavenumbers two and three and constructive interference between these waves in the Pacific sector. The poleward heat transport by wavenumber one during the Atlantic blocking was positive but not large. The blocking was accompanied by a decrease in the zonal wind speeds at $50^{o}$N and easterly sea-level winds.

## 4.4 General Conclusions from Case Studies

Blocking never commences with the amplification of a single wavenumber in isolation, but with a local reinforcement of long waves at 500 mb. In the Atlantic sector this reinforcement is either between wavenumbers one and two or between wavenumbers one and three. In the Pacific sector this initial reinforcement is between wavenumbers two and three, but this only manifests itself as blocking if wavenumber one is small. For example, Pacific blocking is likely to occur if there is destructive interference between a stationary and travelling wavenumber one. The long waves which contribute to the initiative of blocking have amplitudes which are large compared with those on normal charts, but generally have near-normal phases.

Thus the Fourier analysis has confirmed the synoptic impression that blocking anticyclones are initially spatially ''isolated'' phenomena. However, it has shown that blocking in different regions is associated with different combinations of wavenumbers. Because of the variation of energy transports with wavenumber, this result shows that it is important to specify the type of blocking being discussed before making statments on, for example, the typical change in poleward heat transfer during blocking. For example, the initiation of an Atlantic block is associated with an amplification of wavenumber one and, at least in the first few days of the block, enhanced poleward heat transport by wavenumber one. This is not true for Pacific blocking. This enhanced heat transport by wavenumber one is consistent with the decrease in ZAPE associated with Atlantic blocking (see Chapter Two). ZAPE and the mean wind shear are directly related through the thermal wind equation. Fig. 4(18)

FIGURE 4 (17)

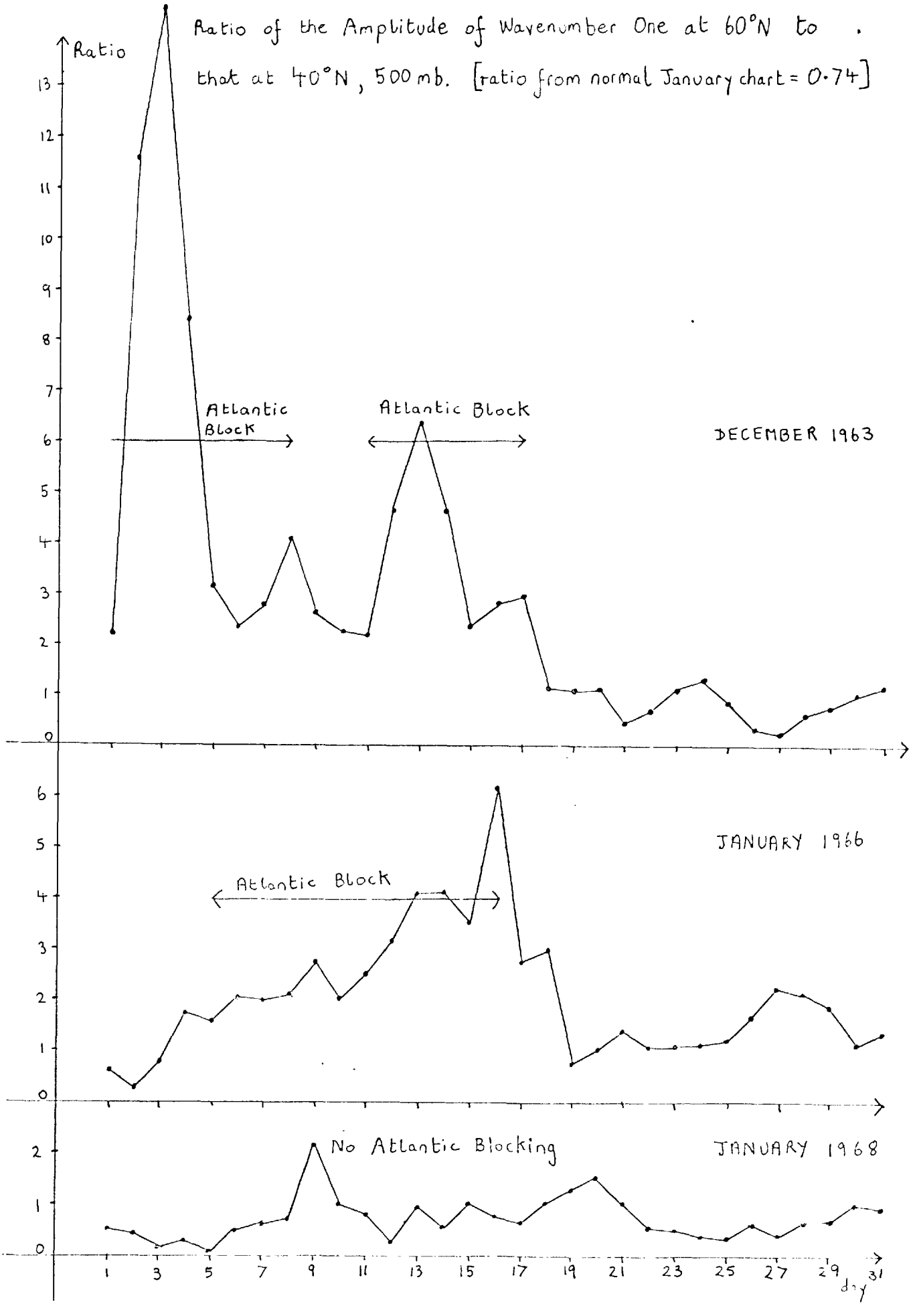
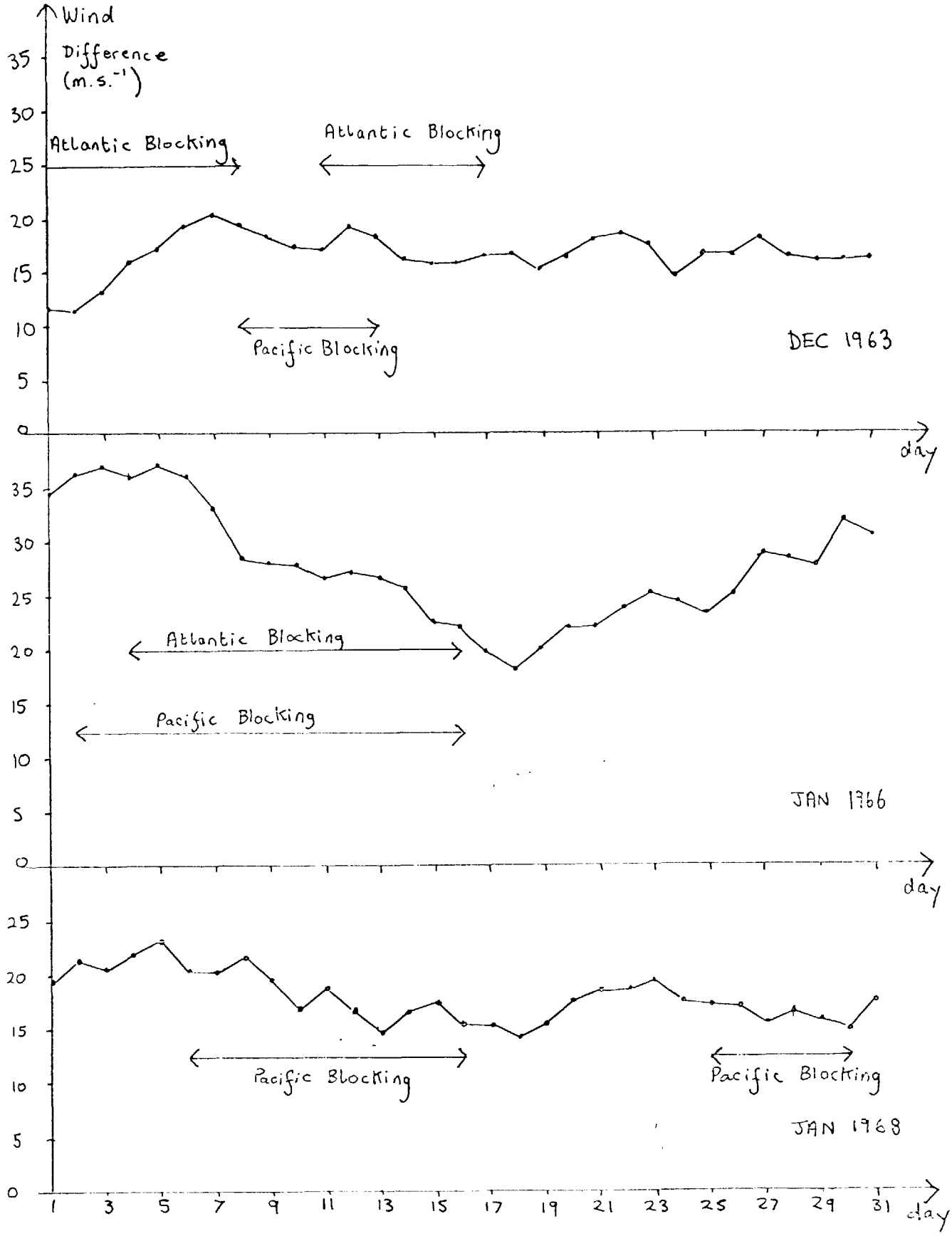

Ratio of the Amplitude of Wavenumber One at 60°N to that at 40°N, 500 mb. [ratio from normal January chart = 0·74]
Ratio
Atlantic Block
Atlantic Block
DECEMBER 1963
Atlantic Block
JANUARY 1966
No Atlantic Blocking
JANUARY 1968
day

Figure 4 (18)

Wind Difference between sea-level and 500mb. of the Zonal Mean Geostrophic Wind, 50°N.



shows the zonal wind difference between sea-level and 500 mb. for the three case studies. In January 1966 the month commenced with a very high value of wind shear which decreased rapidly as Atlantic blocking set in. December 1963 commenced with an established Atlantic block and a very low value for the wind shear, which increased as the blocking broke down. In January 1968 there was no Atlantic blocking but the wind shear did decrease during the first period of Pacific blocking. This could have been due to enhanced poleward heat transport by wavenumber four. Thus these results do tend to support previous observations which indicate blocking, in particular Atlantic blocking, is associated with a decrease in ZAPE.

These case-studies have concentrated on the zonal wavenumbers associated with blocking patterns and no mention has been made yet of the meridional scale of the motion; this obviously decreases when a split jet-stream is involved. It was not possible to calculate meridional wavenumbers from the data analysed, but an attempt was made to detect a change in meridional scale by comparing the amplitudes of the waves at $60^{\circ}N$ with their amplitudes at $40^{\circ}N$. These results for wavenumber one are shown in Fig. 4(17). The decrease of meridional scale of wavenumber one during Atlantic blocking is striking. Interestingly, this close correlation between the decrease in meridional scale and blocking (Atlantic or Pacific) was not found for wavenumbers two and three. This is consistent with the subjective impression that Pacific blocking is often just a warm ridge extending poleward from the tropics while Atlantic blocking almost always consists of a ''cut-off'' high and a split jet-stream. Thus the criterion for initiating Atlantic blocking seems to be a large amplitude, stationary wavenumber one, with high meridional wavenumber and near-normal phase, interfering with

wavenumbers two or three at 500 mb. It will be argued later that 500 mb. rather than the surface, is the important height for interference between long waves because this is very near the steering level of baroclinic waves. From the point of view of general circulation models, it is important to predict the phases of wavenumbers one, two and three correctly to represent this interference. The data suggests that the phases should be correct to within $10^{o}$ of longitude at 500 mb. Possible errors in the phases of the long waves analysed in these case studies will be discussed in Appendix Two.

Fourier analysis also showed that an isolated blocking anticyclone, once established, can then develop into a global scale disturbance characterised by a single wavenumber, for example wavenumber four in January 1968. This indicates that an additional mechanism is at work in a persistent blocking situation; one of the manifestations of this mechanism is thetransport of westerly momentum out of mid-latitudes.

Another surprising feature shown by the Fourier analysis is that the long waves lean to the west with height during the early stages of blocking, despite the blocking anticyclone itself being warm and having no obvious vertical phase tilt. This is mainly due to the long waves having a much closer phase coincidence at 500 mb. than at the surface, so that the surface anticyclone is actually rather ill-defined. However, in the strong Atlantic blocking of Jan. 5th to Jan. 17th 1966 wavenumber one lost its phase tilt with height during the peak of the blocking, causing the associated poleward heat transportto fall to zero. This loss of phase tilt with height of wavenumber one may be yet another feature which distinguishes a persistent blocking situation from a short-lived one.

These general features of blocking have been deduced from the three months analysed and need to be tested in a more rigorous case-study. This case study would involve analysing hemispheric data into spherical harmonics at many levels in the troposphere and stratosphere. However, the implication from the results presented here is that it is the long waves due to topographic forcing which need to be predicted correctly in order to forecast the initiation of a block. This is because the long waves which contribute to blocking initiation have phases close to those of waves on normal charts. The waves on normal charts are assumed to represent the steady-state response of the atmosphere to topographic forcing. In many ways the correct prediction of wavenumber one is the key to the problem because its presence can lead to Atlantic blocking and its absence can lead to Pacific blocking.

The remaining chapters will be concerned with identifying mechanisms relevant to sustaining persistent blocking situations.

# Chapter FIVE

# THE INTERACTION BETWEEN THE LONG WAVES AND THE BAROCLINIC WAVES

## PART ONE - TRANSFER OF HEAT

# Chapter Five The Interaction between the Long Waves and the Baroclinic Waves

## Part One - Transfer of Heat

### 5.1 Introduction

Long Rossby waves, produced by flow over forcing, and baroclinic waves have been separately discussed as possible mechanisms responsible for blocking. However, an interaction between these two types of wave has not yet been investigated. This interaction would initially arise from the long waves distorting the basic - state baroclinity, thus possibly affecting the growth rates, wavelength of maximum instability and direction of propagation of the baroclinic waves. In turn the baroclinic waves would transport heat down the temperature gradients set up by the long waves. This may provide a significant energy sink for the very long waves. Furthermore, this transport of heat by the baroclinic waves would be accompanied by a non-Fickian transfer of momentum. The importance of momentum transfer by baroclinic waves is well known and this will be discussed in the next chapter. This chapter will be concerned exclusively with the effect of heat transfer by short baroclinic waves growing in the baroclinic zones of very long waves.

### 5.2 Effect of Eddy Diffusivity of Heat on Stationary Rossby Waves

This section will investigate the effect of small scale baroclinic waves growing in the temperature gradients of a stationary Rossby wave in a barotropic current. Thus there is no mean north-south temperature gradient present.

The effect of small-scale heat transfer can be represented implicitly by including an eddy diffusivity term in the thermodynamic equation

$$\frac{D\phi}{Dt_h} + wB = \text{div}\,(K_H \nabla_h \phi)$$

$$= K_H \nabla_h^2 \phi$$

$K_H$ is a heat-transfer coefficient, which is here assumed to be a constant. The linearised, incompressible, quasi-geostrophic potential vorticity equation 2(ii) then becomes:

$$\bar{u}\frac{\partial}{\partial x}\left[\nabla_h^2\psi + \frac{f_o^2}{gB}\frac{\partial^2\psi}{\partial z^2}\right] + \beta\frac{\partial\psi}{\partial x} = \frac{K_H f_o^2}{gB}\nabla_h^2\left(\frac{\partial^2\psi}{\partial z^2}\right)$$

Taking the separable solution

$$\psi = Re\left\{A e^{i(kx+\nu z)} + B e^{i(kx-\nu z)}\right\}\cos\mu y$$

gives $\nu^2 = \dfrac{ik(\beta - \bar{u}P^2)}{Q^2(\bar{u}ik + P^2K_H)}$ where $P^2 = (k^2+\mu^2)$, $Q^2 = \dfrac{f_o^2}{gB}$

Note that the critical wind speed for wave trapping ($\beta = U_c P^2$) is not affected by the presence of diffusion.

Let $\dfrac{K_H P^2}{\bar{U}k} = \varepsilon$

$$\therefore \nu = \pm\frac{1}{Q}\left[\frac{\beta - \bar{u}P^2}{\bar{u}(1+\varepsilon^2)}\right]^{1/2}(1+i\varepsilon)^{1/2}$$

Typical value for $\varepsilon$ : $\varepsilon \sim \dfrac{K_H P}{\bar{U}}$

From Green (1970), $K_H \sim 4.4 \times 10^7\ \Delta\phi$ m.$^2$ s.$^{-1}$ where $\Delta\phi$ is the entropy difference between pole and equator. Typically, temperature differences between warm highs and cold lows at 500 mb. are 15°C to 20°C, which yields $K_H \sim 3 \times 10^6$ m$^2$.s.$^{-1}$

$$k \sim 0.4 \times 10^{-6} \text{m.}^{-1} \quad \text{and} \quad \bar{U} \sim 10 \text{ m.s.}^{-1} \rightarrow \varepsilon \sim 0.12$$

As $\varepsilon \ll 1$, a binomial expansion for $\lambda$ can be used.

$$\lambda = \pm \frac{1}{Q} \left( \frac{\beta - \bar{u} p^2}{\bar{u}(1+\varepsilon^2)} \right)^{1/2} \left( 1 + \frac{i\varepsilon}{2} + \frac{\varepsilon^2}{8} \ldots \right)$$

In order for the solution for $\psi$ to be realistic for very long waves, whose energy is not trapped in the troposphere, we take $B = 0$ and choose the real positive root for $\lambda$.

For $\beta > \bar{U}P^2$,

$$\psi = A\, e^{i(kx + \lambda_R z)}\, e^{-\lambda_i z} \qquad \text{where} \quad \lambda_R = \text{real part of } \lambda$$
$$\lambda_i = \text{imag. part of } \lambda$$

Thus to first order in $\varepsilon$,

$$\lambda_R = \lambda_o, \quad \text{where } \lambda_o \text{ represents the undamped solution}$$

Typical values give $\lambda_R \sim 10^{-4} \text{ m}^{-1}$.

$$\frac{2\pi}{\lambda_R} \sim 60 \text{ km.}$$

$$\lambda_i = \frac{\lambda_R \varepsilon}{2} \sim 10^{-5} \text{ m.}^{-1}$$

Thus the exponential damping height is of the order of 100 km. which is negligible, particularly as the diffusion coefficient used is only typical of the very active baroclinic waves confined to the bottom 10 km. of the atmosphere.

Mountain Forcing

The effect of heat diffusion upon the surface amplitude of the long

wave can be investigated in a simple case of, for example, mountain forcing. The linearised lower boundary condition is

$$w\Big|_{z=0} = \mathrm{Re}\left\{\frac{Dh}{Dt}\right\} \quad \text{where } h\ (\text{mountain profile}) = h_0 e^{ikx}\cos My$$

$$\psi = A\, e^{i(kx + \nu_R z)}\, e^{-\nu_i z}$$

$$\therefore \frac{g\beta \bar{u} i k h_0}{f_0} = A\left(-K_H P^2 - ik\bar{u}\right)\left(i\nu_R - \nu_i\right)$$

$$= -A\,\nu_R\,\bar{u}k\,(\varepsilon + i)\left(i - \varepsilon/2\right)$$

$$\therefore A = \frac{g\beta h_0}{\nu_0 f}\left(i - \varepsilon/2\right)$$

to first order in $\varepsilon$, with $\nu_0 \sim \nu_R$

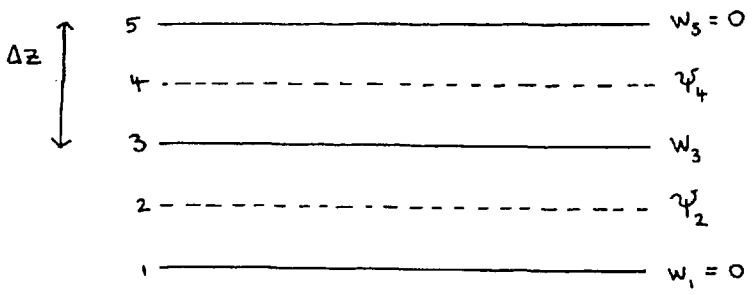
$$\therefore \psi = \frac{g\beta h_0}{\nu_0 f_0}\left[\underbrace{-\sin\left(kx + \nu_0 z\right)}_{\text{solution without diffusivity}} - \varepsilon/2\cos\left(kx + \nu_0 z\right)\right] e^{-\nu_i z}$$

Thus the surface amplitude and phase of the wave closely resembles that of the undamped solution. Although the ''main'' temperature field is $\pi/2$ out of phase with the ''main'' streamfunction, there is also a ''small'' temperature field $\pi$ out of phase with the ''main'' stream function. This is consistent with the amplitude of the stream function being gently damped with height. This vertical structure in no way resembles blocking.

Thus it has been shown that baroclinic heat transfer has a negligible effect upon stationary Rossby waves in a basic-state barotropic current. However, this heat transfer may be important in the presence of a basic-state baroclinity which, in conjunction with the Rossby wave, gives rise to areas of intensified temperature gradients. One way of investigating this problem is to look at the effect of heat diffusivity upon long baroclinically unstable waves.

## 5.3 A Two-Layer Baroclinic Model

In this section the effect of eddy diffusivity of heat on baroclinic instability is investigated. Although a simple two-layer model of baroclinic instability gives slightly incorrect absolute values of growth rates and phase speeds, it can give a useful indication of the effect of diffusivity. It cannot however be used to reliably predict, for example, whether any of the long waves will have their phase speeds reduced to zero.




The vorticity equation $\frac{D}{Dt}\left(\nabla_h^2\psi + f\right) = f_0 \frac{\partial w}{\partial z}$ is evaluated at levels 2 and 4 and the thermodynamic equation $\frac{D\phi}{Dt} = K_H \nabla_h^2 \phi$ at level 3. The flow is vertically bounded by rigid smooth surfaces and is infinite in the north-south direction. Vertical derivatives are approximated by first-order finite differences.

The equations are then linearised about a basic state zonal wind so that:

$$\psi_2 = -U_2 y + \psi_2'(x,t)$$

$$\psi_4 = -U_4 y + \psi_4'(x,t)$$

and $$\psi_3 = \frac{\psi_2 + \psi_4}{2}$$

Perturbation stream functions are now understood in the following equations.

$$\left(\frac{\partial}{\partial t} + \frac{U_2+U_4}{2}\frac{\partial}{\partial x}\right)(\psi_4 - \psi_2) - \frac{(U_4-U_2)}{2}\frac{\partial}{\partial x}(\psi_2+\psi_4) + w_3 \Delta z \frac{g\beta}{f_0} - \frac{K_H}{2}\frac{\partial^2}{\partial x^2}(\psi_4 - \psi_2) = 0$$

$$\left(\frac{\partial}{\partial t} + U_2\frac{\partial}{\partial x}\right)\frac{\partial^2\psi}{\partial x^2} + \beta\frac{\partial\psi_2}{\partial x} - f\frac{w_3}{\Delta z} = 0$$

$$\left(\frac{\partial}{\partial t} + U_4\frac{\partial}{\partial x}\right)\frac{\partial^2\psi_4}{\partial x^2} + \beta\frac{\partial\psi_4}{\partial x} + f\frac{w_3}{\Delta z} = 0 \quad \text{—— Equations 5(i)}$$

Letting $\psi_2$, $\psi_4$ and $w_3$ all vary as $\exp[ik(x - ct)]$ and substituting these expressions in equations 5(i) leads eventually to an expression for c.

$$c = U_M - \frac{\beta(k^2+\nu^2)}{k^2(k^2+2\nu^2)} - \frac{i\nu^2 K_H k}{2(k^2+2\nu^2)} \pm \left[k^4(k^2+2\nu^2)(k^2-2\nu^2)U_T^2 + \beta^2\nu^4 - \frac{K_H^2\nu^4 k^6}{4} - i\beta\nu^4 k^3 K_H\right]^{1/2}$$

where $U_M = \frac{U_2 + U_4}{2}$ , $U_T = \frac{U_4 - U_2}{2}$

$\lambda^2 = \frac{f_o^2}{gB(\Delta z)^2}$ ie. a scaled vertical wavenumber.

SPECIAL CASES

1) $U_T = 0, \quad K_H = 0, \quad \beta \neq 0$

$$c = U_M - \frac{\beta(k^2+\lambda^2)}{k^2(k^2+2\lambda^2)} \pm \frac{\beta\lambda^2}{k^2(k^2+2\lambda^2)}$$

$$\therefore \quad c = U_M - \frac{\beta}{k^2} \quad \text{or} \quad c = U_M - \frac{\beta}{(k^2+2\lambda^2)}$$

These solutions represent the first two barotropic Rossby modes.

2) $U_T = 0, \quad \beta = 0, \quad K_H \neq 0$

$$c = U_M - \frac{i\lambda^2 K k}{2(k^2+2\lambda^2)} \pm \frac{i k^3 K_H \lambda^2}{2k^2(k^2+2\lambda^2)}$$

$C = U_M$ (barotropic wave with no vertical variations)

or $C = U_M - \frac{ikK_H\lambda^2}{(k^2+2\lambda^2)}$ (barotropic wave with temperature perturbations produced by vertical velocities)

Scale Analysis: Let $\sigma = kC_i$ where $C_i$ = imag. part of C

$$\sigma = \frac{k^2 K_H \lambda^2}{(k^2+2\lambda^2)}$$

$k \sim \lambda \sim 10^{-6}$ m.$^{-1}$ , $K_H \sim 5 \times 10^6$ m.$^2$ s.$^{-1}$

$\sigma \sim 10^{-6}$ s.$^{-1}$

Thus the exponential damping time is of the order of ten days.

3) $\beta = 0, \quad U_T \neq 0, \quad K = 0$

$$c = U_M \pm \frac{1}{(k^2+2\lambda^2)} \left[(k^2+2\lambda^2)(k^2-2\lambda^2) U_T^2\right]^{\frac{1}{2}}$$

Now all waves with $k < \lambda\sqrt{2}$ are unstable

Undamped Growth Rate $\sigma_o = kC_i = U_T k \left(\frac{2\lambda^2 - k^2}{2\lambda^2 + k^2}\right)^{\frac{1}{2}}$, taking the positive square root.

The fastest growing wave $\left(\frac{\partial \sigma_o}{\partial k} = 0\right)$ is given by $k^2 = 2(\sqrt{2}-1)\lambda^2$.

4) $U_T \neq 0, \quad K_H \neq 0, \quad \beta = 0$

$$c = U_M + \frac{1}{(k^2+2\lambda^2)}\left[\frac{-i\lambda^2 K_H k}{2} \pm \left(\left(k^4 - 4\lambda^4\right)U_T^2 - \frac{K_H^2 \lambda^4 k^2}{4}\right)^{1/2}\right]$$

Let $\frac{k}{\lambda} = p$ and $\lambda\frac{K_H}{U_T} = E$

Now instability occurs for $p^4 - 4 - \frac{p^2E^2}{4} > \frac{p^2E^2}{4}$

The critical wavelength is given by:

$$p^4 - 4 - \frac{p^2E^2}{2} = 0$$

$$\therefore 2p^2 = \frac{E^2}{2} \pm \sqrt{\frac{E^4}{4} + 16}$$

Typical value for $E \sim 1$

→ critical value of $p \sim \sqrt{2.26}$ in comparison to $p = \sqrt{2}$ in undamped case.

Thus diffusion has a negligible effect upon the critical wavelength for instability.

The growth rate of unstable disturbances is given by:

$$kc_i = \frac{k}{(k^2+2\nu^2)}\left[\frac{-i\nu^2 K_H k}{2} \pm \left(\left(k^4+\nu^4\right)U_T^2 - \frac{K_H^2 \nu^4 k^2}{4}\right)^{1/2}\right] \qquad \text{Equation 5(ii)}$$

$$\text{for } U_T = 0, \text{ either } kc_i = 0 \text{ or } kc_i = -\frac{k^2\nu^2 K_H}{(k^2+2\nu^2)} = D_1$$

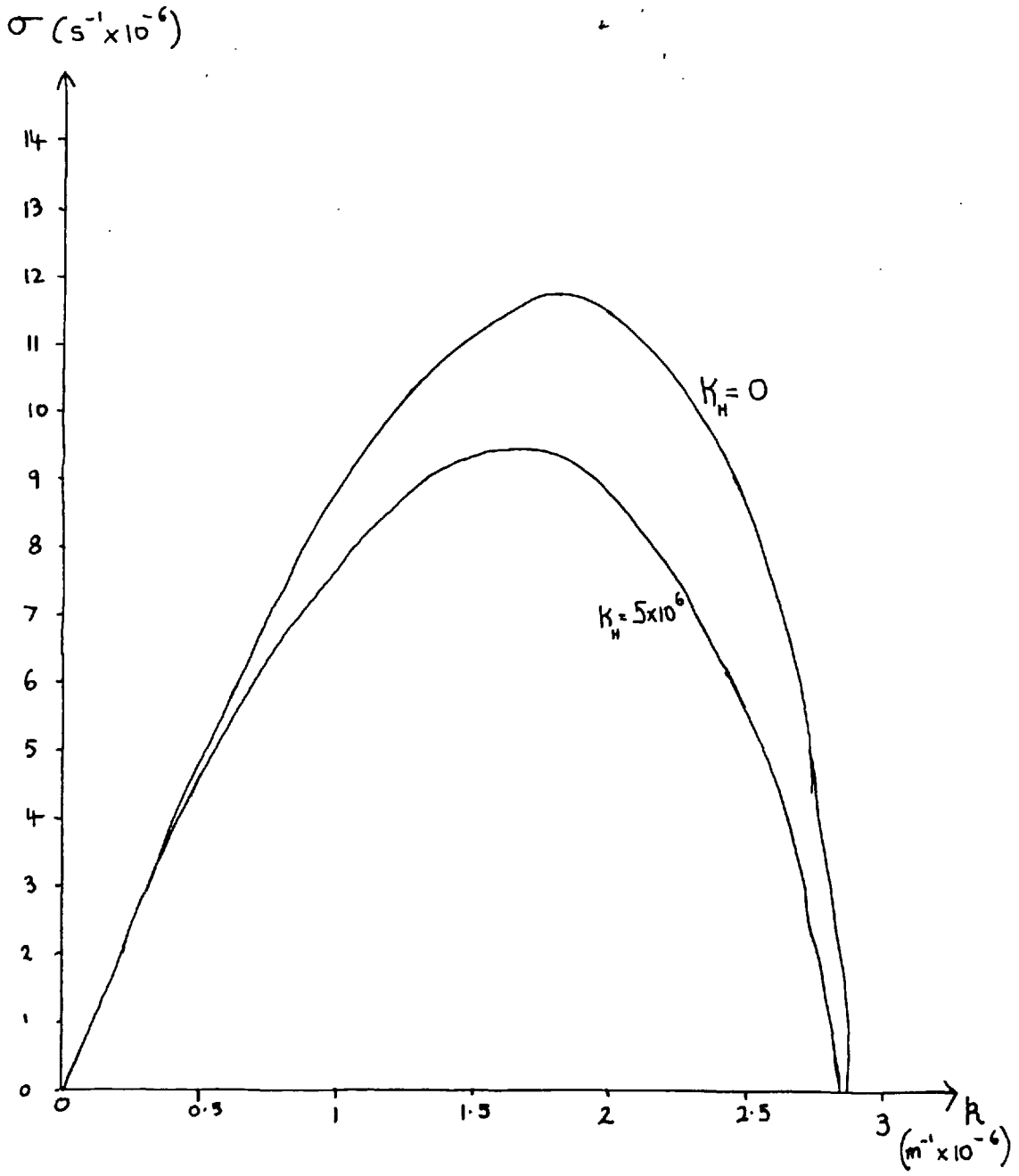
Thus it can be seen that the damping of the barotopic modes is given either by exp. $(-D_1 t)$ or by unity (no temperature perturbations). Let the damping of the growing baroclinic modes be given by $D_2$, so that the total growth rate is given by the expression exp. $[\sigma_o - D_2]t$. It can then be seen from equation 5(ii) that

$$0 < D_2 < D_1$$

This interesting result shows that growing baroclinically unstable waves are actually affected <u>less</u> by heat diffusion than vertically varying waves in a barotropic current. The growth-rate curves for different values of $K_H$ are shown in Fig. 5(1). The very long waves are hardly affected at all by the presence of heat diffusion. The implication of these results is that, in the presence of heat diffusion, the particle-paths in the baroclinic waves are steepened. The damping of the temperature perturbations by diffusion is then compensated by increased adiabatic warming and cooling. This is consistent with the potential energy release being greater than one might initially have expected.

Figure 5(1)

Growth Rate curves from a two-layer baroclinic model with $K_H = 0$ and $K_H = 5 \times 10^6 \ m^2 s^{-1}$ $\left(\begin{matrix} U_T = 10 ms^{-1} \\ \Delta z = 5 \ km \end{matrix}\right)$



## 5.4 Conclusion

The effect of small scale heat transfer on the long waves is insignificant. In the case of stationary Rossby waves, the vertical damping height is of the order of 100 km. In the case of long, baroclinically unstable waves, the diffusion damping time is of the order of 20 days.

# Chapter SIX

# THE INTERACTION BETWEEN THE LONG WAVES AND THE BAROCLINIC WAVES

## PART TWO - TRANSFER OF MOMENTUM

# Chapter Six The Interaction between the Long Waves and the Baroclinic Waves

## Part Two - Transfer of Momentum

### 6.1 Introduction

It is well known that a consequence of the poleward transport of heat by baroclinic waves is a convergence of momentum in mid-latitudes. This convergence intensifies the jet-stream in mid-latitudes and maintains westerly winds there against surface friction. There are easterly winds in high and low latitudes as a consequence of the transport of westerly momentum out of these regions. The maintenance of surface winds by baroclinic waves causes cross-isobar flow in the surface friction layer and this gives rise to the observed meridional circulation. The observed pattern of surface winds was shown by Green (1970) to be a direct consequence of the mixing of two conservative quantities, namely potential temperature and potential vorticity, by the baroclinic waves.

It is therefore reasonable, but not obvious, to suppose that the existence of two main baroclinic zones in the North-South direction will give rise to the convergence of westerly momentum into these zones. Furthermore, there is data to support this hypothesis. January 1963 was a month in which there was a pronounced split jet-stream in the mean zonal winds; this data is shown by Oort and Rasmussen (1971). Fig. 6(1) shows the zonal mean of the transient momentum flux (private communication from Oort) for January 1963 and Fig. 6(2) shows the divergence of this momentum flux. It can be seen that there are two regions of convergence, coinciding with the two branches of the jet-stream. The implication is, therefore, that baroclinic waves travelling in a split jet-stream will tend to intensify these jets and so enhance the regions of anticyclonic and cyclonic shear.

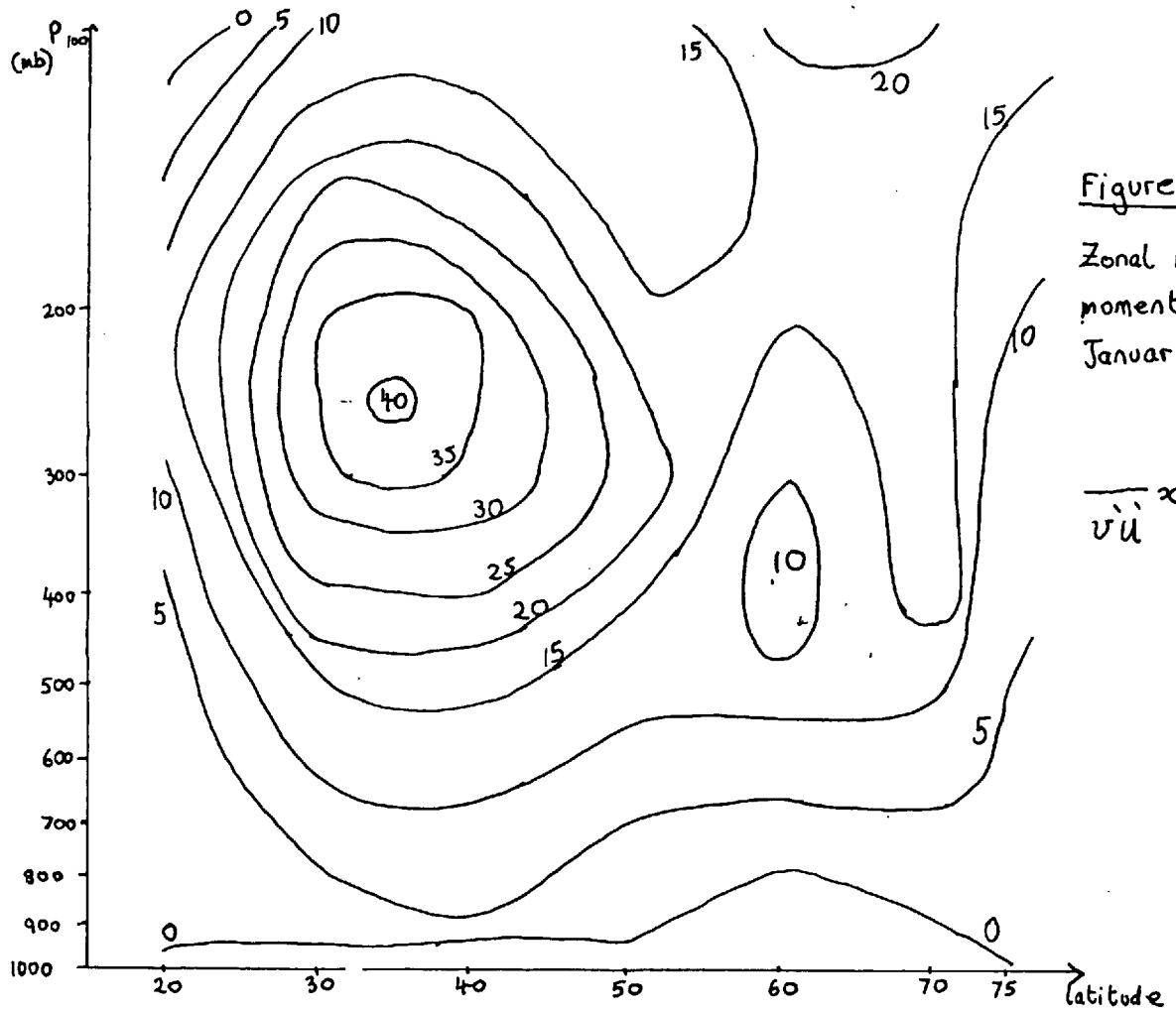



Figure 6(1)

Zonal mean of transient momentum flux for January 1963

$\overline{v'u'}^{x}$ $(m^2 s^{-2})$

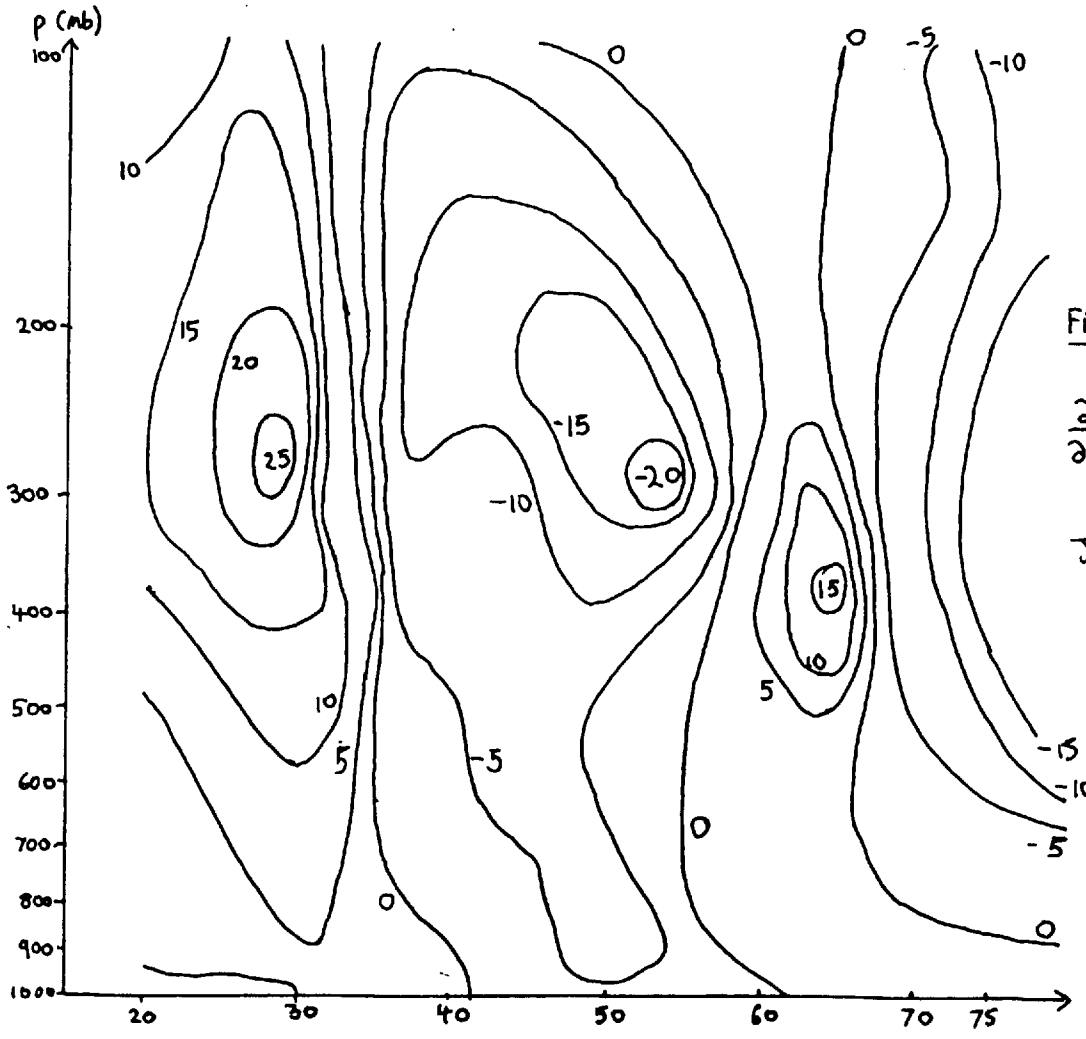
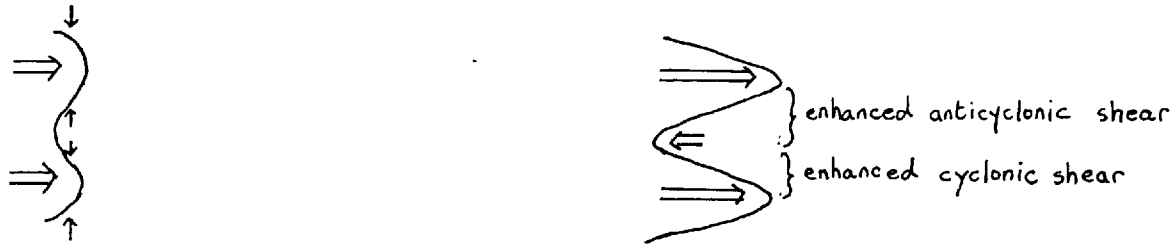



Figure 6(2)

$\frac{\partial}{\partial y}\overline{v'u'}^{x}$ $(ms^{-2} \times 10^{-6})$

January 1963

Initial Weak Split Jet leads to Intensified Split Jet

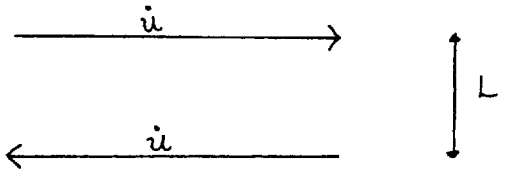



⟹ zonal flow

⟶ direction of momentum transport by baroclinic waves

This process (ie. intensification of the jets) obviously cannot continue ad infinitum because it will eventually be limited by friction.

The importance of the eddy transfer of momentum in a split jet was pointed out by Green (1977) in his study of the British drought of 1976. Green calculated the transient momentum flux around the blocking anticyclone and found that it was sufficient to produce the observed mean anticyclonic vorticity of $2 \times 10^{-5}\ S^{-1}$ in about four days. He then assumed that Ekman friction in the low-levels of the anticyclone would be sufficient to balance the vorticity forcing and hence a steady-state would be established.




Consider an atmosphere of height H in a channel of width L, with momentum sources $+\dot{u}$ (constant with height) at the northern boundary and $-\dot{u}$ at the southern boundary. Let the vorticity be $\zeta$.
Using standard notation:

$$\int_0^H \frac{\partial \zeta}{\partial t}\, dz = \int_0^H \frac{2\dot{u}}{L}\, dz + \int_0^H f \frac{\partial w}{\partial z}\, dz = 0 \quad \text{in the steady state}$$

Let $w = 0$ at $z = H$

$$\therefore \zeta w\Big|_{z=0} = \frac{2\dot{u}H}{L}$$

Assuming Ekman friction

$$w\Big|_{z=0} = \frac{K\zeta}{f}$$

where K is a constant stress coefficient

$$\zeta = \frac{2\dot{u}H}{LK}$$

$\left(\frac{2\dot{u}}{L}\right)$ = 5m.s.$^{-1}$ per 1000km. per day (from Green's data)
= $5 \times 10^{-11}$ s$^{-2}$.

$H = 10^4$ m.

$K = 2 \times 10^{-2}$ m.s.$^{-1}$
$= 5 \times 10^{-5}$ s.$^{-1}$

This value is very close to the observed mean vorticity. However, a difficulty with this description is that the thermodynamics, which is not used, is not in a steady-state with the air warming indefinitely as it sinks.

Hence the problem of momentum forcing needs to be investigated further. In particular, it is important to discover what is the effect of momentum forcing varying with height as it is observed that eddy momentum transfer peaks near the tropopause.

## 6.2 Momentum Forcing Constantwith Height

Initially consider the atmospheric response to a wave-like pattern of momentum forcing which is constant with height. This is due to baroclinic waves growing in the temperature gradients set

up by a long wave.

From equation 2(ii) : (steady-state, adiabatic and incompressible)

$$\bar{u}\frac{\partial}{\partial x}\left(\nabla_h^2\psi + \frac{f_o^2}{gB}\frac{\partial^2\psi}{\partial z^2}\right) + \beta\frac{\partial\psi}{\partial x} = V$$

where $\psi$ is now understood to be a perturbation stream function

$V$ is the vertical component of the curl of the momentum forcing and is a vorticity-forcing term.

In this case $V = Re\left\{V_o e^{ikx}\cos\mu y\right\}$ $V_o$ = magnitude of vorticity forcing.

The following boundary conditions are used:

Periodic in x.

$\psi = 0$ at the north and south boundaries (from observations).

Rigid smooth surfaces at $z = 0$ and $z = H$. These are energy-reflecting boundary conditions which are thought to be appropriate for the scale of blocking waves.

Let $\psi = Re\left\{e^{ikx}\cos\mu y\, F(z)\right\}$

$$\bar{u}ik\left(-(k^2+\mu^2)F + \frac{f_o^2}{gB}\frac{d^2F}{dz^2}\right) + \beta ikF = V_o$$

$$\frac{d^2F}{dz^2} + \nu^2 F = -iY$$

where $\frac{gB}{f_o^2}\left(-(k^2+\mu^2) + \frac{\beta}{\bar{u}}\right) = \nu^2$ and $Y = \frac{gB}{f_o^2}\frac{V_o}{\bar{u}k}$

Solution for F: $F = Ce^{i\nu z} + De^{-i\nu z} - \frac{iY}{\nu^2}$

where C and D are arbitrary constants.

Application of boundary conditions:

At $z = 0$, $w = -\frac{\bar{u}}{B}\frac{\partial}{\partial x}\left(\frac{f_o}{g}\frac{\partial\psi}{\partial z}\right) = 0$

$$\therefore \frac{dF}{dz} = 0$$

$$\Rightarrow C = D$$

At $z = H$, $w = 0 \Rightarrow Ce^{i\lambda H} = De^{-i\lambda H}$

Therefore either $C = D = 0$

or $e^{i\lambda H} = e^{-i\lambda H}$. This solution represents free Rossby internal modes. If these modes are present at $t = 0$ then they will always be present and may be important from the point of view of interference patterns. However, they are not fundamental to the problem.

Thus the result $C = D = 0$ is used.

$$\therefore \psi = Re\left\{\cos\mu y\, e^{ikx}\frac{(-i)Y}{\lambda^2}\right\}$$

But $\lambda^2$ can be positive or negative.

If $\lambda^2$ is positive, $\beta > \bar{U}(k^2+\mu^2)$ horizontal advection of planetary vorticity is greater that that of relative vorticity.

If $\lambda^2$ is negative, $\beta < \bar{U}(k^2+\mu^2)$ advection of relative vorticity is greater than advection of planetary vorticity.

$\underline{\lambda^2 > 0}$ ($\beta$ dominates relative advection)

$$\psi = \frac{Y\cos\mu y}{\lambda^2}\sin kx$$

$\therefore \nabla_h^2\psi$ is proportional to $-\sin kx$

Note that the maximum vorticity of the forced wave lies $\pi/2$ <u>upstream</u> of the maximum vorticity of the forcing and the forcing function is balanced by the advection of planetary vorticity. This is illustrated schematically below.

| | | | | | | |
|---|---|---|---|---|---|---|
| Forcing ($\cos kx$) | $\xi^+$ | | $\xi^-$ | | $\xi^+$ | |
| $\psi$ ($\sin kx$) | $\uparrow$ $v f^-$ | H | $\overline{v f^+}$ $\downarrow$ | L | $\uparrow$ $v f^-$ | H |
| $\nabla_h^2 \psi$ ($-\sin kx$) | | $\xi^-$ | | $\xi^+$ | | $\xi^-$ |

The horizontal advection of relative vorticity is also balanced, along with the forcing, by the dominant advection of planetary vorticity.

$\underline{\nu^2 < 0}$ (relative advection dominates $\beta$)

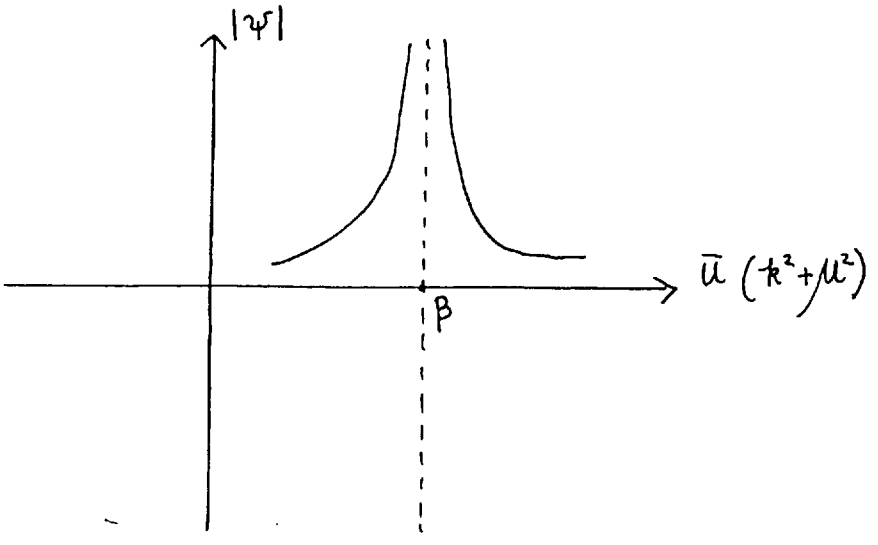
$$\psi = \frac{Y \cos \mu y}{|\nu|^2} (-\sin kx)$$

$\therefore \nabla_h^2 \psi$ is proportional to $\sin kx$

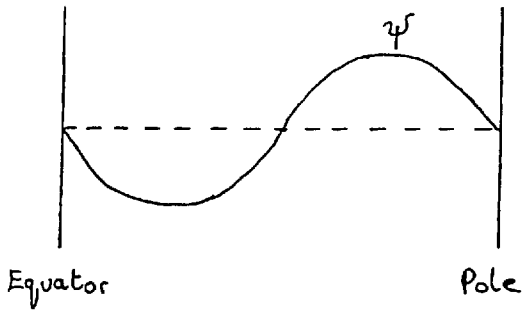
Now the vorticity maximum of $\psi$ lies $\pi/2$ <u>downstream</u> of the maximum of the forcing and advection of relative vorticity balances both the forcing and the advection of planetary vorticity.

$\underline{\nu = 0}$

Now the two mechanisms capable of balancing the vorticity forcing cancel each other out and, as there are no vertical velocities anywhere to provide vortex stretching or compression, the amplitude of $\psi$ goes to infinity.



It is interesting to compare this resonance condition with values taken from a "blocking wave". Typically this would be wavenumber four in the x direction and have the meridional variation illustrated below.




It is more accurate to consider the problem in spherical geometry so this wave would be described by the Associated Legendre Polynomial $P_n^m(\cos\theta)e^{im\phi}$, where $m \equiv$ zonal wavenumber

$(n-m)$ = number of zeros of the function between the geographic poles.

$$n \geq m$$

If $m = 4$ and $(n-m) = 3$, then $\underline{n = 7}$

The resonance condition in spherical geometry is given by:

$$\frac{\beta}{\bar{U}} = \frac{(n-1)(n+1)}{R^2} \quad \text{from equation } 2(vi)$$

but $$\frac{\beta}{\bar{U}} \sim \frac{1.5 \times 10^{-11}}{10} \text{ m.}^{-2} \sim 1.5 \times 10^{-12} \text{ m.}^{-2}$$

and $$\frac{(n-1)(n+1)}{R^2} \sim \frac{63}{39 \times 10^{12}} \text{ m.}^{-2} \sim 1.6 \times 10^{-12} \text{ m.}^{-2}$$

Thus the wavenumber of blocking observed in the atmosphere is almost identical to the wavenumber of the forcing which will produce a resonance.

However, one important feature is missing in this description – there are no temperature perturbations anywhere. Perhaps the presence of friction will make the anticyclones warm and the cyclones cold in the troposphere.

6.3 Effect of Friction

$$\psi = \mathrm{Re}\left\{e^{ikx}\cos\mu y\, F(z)\right\} \quad \text{where } F(z) = Ce^{\lambda z} + De^{-\lambda z} - \frac{iY}{\lambda^2}$$

Taking Ekman friction at the lower boundary:

$$w\big|_{z=0} = \frac{K}{f}\nabla_h^2\psi = -\frac{f_0\bar{u}}{gB}\frac{\partial}{\partial x}\left(\frac{\partial\psi}{\partial z}\right)$$

$$-\frac{K}{f_0}(k^2+\mu^2)\left(C+D-\frac{iY}{\lambda^2}\right) = -\frac{f_0\bar{u}}{gB}ik\left(\lambda C - \lambda D\right)$$

$$\underbrace{\frac{-(k^2+\mu^2)KgB}{k\lambda\bar{u}f_0^2}}_{=P}\left(C+D-\frac{iY}{\lambda^2}\right) = (C-D)$$

From the scale analysis,

$$(k^2+\mu^2) \sim 10^{-12}\,\mathrm{m.}^{-2}, \qquad \lambda \sim 10^{-4}\,\mathrm{m.}^{-1}, \qquad K \sim 10^{-2}\,\mathrm{m.s.}^{-1}$$

$$k \sim 10^{-6}\,\mathrm{m.}^{-1}, \qquad \bar{u} \sim 10\,\mathrm{m.s.}^{-1}, \qquad \frac{gB}{f_0^2} \sim 10^4$$

$$\therefore \quad \underline{P \sim 0.1}$$

$$D = \frac{(1+P)}{(1-P)}C - \frac{P}{(1-P)}\frac{Y}{\lambda^2}$$

At $z = H, \quad w = 0$

$$\therefore \frac{dF}{dz} = 0 \quad \Rightarrow \quad D = e^{2i\partial H} C$$

$\underline{\partial^2 > 0}$

$$C = \frac{PY e^{-i\partial H}}{2\partial^2} \frac{(iP\cos\partial H - \sin\partial H)}{(\sin^2\partial H + P^2\cos^2\partial H)}$$

$$D = \frac{PY e^{i\partial H}}{2\partial^2} \frac{(iP\cos\partial H - \sin\partial H)}{(\sin^2\partial H + P^2\cos^2\partial H)}$$

$$\psi = Re\left\{e^{ikx}\left(Ce^{i\partial z} + De^{-i\partial z} - \frac{iY}{\partial^2}\right)\right\}\cos\mu y$$

$$\psi = \frac{Y}{\partial^2}\cos\mu y\left[\sin kx - \frac{P(P\cos\partial H\sin kx + \cos kx\sin\partial H)\cos\partial(H-z)}{(\sin^2\partial H + P^2\cos^2\partial H)}\right]$$

Check: If $P = 0$, $\psi = \frac{Y}{\partial^2}\cos\mu y \sin kx$ which is the frictionless solution. When $P \to \infty$, $\psi = 0$ at $z = 0$ which is a non-slip lower boundary condition. As $P \sim 0{\cdot}1$, the approximation can be made that $P \ll 1$.

Using a binomial expansion:

$$\frac{P(P\cos\partial H\sin kx + \sin\partial H\cos kx)}{\sin^2\partial H(1 + P^2\cot^2\partial H)} \sim \frac{P(P\cos\partial H\sin kx + \sin\partial H\cos kx)}{\sin^2\partial H}\left(1 - P^2\cot^2\partial H \ldots\right)$$

N.B. For typical atmospheric values $\partial \sim \frac{2\pi}{40\ km.}$, $H \sim 10\ km.$

$\therefore \sin\partial H \sim 1$ and $\cos\partial H$ is very small, so the above expansion is valid.

So, to first order in P:

$$\psi = \frac{Y}{\nu^2} \cos \mu y \left( \sin kx - \frac{P \cos kx \cos \nu (H-z)}{\sin \nu H} \right)$$

So the solution consists of the original barotropic wave plus a "small" baroclinic wave which is $\pi/2$ out of phase with the barotropic wave.

$$w = -\frac{\bar{u}}{\beta} \left( \frac{\partial \phi}{\partial x} \right) = \frac{\bar{u} Y k f_0 (-\sin kx) P \sin \nu (H-z) \cos \mu y}{\beta \nu g \sin \nu H}$$

$$w\Big|_{z=0} = \frac{\bar{u} Y k P f_0}{\beta \nu g} \cos \mu y \, (-\sin kx)$$

Compare this with the lower boundary condition applied to the zeroth-order barotropic term.

$$w\Big|_{z=0} = \frac{K}{f_0} \nabla_h^2 \psi = -\frac{K}{f_0} (k^2 + \mu^2) \frac{Y}{\nu^2} \cos \mu y \sin kx$$

but $$P = \frac{(k^2+\mu^2)}{k\nu} \frac{K_q \beta}{\bar{u} f_0^2}$$

$$\therefore \; w\Big|_{z=0} = \frac{\bar{u} Y k P f_0}{\beta \nu g} \cos \mu y \, (-\sin kx)$$

This result can be interpreted as follows: The zeroth-order term in is barotropic and is the same as for the frictionless case, with the vorticity maximum $\pi/2$ upstream of the vorticity maximum of the forcing

(for $\gamma^2 > 0$ in this case). Weak vertical velocities are induced by Ekman friction and so the first-order term provides the temperature field necessary to balance the effect of these vertical velocities in the thermodynamic equation. The first order term in $\psi$ then induces even weaker Ekman vertical velocities which are balanced in the thermodynamic equation by the second-order term in $\psi$ and so on.

Thus the inclusion of friction in the steady-state model produces "small" temperature perturbations which are $\pi/2$ out of phase with the pressure perturbations. This does not resemble the structure of warm highs and cold lows observed in blocking. It is therefore necessary to see whether this temperature structure is due to the momentum forcing varying with height.

## 6.4 Momentum Forcing Varying with Height

Now consider the case in which the momentum is supplied to the atmosphere at a discreet height $H_1$. This is intended to represent the transfer of momentum by baroclinic eddies, occuring in a narrow band of heights near the tropopause.

From equation 2(ii)

$$\bar{u}\frac{\partial}{\partial x}\left(\nabla_h^2\psi + \frac{f_0^2}{g\theta}\frac{\partial^2\psi}{\partial z^2}\right) + \beta\frac{\partial\psi}{\partial x} = Re\left\{V_0 e^{ikx}\delta(z-H_1)\right\}\cos\mu y$$

in this case

Boundary Conditions: periodic in x
$\psi = 0$ at north and south boundaries. Rigid, smooth surfaces at $z=0$ and $z = H_2$.

Let $$\psi = Re\left\{e^{ikx}\cos\mu y\, F(z)\right\}$$

Then the resulting equation for F is:

$$\frac{d^2F}{dz^2} + \nu^2 F = -i\gamma\,\delta(z-H_1) \qquad \text{Equation 6(i)}$$

This equation is easily solved and the solution for $F$ is:

$$F = Ae^{i\lambda z} + \grave{B}e^{-i\lambda z} \qquad \text{for} \quad z > H_1$$

$$F = Ce^{i\lambda z} + De^{-i\lambda z} \qquad \text{for} \quad z < H_1$$

where $A$, $\grave{B}$, $C$ and $D$ are arbitrary constants.

Two further boundary conditions are necessary at $z = H_1$.

At $z = H_1$, the right-hand side of equation 6(i) has a discontinuity and is infinitely large. On the left-hand side $F$ cannot have a discontinuity because, as it represents pressure, it must be continuous in order to avoid infinite accelerations. Therefore the discontinuity must be in $\frac{d^2F}{dz^2}$ and this term must be large to balance the equation.

$$\frac{d^2F}{dz^2} = -iY\,\delta(z - H_1) \quad \text{in the region of} \quad z = H_1$$

$$\left[\frac{dF}{dz}\right]_{H_1-\varepsilon}^{H_1+\varepsilon} = -iY\int_{H_1-\varepsilon}^{H_1+\varepsilon}\delta(z - H_1)\,dz \qquad \text{as} \quad \varepsilon \to 0$$

$$= -iY$$

Therefore the boundary conditions at $H_1$ are as follows:

1) $$\left[\frac{dF}{dz}\right]_{H_1-\varepsilon}^{H_1+\varepsilon} = -iY$$

2) F continuous

Applying all the boundary conditions to the solutions:

$$\psi = \mathrm{Re}\left\{e^{ikx}(Ae^{i\lambda z} + \grave{B}e^{-i\lambda z})\right\}\cos\mu y \qquad H_1 < z \leq H_2$$

$$\psi = \mathrm{Re}\left\{ e^{ikx}(Ce^{i\lambda z} + De^{-i\lambda z}) \right\} \cos \mu y \qquad 0 \leq z < H_1$$

yields the following values for the constants.

$$C = D = -\frac{iY}{2\lambda} \frac{\cos\lambda(H_2 - H_1)}{\sin \lambda H_2}$$

$$A = -\frac{iY}{2\lambda} e^{-i\lambda H_2} \frac{\cos \lambda H_1}{\sin \lambda H_2}$$

$$B = -\frac{iY}{2\lambda} e^{i\lambda H_2} \frac{\cos \lambda H_1}{\sin \lambda H_2} \qquad \text{——} \qquad \text{Equations 6(ii)}$$

$\underline{\lambda^2 > 0}$ ie very large scales of motion where $\beta$ dominates advection of relative vorticity.

Upper Region: $\psi = \frac{Y}{\lambda} \frac{\cos \lambda H_1}{\sin \lambda H_2} \cos \mu y \sin kx \cos \lambda (H_2 - z)$

Lower Region: $\psi = \frac{Y}{\lambda} \frac{\cos \lambda (H_2 - H_1)}{\sin \lambda H_2} \cos \mu y \sin kx \cos \lambda z$

Note that, as in the case with the momentum forcing constant with height, the vorticity maximum of the forced wave leads the vorticity maximum in the forcing by $\pi/2$. However, the vertical velocities developed have now induced temperature perturbations.

Upper Region: $\psi$ is proportional to sin kx cos $(H_2 - z)$

$\phi$ is proportional to sin kx sin $(H_2 - z)$

W is proportional to -cos x sin $(H_2 - z)$

ie. warm highs and cold lows.

Lower Region: $\psi$ is proportional to sin kx cos z

$\phi$ is proportional to -sin kx cos z

W is proportional to cos kx sin z

ie. cold highs and warm lows.

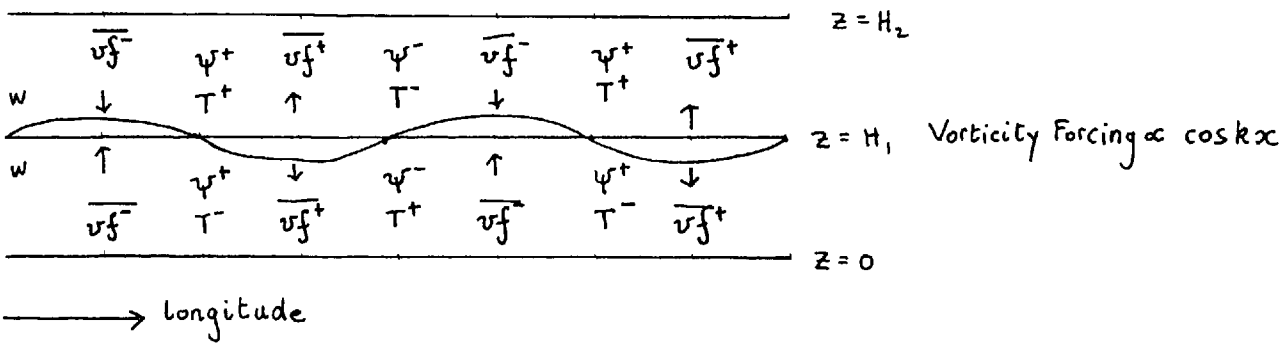
In the lower region there are cold highs and warm lows and the amplitude of $\psi$ decreases with height to reach its minimum value at $z = H_1$. In the upper region there are warm highs and cold lows and the amplitude of $\psi$ increases with height. The vorticity forcing function at $z = H_1$ is exactly balanced by the vortex stretching across it.

At $z = H_1$,

$$f_0 \left[ w \right]_{H_1 - \varepsilon}^{H_1 + \varepsilon} = \frac{\bar{u} f_0^2 \gamma k}{g\beta} \cos \mu y \, (-\cos kx)$$

$$= - V_0 \cos kx \cos \mu y$$

This is a limit case where the forcing is injected in an infinitely thin layer of the atmosphere; it is balanced by the vortex stretching produced by a near-discontinuity in the vertical velocity. The vorticity is then communicated to the rest of the atmosphere by vortex stretching and compression between the level $H_1$ and the boundaries. In this case, this is counteracted by the advection of planetary vorticity. This advection of planetary vorticity balances both the vorticity forcing and the advection of relative vorticity.




The thermodynamics is steadily balanced in both layers because warm air is also rising and vice-versa.

Because of the phasing of the pressure and temperature fields this solution does not resemble blocking but seems more like the Siberian

anticyclone described in Chapter One. Perhaps, on very large space scales, momentum forcing by baroclinic waves may be capable of intensifying the Siberian anticyclone, providing this first split the jet.

$\underline{\lambda^2 < 0}$ ie. smaller scales of motion where advection of relative vorticity dominates $\beta$.

Substituting $\lambda = i|\lambda|$ in existing expressions for A, $\bar{B}$, C and D, given in equations 6(ii), yields for $\Psi$ :

Upper Region: $$= \frac{-Y}{|\lambda|} \cos \mu y \frac{\cosh |\lambda| H_1}{\sinh |\lambda| H_2} \sin kx \cosh |\lambda| (H_2 - z)$$

Lower Region: $$= \frac{-Y}{|\lambda|} \cos \mu y \frac{\cosh |\lambda| (H_2 - H_1)}{\sinh |\lambda| H_2} \sin k x \cosh |\lambda| z$$

Notice now that the vorticity maximum of $\Psi$ is $\pi/2$ downstream from the maximum of the vorticity forcing, as opposed to $\pi/2$ upstream when $\lambda^2 > 0$. The temperature perturbations are as follows:

Upper Region:

$\Psi$ is proportional to $- \sin kx \cosh |\lambda| (H_2 - z)$

$\phi$ is proportional to $\sin kx \sinh |\lambda| (H_2 - z)$

W is proportional to $- \cos kx \sinh |\lambda| (H_2 - z)$

ie. cold highs and warm lows.

Lower Region:

$\Psi$ is proportional to $- \sin kx \cosh |\lambda| z$

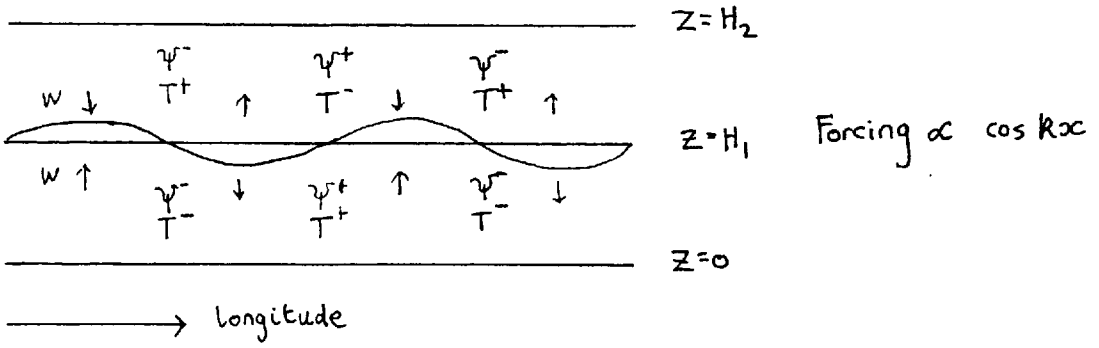
$\phi$ is proportional to $- \sin kx \sinh |\lambda| z$

W is proportional to $\cos kx \sinh |\lambda| z$

ie. warm highs and cold lows.

The amplitude of $\Psi$ increases with height in the lower region until it reaches its <u>maximum</u> value at $z = H_1$. In the upper region the amplitude

of $\Psi$ decreases with height. As in the case with $\gamma^2 > 0$, the vorticity forcing at $z = H_1$ is balanced by a near-discontinuity in the vertical velocity at that level. The vorticity communicated to the rest of the atmosphere by vortex stretching and compression is counteracted by advection of relative vorticity. This balances both the forcing and the advection of planetary vorticity. The thermodynamics are in equilibrium.




This structure does seem similar to that observed in blocking. It only occurs for $\gamma^2 < 0$, which is consistent with the zonal and meridional wavenumbers typical of blocking in the atmosphere. Thus blocking can by hypothesised as follows. The long waves initially interfere to split the jet in a certain region at 500 mb., which is near the steering level of the baroclinic waves. This causes depressions to be "steered" to the north and the south, which produces the anomalous vorticity forcing. This then establishes blocking in the region, with warm highs and cold lows up to the level of the forcing, and cold highs and warm lows above that so the amplitude of the disturbance decreases with height in the stratosphere.

In view of these encouraging results, it was decided to pursue the problem further and to make it more realistic. This was done by introducing spherical geometry, compressibility, a basic state wind shear and a radiation upper-boundary condition. This upper boundary

condition was used to check whether blocking-scale waves really are trapped in the troposphere.

6.5 Inclusion of Spherical Geometry and Wind Shear

From equation 2(iv)

$$\frac{D}{Dt_h}\left[\nabla_h^2\psi + 2\Omega\cos\theta + \frac{f_0}{\rho}\frac{\partial}{\partial z}\left(\frac{\rho}{B}\phi'\right)\right] = V$$

The thermodynamic source term S is assumed zero and V is a vorticity source term, which is the vertical component of the curl of momentum forcing function.

In Chapter two it was shown that a separable solution to this equation exists.

Taking $\psi' = Re\{F(z)\Theta(\theta)\exp(im\phi)\}$ where $\psi = \bar{\psi} + \psi'$

$$V = Re\{iV_0(z)\Theta(\theta)\exp(im\phi)\}$$

again leads to solutions $\Theta(\cos\theta) = P_n^m(\cos\theta)$ . The equation for the complex vertical structure is:

$$\frac{d^2F}{dz^2} + \frac{B}{\rho}\frac{d}{dz}\left(\frac{\rho}{B}\right)\frac{dF}{dz} + \frac{gB}{f_0^2}\left[\frac{2\Omega}{\bar{\psi}} - \frac{f_0^2}{g\rho}\frac{1}{\bar{\psi}}\frac{d}{dz}\left(\frac{\rho}{B}\frac{d\bar{\psi}}{dz}\right) - \frac{(n-1)(n+2)}{R^2}\right]$$

$$= \frac{gBR^2}{f_0^2 m\bar{\psi}}V_0 \qquad \text{- Equation 6(iii)}$$

The basic-state density variation is now taken to be $\rho = \rho_0 e^{-z/H_0}$.

This equation can be solved analytically when the angular rotation of the atmosphere is a linear function of height and the static stability is constant. However, the solutions are confluent hypergeometric functions and in practice need to be evaluated on a computer. Thus it is simpler to solve equation 6(iii) directly, using a numerical integration scheme.

Method of Numerical Integration

This method of numerical integration is taken from an article by

Lindzen and Kuo (1969). All second-order linear differential equations with variable coefficients of the form:

$$\frac{d^2f}{dz^2} + g(z)\frac{df}{dz} + h(z)\,f(z) = r(z) \qquad \text{- Equation 6(iv)}$$

with linear first-order boundary conditions of the form:

$$\frac{df}{dz} + a_1 f = b_1 \quad \text{at} \quad z = z_1, \qquad \text{- Equation 6(v)}$$

$$\frac{df}{dz} + a_2 f = b_2 \quad \text{at} \quad z = z_2$$

are integrable by this method, provided that $g(z)$, $h(z)$ and $r(z)$ do not contain singularities in the range of integration.
Comparison of equation 6(iv) with equation 6(iii) for the height structure yields:

$$f(z) = F(z)$$

$$g(z) = \frac{B}{\rho}\frac{d}{dz}\left(\frac{\rho}{B}\right)$$

$$h(z) = \frac{g\beta}{f_0^2}\left[\frac{2\Omega}{\bar{\psi}} - \frac{f_0^2}{gq}\frac{1}{\bar{\psi}}\frac{d}{dz}\left(\frac{\rho}{B}\frac{d\bar{\psi}}{dz}\right) - \frac{(n-1)(n+2)}{R^2}\right]$$

$$r(z) = \frac{gBR^2}{f_0^2 m\bar{\psi}}\,V_0$$

Dividing the integration range in $N$ segments of length $\delta z$, we may write $z_i = i\,\delta z_i$ with $0 \leq i \leq N$.
We adopt the convention that $f(z_i) = f_i$, $g(z_i) = g_i$ etc. and express

the first and second derivatives in finite difference form as:

$$\frac{df}{dz}(z_n) = \frac{f_{n+1} - f_{n-1}}{2\delta z}$$

$$\frac{d^2f}{dz^2}(z_n) = \frac{f_{n+1} + f_{n-1} - 2f_n}{\delta z^2}$$

Substituting these expressions into equation 6(iv) gives

$$\frac{f_{n+1} + f_{n-1} - 2f_n}{\delta z^2} + \frac{g_n}{2\delta z}(f_{n+1} - f_{n-1}) + h_n f_n = r_n$$

On collectingterms:

$$A_n f_{n-1} + B_n f_n + C_n f_{n+1} = D_n \qquad \text{- Equation 6(vi)}$$

where $A_n = \frac{1}{\delta z^2} - \frac{g_n}{2\delta z}$, $\quad B_n = h_n - \frac{2}{\delta z^2}$

$C_n = \frac{1}{\delta z^2} + \frac{g_n}{2\delta z}$, $\quad D_n = r_n$

Equation 6(vi) can be used at all interior points $1 \leq n \leq N - 1$ since at the boundaries fictitious points are involved. The boundary conditions, equation 6(v), are given by :

$$\frac{f_1 - f_{-1}}{2\delta z} + a_1 f_o = b_1 \quad \text{at} \quad z = 0 \qquad \text{- Equation 6(vii)}$$

$$\frac{f_{N+1} - f_{N-1}}{2\delta z} + a_2 f_N = b_2 \quad \text{at} \quad z = N\delta z \qquad \text{- Equation 6(viii)}$$

and involve the fictitious values $f_{-1}$ and $f_{N+1}$.

Using equation 6(vi), the fictitious values may be expressed in terms

of two real point values. Substituting in equation 6(vii) for $f_{-1}$ gives:

$$f_1\left(1 + \frac{C_o}{A_o}\right) + f_o\left(\frac{B_o}{A_o} + 2\delta z\, a_1\right) = \frac{D_o}{A_o} + 2\delta z\, b_1$$

Similarly, eliminating $f_{N+1}$ from Equation 6(viii) gives:

$$f_{N-1}\left(1 + \frac{A_N}{C_N}\right) - f_N\left(2\delta z\, a_2 - \frac{B_N}{C_N}\right) = \frac{D_N}{C_N} - 2\delta z\, b_2$$

The upper and lower boundary conditions may now be written as:

$$A_b f_o + B_b f_1 = D_b \qquad \text{(lower boundary condition)}$$

$$A_t f_{N-1} + B_t f_N = D_t \qquad \text{(upper boundary condition)}$$

where $A_b = \frac{B_o}{A_o} + 2\delta z a_1$, $B_b = 1 + \frac{C_o}{A_o}$, $D_b = \frac{D_o}{A_o} + 2\delta z b_1$

$$A_t = \left(1 + \frac{A_N}{C_N}\right), \quad B_t = \frac{B_N}{C_N} - 2\delta z a_2, \quad D_t = \frac{D_N}{C_N} - 2\delta z\, b_2$$

This integration method works by expressing the function $f_n$ at $z_n$ in terms of the adjacent point value so that:

$$f_n = \alpha_n f_{n+1} + \beta_n \qquad \text{- Equation 6(ix)}$$

or $f_{n-1} = \alpha_{n-1} f_n + \beta_{n-1}$ ($\alpha_n$ and $\beta_n$ are sets of constants)

The above equation for $f_{n-1}$ is substituted into equation 6(vi) giving an expression for $f_n$ in terms of $f_{n+1}$.

$$f_n = \left(-\frac{C_n}{A_n \alpha_{n-1} + B_n}\right) f_{n+1} + \frac{D_n - A_n \beta_{n-1}}{A_n \alpha_{n-1} + B_n}$$

which on comparison with equation 6(ix) yields:

$$\alpha_n = \frac{-C_n}{A_n\alpha_{n-1} + B_n} \quad \text{and} \quad \beta_n = \frac{D_n - A_n\beta_{n-1}}{A_n\alpha_{n-1} + B_n} \quad \text{- Equations 6(X)}$$

Equations6(x) are recurssion relations for the $\alpha_n$'s and $\beta_n$'s with the values of $A_n$, $B_n$, $C_n$, and $D_n$ determined by the variable coefficients of the differential equation. Once the values of $\alpha_o$ and $\beta_o$ are known, the rest of the values of $\alpha_n$ and $\beta_n$ may be generated. $\alpha_o$ and $\beta_o$ can be determined from the lower boundary condition using equation 6(ix) and are found to be:

$$\alpha_o = \frac{-B_b}{A_b} \quad \text{and} \quad \beta_o = \frac{D_b}{A_b}$$

Knowledge of $f_N$ will permit the calculation of all the values of $f_n$ and this may be obtained from the upper boundary condition as follows:

Rearranging the upper boundary condition gives:

$$f_{N-1} = \frac{D_t}{A_t} - \frac{B_t}{A_t} f_N$$

and eliminating $f_{N-1}$ with equation 6(ix) gives an expression for $f_N$ in terms of known quantities:

$$f_N = \frac{D_t - A_t B_{N-1}}{\alpha_{N-1} A_t + B_t}$$

and hence equation 6(ix) is again used to generate the remaining values of f. All parameters may assume complex values.

## 6.6 Energy – Transmitting Upper Boundary Condition

In the analytic solutions presented so far, an upper boundary condition of W=0 was considered realistic for blocking-scale waves. However, Shutts (1976) has shown that the escape of energy to the stratosphere is the dominant energy sink for long waves. For this reason an energy transmitting upper boundary condition, described by Shutts, is used in the numerical solutions.

Energy transmission is allowed by keeping the angular rotation rate of the atmosphere constant above the upper boundary and selecting the purely upward energy radiating solution there. This upper solution is connected to the motion below by demanding continuity of stream function and vertical velocity across the boundary. The static stability and $\bar{U}$ are continuous across the boundary.

$$\Psi = Re\left\{ C \exp\left( i(m\phi + \nu z) + \frac{z}{2H_0} \right\} P_n^m(\cos\theta) \right\} \qquad z = H_2$$

$$\Psi = Re\left\{ F(z) \exp(im\phi) \right\} P_n^m(\cos\theta)$$

C is an undetermined complex constant in the upper layer.

The connecting conditions at $z = H_2$ are:

$$C \exp\left( i\nu H_2 + \frac{H_2}{2H_0} \right) = F(H_2)$$

(continuity of stream function)

and

$$\left( \bar{\Psi}(H_2) \frac{dF}{dz} - F \frac{d\bar{\Psi}}{dz} \right)\Bigg|_{z=H_2} = \bar{\Psi}(H_2) \left( i\nu + \frac{1}{2H_0} \right) C$$

(continuity of vertical velocity)

Elimination of C between them yields the complex boundary condition:

$$\frac{dF}{dz} - \left( \frac{1}{\bar{\psi}} \frac{d\bar{\psi}}{dz} + \frac{1}{2H_o} + i\nu \right) F = 0 \qquad \text{at} \quad z = H_2$$

This first order boundary condition will be used at $z = H_2$ while $w=0$ will be applied at $z = 0$.

## 6.7 Numerical Solutions

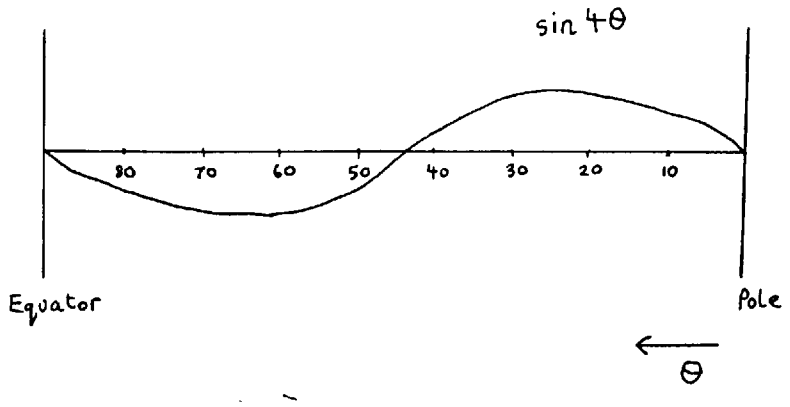
The integration was carried out between 0 and 10km. with $N = 1000$. Doubling the value of N caused a change in the numerical value of $F(z)$ of less than 0.1%. The wind shear was taken to be constant, with the wind speed varying linearly from $5 m.s.^{-1}$ at the ground to $15 m.s.^{-1}$ at 10 km. The following numerical values for the other parameters were used:

$B = 2.5 \times 10^{-5} \ m.^{-1}$ (typical of the troposphere)

$H_o = 7.5 \times 10^{3} \ m.$

$V_o = 3 \times 10^{-11} \sin^4 \left(\frac{\pi z}{H_2}\right) \ s.^{-2}$ (calculated from data for January 1963 shown in Fig.6 (2))

The spatial variation of the forcing was defined by $m = 4$ for the East-West direction and $\sin 4\theta$ in the North-South direction. This North-South variation of the forcing was represented by a truncated series (ten terms) of Associated Legendre Polynomials.



| $\theta$ | sin $4\theta$ | Series Approx. to sin $4\theta$ |
|---|---|---|
| 10 | 0.643 | 0.090 |
| 20 | 0.985 | 0.728 |
| 30 | 0.866 | 1.023 |
| 40 | 0.342 | 0.283 |
| 50 | -0.342 | -0.349 |
| 60 | -0.866 | -0.821 |
| 70 | -0.985 | -1.046 |

The North-South variation of the forcing was represented by a series in order to account for an intensified split jet stream. The vertical variation of $V_o$ was taken as $\sin^4 (\frac{\pi z}{H_2})$ as this realistically peaks sharply in the mid-troposhere.

The results at $60^oN$ were as follows:

| Height (km) | Amplitude (m) | Phase of ridge ($^oW$ of wave cycle) | T($^oC$) | Phase of T ridge ($^oW$ of wave cycle) |
|---|---|---|---|---|
| 10 | 63.0 | 179.6 | 1.6 | 4.1 |
| 9 | 70.4 | 180.0 | 1.9 | 3.1 |
| 8 | 78.9 | 180.3 | 2.2 | 2.4 |
| 7 | 87.6 | 180.5 | 2.1 | 2.1 |
| 6 | 94.6 | 180.7 | 1.3 | 2.5 |
| 5 | 97.5 | 180.8 | 0.1 | 17.7 |
| 4 | 95.1 | 180.8 | 1.2 | 178.9 |
| 3 | 88.5 | 181.0 | 2.1 | 179.9 |
| 2 | 78.9 | 181.0 | 2.5 | 180.4 |
| 1 | 68.6 | 181.0 | 2.7 | 180.8 |
| 0 | 57.3 | 181.1 | 2.8 | 181.1 |

This solution closely resembles the analytic case with no shear and $\nu^2 < 0$. The phase of $\nabla^2\psi$ is $\pi/2$ downstream from the vorticity forcing and the amplitude of $\psi$ reaches its maximum value at the level of the forcing. There are warm highs and cold lows below the forcing and cold highs and warm lows above it.

The solution with wind shear is more realistic than the constant zonal wind case in that it produces temperature perturbations on the horizontal boundaries. These are due to horizontal advection of the basic-state temperature field and is consistent with the observation that blocking highs are warm at the ground. In fact, the barotropic solutions could be used to calculate the surface advection of T and this would provide quite satisfactory results. From the thermodynamic equation at $z = 0$:

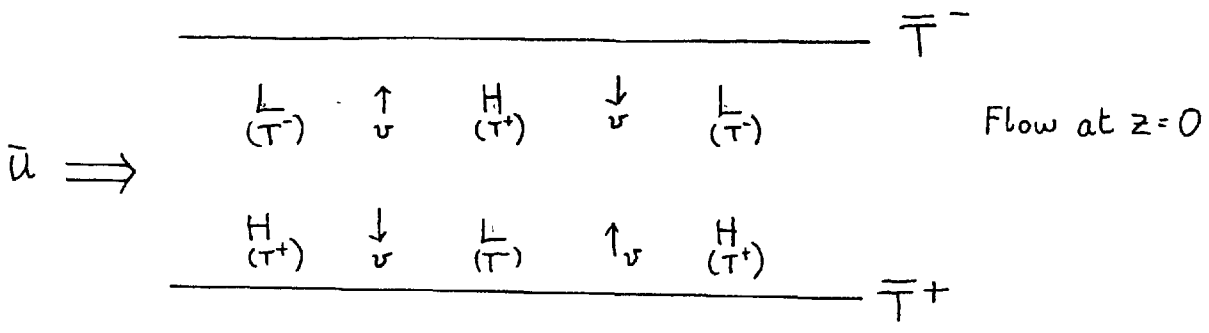
$$\bar{u}\frac{\partial \phi'}{\partial x} + v'\frac{\partial \bar{\phi}}{\partial y} = 0$$

Let $\frac{\partial \bar{\phi}}{\partial y} = -A$ and $v' = |v'| \sin kx \cos ly$

$$\therefore \frac{\partial \phi'}{\partial x} = \frac{A v'}{\bar{u}} \sin kx \cos ly$$

$$\phi' = -\frac{A|v'|}{\bar{u}k} \cos kx \cos ly + \text{constant}$$

Substitution of typical values yields a value of about $1^{\circ}C$ for surface T'. The highs are warm and the lows cold.




In other respects the similarities between the solutions with linear shear and no shear are so marked that it seems probable that the inclusion of a more realistic wind profile in the numerical solution would not have a significant effect.

The most important analytic result which was confirmed by the numerical model in the presence of wind shear is that the vorticity maximum of the forced wave should be $\pi/2$ downstream from the maximum of the vorticity forcing. This then raises the difficult question of the phase of the forcing relative to the original long waves. The mechanism proposed by Green (1977) implied that the main North-South baroclinic zones, the momentum convergence and the blocking wave were all in phase. It was pointed out earlier in this chapter that this situation is not consistent with a steady-state. Furthermore, the analysis of the flow in January 1968 (Chapter Three) showed that when wavenumbers two and three interfered to produce a ridge at 500 mb. over the Pacific, this gave rise to a ''blocking'' wavenumber four which was not in phase with the original ridge.

Savijarvi (1977) has produced results on the vorticity balance of the atmosphere in high and low (blocking) index cases. The distribution of the vorticity forcing due to transient eddies is shown in Figure 3 of his paper.* In the low index case there is an area of anticyclonic vorticity forcing on the upwind and downwind edges of the position of the mean anticyclone. There is also a

* See Figs. 6(3) and 6(4)

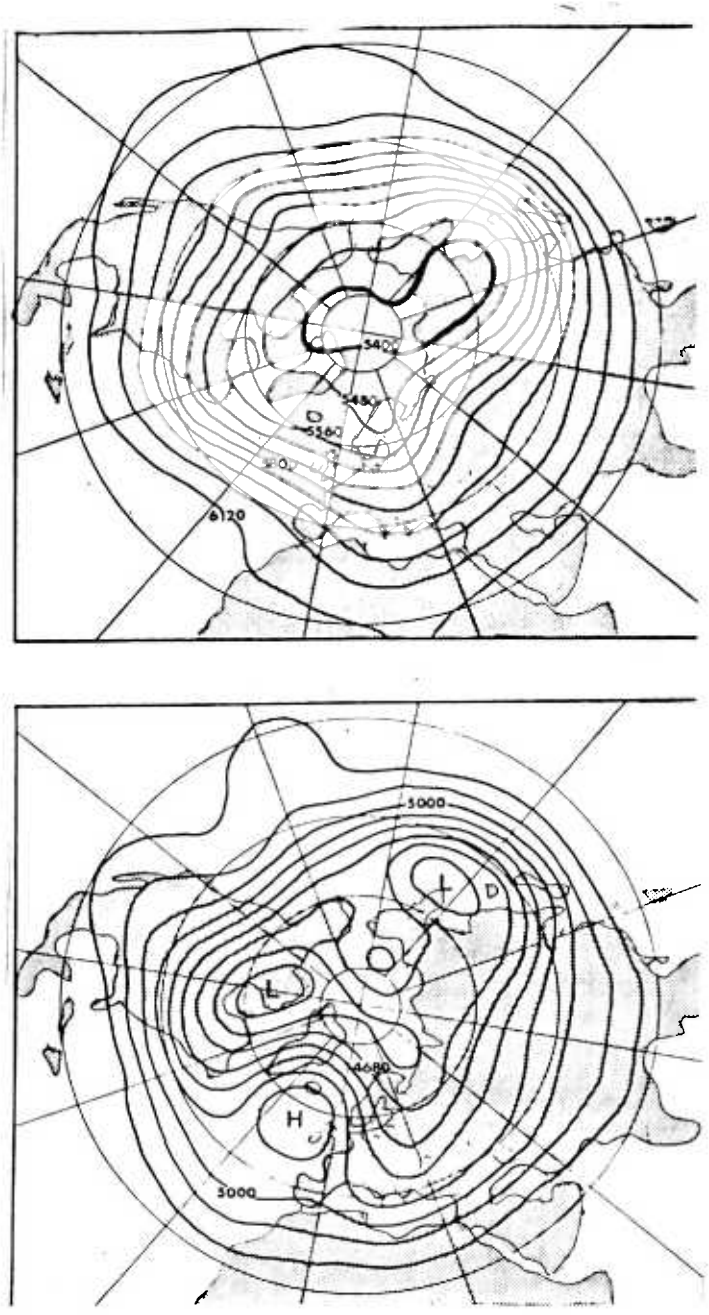
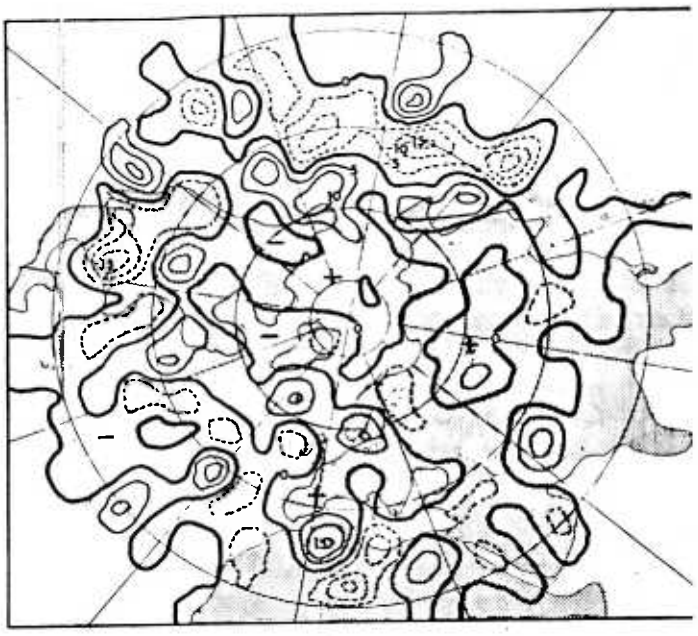
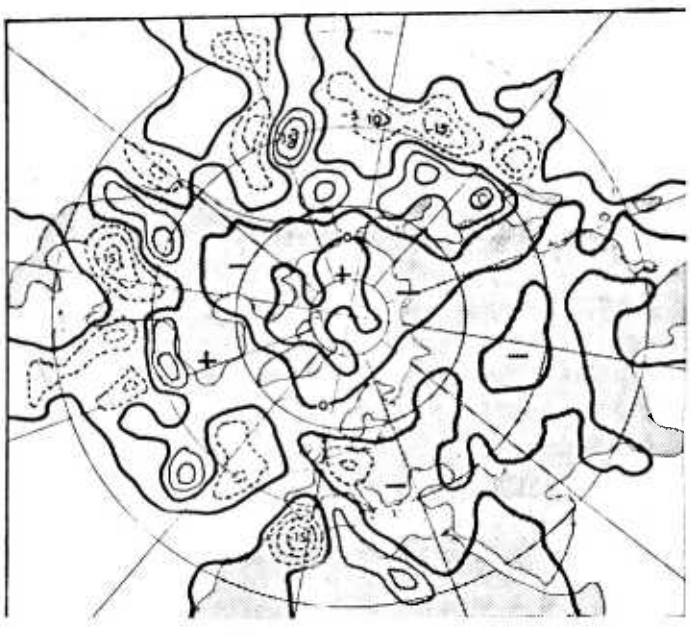



Figure 6(3) Monthly Mean Height Fields $\bar{z}$ averaged vertically for the two periods in 1965. Unit: m.

(From Savijärvi, 1977)



December 1965



February 1965

Figure 6(4) Distribution of $\hat{k} \cdot \nabla \wedge A_H$ averaged vertically.
Units: $10^{-11} s^{-2}$.

$\hat{k} \cdot \nabla \wedge A_H$ is the vorticity forcing due to transient effects.

$A_H = A_x \underset{\sim}{i} + A_y j$ where $A_x = -\overline{\nabla . u'V'}$

$A_y = -\overline{\nabla . v'V'}$

(From Savijärvi, 1977)

strong area of cyclonic forcing over Japan, where there was a well developed low on the monthly mean chart. Savijari did not attach much significance to these results which is surprising because the central magnitude of the relevant areas of forcing was of the order of $10^{-10}$ $s^{-2}$. This is very large, considering that the results represent a vertical average. For comparison, Green's calculation of the momentum convergence around a blocking anticyclone in July 1976 produced a value for the vorticity forcing of $5 \times 10^{-11}$ $s.^{-2}$ at 500 mb. and calculations from the zonal mean data for January 1963 produced a peak value of $3 \times 10^{-11}$ $s.^{-2}$ at 400 mb. This is the value of the forcing which was used in the numerical model and it produced realistic, if a little small, magnitudes of the height fields when compared with data on long waves analysed in Chapters Three and Four. Thus it seems that the areas of transient vorticity forcing identified by Savijarvi during blocking must have had large repercussions on the monthly mean flow. However, the problems of phase relationships will not be properly understood until more is known about the momentum transfer due to an isolated travelling depression.

## 6.8 Conclusion

In this chapter it was shown that a simple barotropic model of momentum forcing which was sharply peaked with height produced results which closely resembled blocking waves, providing $\nu^2 < 0$. ( $\nu$ is the vertical wavenumber). The height structure and zonal and meridional scales produced were particularly realistic. A resonance was possible as the vertical wavenumber approached zero. This structure of blocking waves was confirmed in a numerical model which included wind shear.

Appendix One

Blocking Catalogue for the Atlantic Sector, 1966-1976

The definition of blocking used here is that a stationary anticyclone should persist for at least six days, with its centre lying in the region $20^{\circ}E$ to $50^{\circ}W$ and $50^{\circ}N$ to $70^{\circ}N$. A stationary persistent ridge was considered to be a block if it extended up to $60^{\circ}N$. The catalogue was compiled from monthly ''Weather Logs'', published with the magazine ''Weather''.

| Year | First Day of Blocking | Last Day of Blocking |
|---|---|---|
| 1966 | Jan 9 | Jan 19 |
| | Feb 11 | Feb 18 |
| | March 14 | March 21 |
| | April 11 | April 21 |
| | May 27 | June 3 |
| | June 8 | June 17 |
| | Aug 22 | Aug 28 |
| | Sep 20 | Sep 26 |
| | Oct 27 | Nov 1 |
| 1967 | Jan 8 | Jan 14 |
| | April 5 | April 18 |
| | April 27 | May 3 |
| | June 10 | June 17 |
| | Dec 1 | Dec 17 |
| 1968 | Feb 4 | March 12 |
| | April 3 | April 29 |
| | May 16 | June 16 |

| | | | | |
|---|---|---|---|---|
| | July | 19 | Aug | 11 |
| | Aug | 20 | Aug | 28 |
| | Sep | 4 | Sep | 18 |
| | Sep | 26 | Oct | 7 |
| | Nov | 3 | Nov | 20 |
| | Nov | 28 | Dec | 14 |
| | Dec | 26 | | |
| 1969 | | | Jan | 6 |
| | Jan | 31 | Feb | 15 |
| | Feb | 24 | March | 7 |
| | March | 21 | March | 27 |
| | April | 17 | April | 24 |
| | June | 4 | June | 11 |
| | July | 26 | Aug | 16 |
| | Oct | 4 | Oct | 23 |
| | Nov | 21 | | |
| 1970 | | | Jan | 6 |
| | Jan | 15 | Feb | 1 |
| | Feb | 24 | March | 15 |
| | March | 22 | April | 5 |
| | May | 4 | May | 16 |
| | June | 4 | June | 30 |
| | Sep | 20 | Sep | 29 |
| | Oct | 11 | Oct | 16 |
| | Dec | 7 | Dec | 31 |
| 1971 | Feb | 2 | Feb | 7 |
| | Feb | 22 | March | 10 |
| | April | 30 | May | 21 |

| | | |
|---|---|---|
| | May 31 | June 17 |
| | July 2 | July 17 |
| | Sep 4 | Sep 17 |
| | Dec 4 | Dec 11 |
| | Dec 27 | |
| 1972 | | Jan 18 |
| | Jan 28 | Feb 4 |
| | Feb 18 | March 18 |
| | April 18 | April 26 |
| | May 5 | May 21 |
| | July 13 | July 28 |
| | Aug 21 | Oct 20 |
| 1973 | Jan 1 | Jan 12 |
| | March 8 | March 20 |
| | April 5 | April 22 |
| | Aug 11 | Aug 26 |
| | Sep 7 | Sep 15 |
| 1974 | March 1 | March 12 |
| | March 22 | April 26 |
| | May 7 | May 20 |
| | Sep 27 | Oct 12 |
| 1975 | Feb 1 | Feb 8 |
| | Feb 15 | Feb 26 |
| | March 10 | March 20 |
| | March 27 | April 8 |
| | May 3 | June 12 |
| | June 19 | July 7 |

| | | | | |
|---|---|---|---|---|
| | Aug | 2 | Aug | 13 |
| | Oct | 7 | Oct | 12 |
| | Oct | 19 | Oct | 28 |
| | Nov | 6 | Nov | 13 |
| | Dec | 2 | Dec | 27 |
| 1976 | Jan | 28 | Feb | 7 |
| | Feb | 16 | Feb | 23 |
| | March | 2 | March | 24 |
| | April | 18 | April | 30 |
| | June | 21 | Sep | 5 |
| | Nov | 14 | Nov | 25 |
| | Dec | 10 | Dec | 27 |

Appendix Two

Errors in Long Wave Calculations

In Chapter Four it was concluded that the phases of the long waves need to be correctly predicted to within $10^{\circ}$ longitude. This conclusion was based on results from a number of obervational studies. It is therefore necessary to look at the errors which may have been incurred during the calculation of these results. The two most likely sources of error are the use of a grid of observations and possible gaps or errors in these observations.

Errors due to Grid Spacing

$$\text{Say} \int_0^a f(\theta)\, d\theta = \frac{a}{2}\left(f(0) + f(a)\right) + \mathcal{E}$$

where $\mathcal{E}$ is the truncation error.

To second order let

$$f(\theta) = A_o + A_1\theta + A_2\theta^2$$

Then $\mathcal{E} = \frac{A_2 a^3}{3}$ where $A_2 = \frac{1}{2}\frac{d^2f}{d\theta^2}$

Let the fractional error $\gamma = \frac{\mathcal{E}}{fa} = \frac{a^2}{6}\,\frac{1}{f}\,\frac{d^2f}{d\theta^2}$

If $f \sim \cos n\theta$

$$\gamma = -\frac{a^2n^2}{6}$$

The grid spacing of the observations used was $10^{\circ}$ longitude

$$\therefore \tau \sim \frac{1}{200} \quad \text{for} \quad n = 1$$

$$\sim \frac{1}{20} \quad \text{for} \quad n = 3$$

These errors can therefore be expected in the calculation of the Fourier coefficients $a_n$ and $b_n$.

Let $\phi$ be the resultant error in the phases.

Then $\phi \sim \tan \tau$

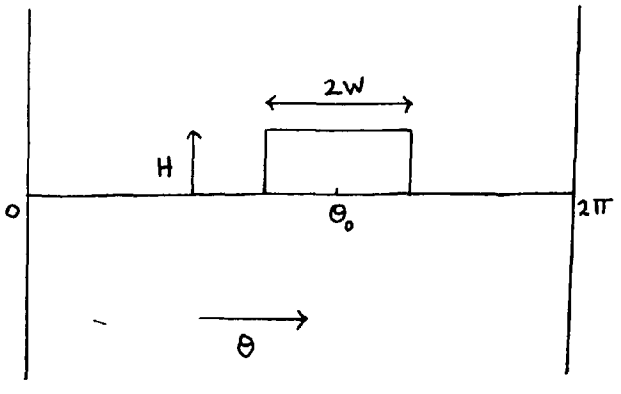
For $n = 1$, $\phi \sim 0.3^{\circ}$ longitude

$n = 3$, $\phi \sim 2^{\circ}$ longitude.

Thus errors in the phases of the long waves due to the grid spacing used were negligible.

Errors due to Gaps in Observations

Although hemispheric data was used in the calculations, the lack of observations over the Pacific could introduce a large error in this data. This error is difficult to assess but it could be significant for the very long waves. The presence of a cyclone or anticyclone aloft which had been missed by the observational network could be represented schematically as follows:



As the boundary conditions are periodic in $\theta$, this disturbance can be represented by a Fourier Series

$$f(\theta) = a_o + \sum_n a_n \cos n\theta + \sum_n b_n \sin \theta$$

where $a_o = \frac{WH}{\pi}$

$$a_n = \frac{4H}{n} \cos n\theta_o \sin nW$$

$$b_n = \frac{4H}{n} \sin n\theta_o \sin nW$$

Let the wavenumber one component of the inaccurate observations be $A \cos \theta$ and let the error in $\theta$ be $\phi$. Then $\phi$ will be a maximum when $\theta_o = \pi/2$.

For wavenumber one:

$$A \cos \theta + b \sin \theta = A \cos (\theta - \phi)$$

Typical values: A = 10dm. , H = 2 dm. , W = $45^o$

$$\text{Tan } \phi = \frac{b}{a} = 0.2828$$

$$\therefore \quad \phi \sim 15^o \text{ longitude}$$

This is obviously a fairly extreme case of observational inaccuracy but the errorin the phase of wavenumber one is disturbingly large. There does not seem to be an immediate solution to this problem as satellite techniques cannot yet cope with pressure measurements in the troposphere.

## Harmonic Analysis of Normal Charts from Eliasen (1958)

$A_m$ in metres and $\delta_m$ in degrees Longitude (position of ridge)

| Latitude | Zonal Wavenumber m | January | | | | July | | | |
|---|---|---|---|---|---|---|---|---|---|
| | | 500 mb. | | 1000 mb. | | 500 mb. | | 1000 mb. | |
| | | $A_m$ | $\delta_m$ | $A_m$ | $\delta_m$ | $A_m$ | $\delta_m$ | $A_m$ | $\delta_m$ |
| 30°N | 1 | 59 | 292 | 16 | 351 | 41 | 312 | 79 | 256 |
| | 2 | 10 | 145 | 16 | 110 | 16 | 175 | 53 | 165 |
| | 3 | 28 | 83 | 17 | 102 | 4 | 17 | 21 | 77 |
| 40°N | 1 | 84 | 326 | 39 | 46 | 38 | 332 | 66 | 262 |
| | 2 | 34 | 42 | 48 | 89 | 12 | 77 | 48 | 179 |
| | 3 | 64 | 98 | 32 | 108 | 12 | 79 | 22 | 83 |
| 50°N | 1 | 84 | 6 | 76 | 66 | 32 | 22 | 38 | 271 |
| | 2 | 79 | 43 | 83 | 85 | 43 | 73 | 32 | 14 |
| | 3 | 80 | 106 | 33 | 2 | 22 | 111 | 12 | 93 |
| 60°N | 1 | 62 | 40 | 71 | 114 | 35 | 73 | 17 | 259 |
| | 2 | 100 | 33 | 64 | 79 | 42 | 58 | 19 | 30 |
| | 3 | 63 | 108 | 43 | 12 | 24 | 114 | 6 | 104 |
| 70°N | 1 | 50 | 84 | 87 | 163 | 39 | 116 | 3 | 274 |
| | 2 | 98 | 21 | 19 | 71 | 40 | 40 | 12 | 23 |
| | 3 | 40 | 108 | 18 | 3 | 14 | 101 | 2 | 110 |

REFERENCES


Charney, J.G. and Drazin, P.G. 1961 "Propagation of Planetary Scale Disturbances from the lower into the upper atmosphere."
J. Geophys. Res. 66, pp 83-110

Eady, E.T. 1949 "Long Waves and Cyclone Waves."
Tellus 1, pp 33-52

Eliasen, E. 1958 "A study of the long Atmospheric Waves on the basis of Zonal Harmonic Analysis."
Tellus 10, pp 206-215

Elliot, R.D. and Smith, T.B. 1949 "A study of the effects of large blocking highs on the general circulation in the Northern Hesmisphere Westerlies."
J. of Meteor. 6, pp 67-85

Everson, P.J. and Davies, D.R. 1970 "On the use of a simple two-level model in General Circulation Studies."
Quart. J.R. Met. Soc. 96, pp 404-412

Geisler, J.E. 1977 "On the Application of Baroclinic Instability and Sensible Heat Exchange to explain Blocking Ridge Development."
J. At. Sci. 34, pp 216-218

Geisler, J.E. and Garcia, R.R. 1977 "Baroclinic Instability at Long Wavelengths on a $\beta$-plane"
J.At. Sci. 34, pp 311-321

Green, J.S.A. 1960 "A problem in baroclinic instability."
Quart. J.R. Met Sci. 86, pp 237-251

Green, J.S.A. 1970 "Transfer Properties of the large scale eddies and the general circulation of the atmosphere."
Quart. J.R. Met. Sci. 96, pp 157-185

Green, J.S.A. 1972 "Large Scale Motion in the upper stratosphere and mesosphere : an evaluation of data and theories."
Phil. Trans. Roy. Soc 271A, pp 577-583

Green, J.S.A. 1977 "The Weather during July 1976 : Some dynamical considerations of the drought." Weather 32, pp 120-128

Haltiner, G.J. 1967 "The Effects of Sensible Heat Exchange on the dynamics of Baroclinic Waves." Tellus 19, pp 183-198

Kane, I.D. 1973 "A numerical investigation into the stability of zonal flows in the atmosphere." Ph.D. Thesis, University of London

Kikuchi, Y 1968 "Numerical Simulation of the Blocking Process." Colorado State Univ., At. Sci. paper 125

Labitzke, K. 1965 "On the Mutual Relation between Stratosphere and Troposphere during Periods of Stratospheric Warmings in Winter." J. Applied Met. 4, pp 91-99

Lamb, H.H. 1972 "Climate: Present, Past and Future." Vol. 1. (Methuen and Co. Ltd.)

Lejenas, H. 1975 "On the breakdown of the Westerlies." Dept. of Meteor., Univer. of Stockholm, Report DM17

Lindzen, R.S. and Kuo, H.L. 1969 "A reliable method for the numerical integration of a large class of ordinary and parital differential equations." Mon. Weath. Rev. 97, pp 732-734

Lorentz, E.N. 1955 "Available potential energy and the maintenance of the general circulation." Tellus 7, pp 157-167

Lorentz, E.N. 1972 "Barotropic Instability of Rossby Wave Motion." J.At. Sci. 29, pp 258-264

Mahlam, J. and Manabe, S. 1972 "Numerical Simulation of the Stratosphere: implications for related Climatic Change Problems." CIAP Survey Conference Proceedings P. 186 (U.S. Dept of transportation)

McNulty, R.P. 1976 "Vertical Energy Flux in Planetary Waves : Observational Results."
J.At. Sci. 33, pp 1172-1183

Miyakoda, K. 1963 "Some characteristic features of the winter circulation in the troposphere and lower stratosphere."
Univ. of Chicago, Tech. Report 14

Montalto, M., Conte, M., and Urbani, M. 1973 "Comparison and Summary of the Characteristics of long and short lived Blocking Systems in the Euro-Atlantic Area."
Rome, Min. Aero.

Oort, A.H. and Rasmussen, E.M. 1971 "Atmospheric Circulation Statistics."
NOAA Professional Paper 5

Perry, J.S. 1967 "Long Wave Energy Processes in the 1963 sudden stratospheric warming."
J. At. Sci. 24, pp 539-550

Rex, D.F. 1951 "Blocking Action in the Middle of Troposphere and its effect upon regional climate."
Part One: Tellus 2, pp 196-211
Part Two: Tellus 2, pp 275-301

Rossby, C.G. 1939 "Relation between variations in the Intensity of the Zonal Circulation of the Atmosphere and the Displacements of Semi-Permanent Centres of Action."
J. Marine Research 2, p. 38

Rossby, C.G. 1950 "On the Dynamics of certain types of Blocking Waves."
J. Chinese Geophys. Soc. 2, pp 1-13

Sanders, R.A. 1953 "Blocking Highs over the Eastern North Atlantic and Western Europe."
Mon. Wea. Rev. 81, pp 67-73

Savijärvi, H.I. 1977 "The Interaction of the Monthly Mean Flow and large scale transient eddies in two different circulation types."
Part II: Geophysica 74, Vol. 2, pp 1-23

Shutts, G.J. 1976 ''The Generation and Propagation of Planetary Rossby Waves.''
Ph.D. Thesis, University of London

Van Loon, H. 1956 ''Blocking Action in the Southern Hemisphere.''
Notes 6, pp 171-175

Wexler, H. 1956 ''Variations in insolation, general circulation and climate.''
Tellus 8, pp 480-494

White, W.B. and Clarke, N.E. 1975 ''On the development of Blocking Ridge Activity over the central North Pacific.''
J.At. Sci. 32, pp 489-502

Wiin-Nielsen, A. 1961 ''On the short and long term variations in quasi-barotropic flow.''
Mon. Wea. Rev. 89, pp 461-476

Wiin-Nielsen, A., Brown J.A. and Drake, M. 1964 ''Further studies of energy exchange between the zonal flow and the eddies.''
Tellus 14, pp 168-180

Winston, J.S. and Kreuger, A.F. 1961 ''Some aspects of a cycle of available potential energy.''
Mon. Weath. Rev. 89, pp 461-476

Woffinden, C.M. 1960 ''Blocking Action.''
Met. Mag. 89, pp 236-240

Acknowledgements

This project was supervised by Dr. J.S.A. Green and his criticisms were invaluable. Many useful discussions were also had with Dr. Andy White and Dr. Glenn Shutts. My thanks go to Mrs. Sue Miller for her careful typing of the manuscript. The work was supported by an N.E.R.C. studentship.